Quantitative Methods to Determine Brain Deposition of Peptides and Proteins after Delivery across the Blood-Brain Barrier

By

Kavisha Raneendri Ulapane

Submitted to the graduate degree program in Chemistry and the Graduate Faculty of the University of Kansas in partial fulfillment of the requirements for the degree of Doctor of Philosophy.

_____

Chair: Dr. Teruna Siahaan

_____

Dr. Susan Lunte

_____

Dr. Robert Dunn

_____

Dr. David Benson

_____

Dr. Thomas Tolbert

Date Defended: 18th July 2019

The dissertation committee for Kavisha R. Ulapane certifies that this is the approved version of the following dissertation:

Quantitative Methods to Determine Brain Deposition of Peptides and Proteins after Delivery across the Blood-Brain Barrier

_____

Chairperson: Dr. Teruna Siahaan

Date Approved: 26th July 2019

Quantitative Methods to Determine Brain Deposition of Peptides and Proteins after Delivery across the Blood-Brain Barrier

Kavisha R. Ulapane

The University of Kansas, 2019

It is very challenging to develop peptide and protein drugs for treatment of brain diseases because it is difficult to deliver them to the brain due to the presence of the blood-brain barrier (BBB). Therefore, there is an urgent need to develop new and alternative methods to deliver these drugs to the brain for treatment of brain diseases. ADTC5 and HAV6 peptides were derived from the binding sequence of the EC1 domain of E-cadherin protein, and these peptides can enhance the in vivo brain delivery of various molecules through the paracellular pathway of the BBB. Therefore, the overall goal of this project was to evaluate the activity of current and new cadherin cyclic peptides to enhance the in vivo brain delivery of peptides and proteins in rats and mice.

The first goal of this project was to evaluate the activity of cadherin peptides (e.g., HAV6, HAV4, cHAVc3, and ADTC5) in delivering peptides (e.g., cIBR and cLABL) and 65 kDa galbumin protein to mouse and rat brains. The brain depositions of peptides and proteins were detected using near IR fluorescence (NIRF) imaging, magnetic resonance imaging (MRI), and mass spectrometry. The brain delivery of unlabeled cIBR7 peptide into rat brains was done to confirm that the intact molecule could be detected in the brain. An efficient extraction method was developed to isolate cIBR7 and ADTC5 from the brain tissue. A novel LC/MS/MS method was developed and validated to quantify cIBR7, an internal standard, and ADTC5 in brain after in vivo delivery. Detection was performed using triple quadrupole tandem mass spectrometry and a

multiple reaction monitoring technique. Our results showed a fourfold increase ($p = 0.013$) in the amount of intact cIBR7 in the brain when it was delivered using ADTC5 compared to cIBR7 alone.

The second goal was to compare the activity of ADTC5 and HAV6 peptides in delivering various sized proteins, including IRdye800cw-labeled-lysozyme (15 kDa), albumin (65 kDa), IgG mAb (150 kDa), and fibronectin (220 kDa) into mouse brains. In addition, a quantitative NIRF imaging method was developed to determine brain depositions of these proteins. The results showed that ADTC5 peptide significantly enhanced brain delivery of lysozyme, albumin, and IgG mAb compared to controls; however, no enhancement was observed for fibronectin. HAV6 peptide could enhance the brain delivery of lysozyme, but not the other proteins.

The third goal was to design and synthesize new cyclic peptides for better modulation of the BBB. An N-to-C terminal cyclization method was utilized to improve the plasma stability and activity to modulate the BBB of the peptide. Linear and cyclic ADTHAV peptides were designed by combining the sequences of ADTC5 and HAV6. Cyclic HAVN1 and HAVN2 peptides were designed as N-to-C terminal cyclic derivatives of linear HAV6 peptide as new BBB modulator peptides. Binding properties of cyclic ADTHAV and ADTC5 peptides to the EC1 domain of E-cadherin were determined using surface plasmon resonance (SPR), and ADTHAV was found to have higher binding affinity ($K_d = 0.114$ μM) than ADTC5 ($K_d = 26.8$ μM). The in vivo activities of these peptides to deliver an IRdye800cw-labeled IgG mAb into the brain were qualitatively and quantitatively determined using NIRF imaging. Cyclic HAVN1 and HAVN2 peptides enhanced brain delivery of IgG mAb compared to HAV6 peptide. Cyclic and linear ADTHAV as well as ADTC5 peptides enhanced brain delivery of IgG mAb. There seems to be a trend that cyclic ADTHAV peptide has better activity than linear ADTHAV under the current conditions ($p = 0.07$).

Overall, these three studies support the potential use of cadherin peptides in transiently modulating the BBB to improve the brain delivery of peptides and proteins.

This thesis is dedicated to:

My Mom: Manel Ranasuriya

My Husband: Sasanka Ulapane

My Daughter: Maya Ulapane

Acknowledgements

My PhD at KU, I find to be an unforgettable memory created by a group of intellectually and emotionally fortified people. This small note is to humbly offer my sincere gratitude for all your support. I would not be where I am today without the love and support from my family, friends, and teachers throughout my graduate work and my education before that. Although many fewer names are included in here, you all have contributed to my success, and I owe you for that.

First, and foremost, I would like to express my sincere gratitude to my advisor Dr. Teruna J. Siahaan for his support, advice, and all the help given at every step in my graduate career. None of this would have been a possibility if it was not for your guidance. You are not just my mentor; you are like a father to me. You gave me wisdom, help, and encouragement I needed when the life is tough, unbonded to lab and research. Specially, thank you for taking me in to your group when I was facing an unexpected tragedy during my 2nd year of graduate school. You always keep telling your students to work smarter not harder, which I will keep it in my mind forever. Thank you for shaping me up to be a smart scientist with all the skills you taught us to solve problems with ("We don't do big steps; we like small steps to make a consistent impact" that's what you believed). I saw your genuine happiness when my research and personal life is successful. You, as a family-oriented person that are always helping and understanding about my personal life as an international student, a wife, and a mother, meant a lot to me. I believe you are a great mentor, and any student is lucky to have you as their research supervisor. Honestly, I can't thank you enough for what you have done for me, and joining your group is the best decision I made in my graduate career.

Dr. Craig Lunte, you were the one who showed me the first step in graduate school. Your separation class was second to none, so as your BBQ ribs. I learned skills including separation

techniques and animal surgeries while I was in your group; eventually, they became very useful along the way. Even though I did not have much time with you, the short time we shared together was always fun and filled with precious moments that I will cherish throughout my life. I miss our Christmas and departmental parties where Craig had lots of fun with his students. Craig, I really wish we had more time together, and you will forever be missed. I may be the last graduate student who was in your group now graduating from KU, but I know your legacy will live on with me here for many years.

Thank you, Dr. Sue Lunte, for everything you have done for me. You were always with me when I was lost and had no idea how to face the future. You always wanted to make sure that we are taken care of and fought our battles with us. You are a kind person as well as an inspirational scientist. Because of you, I am writing a PhD dissertation, not a Master's thesis. Thank you, Sue, I'm grateful to you. Dr. Dunn, you were my favorite teacher in graduate school, I really enjoyed your spectroscopy class as a student. I had the best experience as a TA with you in the instrumental analysis class that we taught together. You are my icon teacher and a great mentor to work with. I would also like to thank Dr. Benson and Dr. Tolbert for agreeing to serve in my defense committee, specially thank you Dr. Tolbert for agreeing my last-minute request to serve as one of my committee members for the defense. I would like to thank Drs. Mario Rivera and Yong Zeng for serving in my orals committee and providing valuable feedback. To Dr. Todd Williams, I would like to thank you for allowing me to use the mass spectroscopy laboratory on my first project, and for all your fun stories (about the Shoe Store!!!). I had promised you that I will help as a dog-sitter, but never got a chance to do so. I still can remember you were saying that how grumpy you are when I first met you, and thinking it was very true at the time. Years have passed, I found out who

you truly are and what a fun-filled person you are. I loved the scientific discussions that we had at the mass spectrometry laboratory in Malott Hall.

Next, I thank all members of the Siahaan's research group, both past and present, for their impact on my research as well as my development as a scientist. I would like to thank Dr. Paul Kiptoo for his guidance and support when I was new to the lab; Dr. Mario Moral for all his help and guidance and training me about protein expression and purification; and Brian Kopec for his tremendous support on all animal studies that we have done. Without you Brian, I will not be able to finish my last two projects on time. Isaac and Ricardo, you have been two wonderful students that I had the privilege to teach and mentor. Isaac, I love how you turned out to be the guardian and housekeeper of our laboratory. For Rucha, Kelly, and Subra, I enjoyed all the fun chats that we had. Jinyan, Aldyn and Darci and all my Craig Lunte group members, Sara, Amanda, Hasitha, Yunan, Michael, Ryan and Nhan, many thanks for all your help during my stay at KU. For my best friend at KU, Lin Zeng, I missed you so much when you left KU after completing your master's degree. We routinely had lunch together even though we were in two different buildings. Thank you for being my best friend, Lin.

I thank Dr. Tahnee Dening, Dr. Michael Hageman, and Dr. Donald Miller and his research group as our Canadian collaborator for numerous help during my research work.

I would like to thank all my teachers from my high school, Visakha Vidyalaya and my undergraduate institute, University of Peradeniya back in Sri Lanka, without whom I would not be here today.

My mom, my best friend, who is my strength should get all the credit for what I'm today. Your commitment and love are boundless. Thank you Ammi (Mom) for everything you have done. I just don't have enough words to say how thankful I am and how much I love you. And my late

Achchiammi (Grandma), who gave a tremendous support to my Mom to raise me will be missed forever. I must thank my wonderful mom- and father-in-laws and my sister, Oshadhi, for all their help when it was needed. All my Sri Lankan friends in Lawrence, you all helped us in many ways when we were new to Lawrence as well as to US. We have shared many moments together; you are my family here. Thank you everyone, you all will be missed. Specially Dr. Shamal Gunawardhana, Dr. Manjula Wijesinghe, and Dr. Kasun Imaduwage, thank you for all the scientific discussions we had about many classes and research matters; you three were the big brains and helped me many times throughout this journey. Gihan and Dimuthu, thank you for taking the time to help me with the hydrogenation reaction and more. Special thanks go to Mr. Nalin Weerasekara and Dr. Chamani Perera, who stood by the Lawrence Sri Lankan community for years.

I fondly am reminded of the support given by KU Department of Chemistry, Department of Pharmaceutical Chemistry, staff personals at Chemistry and Pharm. Chem (Nancy, Andre, Nicole, Michelle, Ruben, Liz, Megan), and KU International Student Services.

Beyond everything, my heartfelt thanks go out to my amazing husband and the best dad to my little princess, Sasanka. We have come a long way since we first met during our freshman year at UOP up to now, getting our PhDs together at KU. You are the best that one can ever ask for, as a husband and as an Appachchi (Dad). It is your love and encouragement that kept me going throughout these tough years. In many times that I was down, you were there to pick me up. Thank you for always being by my side, supporting me for everything I do. I love you immensely, more than I can ever say. I can’t wait to see our future with our newest bundle of joy, Maya who turned one this month. She is the most wonderful gift I ever had who filled our life with love, joy and hope. I love you all so much!

Table of Contents

CHAPTER 1

Peptides and Drug Delivery

1.1. Introduction

Peptides have been successfully developed as therapeutic and diagnostic agents because of their selectivity to bind the respective target receptors.[1-3] Currently, there are more than 60 peptide drugs approved by the US Food and Drug Administration (FDA). Thus, development of peptide drugs has increased significantly in the past decades and, as of today, approximately 140 peptides are in clinical trials as potential drugs. In addition, more than 500 therapeutic peptides are in preclinical development.[3] Available peptide drugs which include oxytocin, calcitonin, octreotide, and exenatide are being used to treat various conditions. Some bioactive peptides have been derived from endogenous substances; however, some peptides were derived from truncation of the active region(s) of the parent proteins. For example, opioid peptides such as enkephalins, endorphins, and dynorphins that are found in the brain have been used as drugs. Oxytocin, an endogenous hormone released by the posterior pituitary, is a cyclic peptide synthesized in the paraventricular nucleus of the hypothalamus.[4] Oxytocin and its analogs work as neurotransmitters in the brain to facilitate breastfeeding, induce labor, and treat postpartum hemorrhage. Calcitonin peptide is a hormone produced by the thyroid gland to control calcium and potassium levels in blood. A synthetic salmon-calcitonin peptide has been used to treat osteoporosis; this peptide was first developed as a nasal spray.[5] Tumors can be treated by octreotide, which inhibits the release of growth hormones[6]. Type-2 diabetes is treated successfully with exenatide (**Table 1.1**), which is a derivative of a glucagon-like peptide-1 agonist (GLP-1; **Table 1.1**).[7] Exenatide was developed to increase the *in vivo* half-life because GLP-1 was ineffective in clinical trials for diabetes treatment due to its short half-life. Exenatide binds to GLP-1 receptor and regulates glucose metabolism and insulin secretion. Both GLP-1 and glucose-dependent insulinotropic peptide (GIP)

hormones are produced upon ingestion of food to stimulate insulin secretion; however, only GLP-1 causes insulin secretion in a diabetic state.

Bioactive peptides can also be derived from the active region(s) of large functional proteins. One example is "Arg-Gly-Asp" (RGD), which is derived from the sequence of extracellular matrix (ECM) proteins such as fibronectin, fibrinogen, vitronectin, von Willebrand factor, laminin, and collagen.[8] RGD sequence on the ECM is recognized by various integrin receptors on the cell surface for cell adhesion to ECM. The ECM-integrin binding is essential in various disease processes such as thrombosis, angiogenesis and tumor metastasis.[9] In thrombosis, the process of vascular blood clotting prevents the normal blood flow from the heart, which involves platelet aggregation. Platelet aggregation results from interactions of fibrinogen and platelets, which are mediated by recognition of RGD sequences on the α- and γ-subunits of fibrinogen by gpIIb/IIIa integrin receptors on platelet surfaces.[10] Therefore, RGD peptides (*e.g.*, integrilin or eptifibatide) and peptidomimetics (*e.g.*, aggrastat or tirofiban) have been used as antithrombic agents in the clinic. Integrilin and aggrastat are selective and potent ligands for gpIIb/IIIa receptors, blocking platelet aggregation during thrombosis. Angiogenesis in solid tumors can be inhibited by RGD peptides (**Table 1.1**), which are designed to bind to cell-surface $\alpha_V\beta_3$ and $\alpha_V\beta_5$ integrins that are overexpressed during tumor angiogenesis.[11] Other cell adhesion peptides, such as those derived from intercellular adhesion molecule-1 (ICAM-1) and lymphocyte function-associated antigen-1 (LFA-1) receptors, have been shown to inhibit T-cell adhesion by adhesion to epithelial and endothelial cells during inflammation.[12]

Table 1.1 Peptide Names and Sequences	
Peptide	**Sequence**
Exenatide	HGEGTFTSDLSKQMEEEAVRLFIEWLKNGGPSSGAPPPS-NH_2
GLP-1	HDEFERHAEGTFTSDVSSYLEGQAAKEFIAWLVKGR - NH_2
ALOS4	Cyclo1,9(CSSAGSLFC)
RGD-1	Cyclo(RGDyK)
Transportan	GWTLNSAGYLLGKINLKALAALAKKIL
Penetratin	RQIKIWFQNRRMKWKK
PAF-26	RKKWFW
Octreotide	Cyclo2,7(fCFwKTCT)
GnRH-1	EHWSYkLRPG-NH_2
GnRH-2	EHWSHkWYPG-NH_2
GnRH-3	EHWSHDWKPG-NH_2
pHLIP	AAEQNPIYWARYADWLFTTPLLLLDLALLVDADEGTCG
MMP-hexapeptide	PVGLIG
ANG	TFFYGGSRGKRNNFKTEEY
ANG-SI	TFFYGGSRGKRNNFK–EVN-sta-VAEF
ANG-PEG-SI	TFFYGGSRGKRNNFK–PEG–EVN-sta-VAEF
ANG-TAT	TFFYGGSRGKRNNFK–TEEYGRKKRRQRRRPPQQ
Biotin-ANG	TFFYGGSRGKRNNF([Biotin)TEEY
Biotin-ANG-TAT	TFFYGGSRGKRNNFK(Biotin)TEEYGRKKRRQRRRPPQQ
T10	HAIYPRH
ERK	MPKKKPTPIQLNP
T10-ERK	HAIYPRH–GGCG–MPKKKPTPIQLNP
PEGA	Cyclo1,10(CPGEPEGAGC)
A54	AGKGTPSLETTP
G3-C12	ANTPCGPYTHDCPVKR
KLA	$D(KLAKLAK)_2$
RGD-2	Cyclo(RGDfC)
Pep-1	Cyclo1,9(CGEMGWVRC)
EGRF	YHWYGYTPQNVI
CPP	CKRRMKWKK
YSA	YSAYPDSVPMMS
RGD-3	CRGDK
OCC2	GVNPQAQMSSGYYYSPLLAMC(Acm)SQAYGSTYLNQYIYHYC(Acm)TVDPQE; Acm = Acetamido methyl
OP_{90-135}	DRGYGTSLLGGSVGYPYGGSGFGSYGSGYGYGYGYGYGYGGYTDPR-NH_2
OP_{90-103}	DRGYGTSLLGGSVG
Lip-OP_{90-103}	Lipid-C12-DRGYGTSLLGGSVG
C1C2	SSVSQSTGQIQSKVFDSLLNLNSTLQATR-NH_2
HAV6	Ac-SHAVSS-NH_2
ADTC5	Cyclo1,7(CDTPPVC)
cIBR7	Cyclo1,8(CPRGGSVC)
cLABL	Cyclo1,12(PenITDGEATDSGC)
C-CPE	SSYSGNYPYSILFQKF
AT-1002	FCIGRL
PN-78	FDFWITP
PN-159	KLALKLALKALKLAALKLA-NH_2

In addition to their use as drugs, bioactive peptides have been used as targeting moieties for the delivery of drug payloads (*e.g.*, anticancer and anti-inflammatory) to specific types of cells in tissues and, ultimately, to reduce their adverse side effects. Some of these peptides are internalized by their respective receptors into cells via a receptor-mediated endocytosis process. Others have been conjugated to drug-loaded nanoparticles for specific delivery to corresponding cell targets of the peptide. Receptor selective peptides were also investigated as diagnostic agents by conjugating them to dyes, radioisotopes, or magnetic resonance imaging (MRI) contrast agents.

The ultimate goal of targeted drug delivery is to direct a drug to diseased cells or organs (*e.g.*, cancer cells), while avoiding normal cells. This results in a drug construct with lower side effects than the free form of its parent drug. This chapter describes the roles of peptides in drug delivery, including the use of peptides as (a) peptide-drug and peptide-particle conjugates for targeting molecules to a specific type of cells and (b) modulators of biological barriers for improving the oral and brain delivery of drugs and diagnostic agents.

1.2 Peptide-Drug Conjugates for Targeted Drug Delivery

Drug targeting methods are normally explored to reduce side effects by directing toxic drugs to cells involved in disease states, leaving normal cells minimally affected. Conjugation of the drug to its peptide carrier (targeting agent) can be done directly or through a chemical linker**.** Thus, as a peptide carrier selectively binds to a specific receptor on the surface of targeted cells (*i.e.*, cancer cells), it carries along the drug or diagnostic molecule with it. As an example, cancer cells have a certain upregulated receptor(s) (*e.g.*, HER-2, EGFR) compared to normal cells. These upregulated receptors become distinguishing and exploitable features to selectively direct populations of conjugated drug molecules into cancer cells over normal cells. Binding of the conjugate to the target receptor is followed by cellular uptake of the ligand-receptor complex into

the early endosomes via receptor-mediated endocytosis.[13] From the endosomes, the conjugate reaches the lysosomes where the drug is released as a result of lowered pH and/or enzyme degradation in the lysosomes. The rate of release of the drug can be controlled by designing the appropriate linker between the drug and the peptide.[13-15] This method has been successfully applied in antibody-drug conjugates such as Adcetris® and Kadcycla® to treat cancer patients.[15, 16] Peptides are smaller than proteins and can rapidly synthesized using solid-phase methods. Unlike proteins, most peptides have only primary and secondary structures. Thus, most peptides do not suffer as much from physical instability as do proteins, which often leads to the formation of aggregates that generate immunogenicity. Due to their small size, peptide-drug conjugates are potentially less immunogenic than protein-drug conjugates. Although their formulation remains challenging, peptide conjugate formulation is usually less complicated than that of protein-drug conjugates.

In designing a peptide-drug conjugate, a functional group (*i.e.*, amine, carboxylic acid, alcohol, or thiol) within the structure of the drug can be used to link the drug directly to a targeting peptide's N- or C-termini, or a side-chain functional group of the Lys, Asp, Glu, Ser, Thr, or Cys residue(s) on the peptide. This direct drug-peptide linkage may be in the form of an amide, ester, or thioether bond. In many cases, the drug may be conjugated to the peptide using a molecular linker (*e.g.*, PEG, maleimido, *etc*.). Other than bridging drug and targeting components of the construct, the vital role of the linker is to provide a distance between the peptide and the drug, which is often crucial to the overall activity and potency of the construct. In one respect, ample distance between the drug and targeting-peptide components prevents interference (or steric hindrance) in binding to their respective receptors. This is because both drug and peptide have a molecular surface recognized by their respective receptors for biological activity. Normally, the conjugation is done at the functional group away from the bioactive region of the peptide or the drug. In addition, the

linker can be designed to control the release of the drug from the conjugate upon reaching the cell targets within the tissue. Premature release of the drug in the systemic or lymphatic circulation before reaching the respective target cells can be harmful and, ultimately, defeats the purpose of drug-targeting.

1.2.1 Peptide-Drug Conjugates for Cancer Therapy and Diagnostics

Chemotherapy remains the treatment of choice for cancer patients.[17] Most chemotherapeutic agents are cytotoxic and kill not only cancer cells but also normal cells in the body. Some drugs have poor solubility, are highly toxic, or cannot cross the cancer cell membranes into the intracellular space. Most cancer cells eventually generate resistance to anticancer drugs after multiple treatments. One of the drug-resistance mechanisms is due to the overexpression of efflux pumps *(i.e.*, Pgp, MRP, MDR1) that expel the anticancer drug from the cancer cell membranes. Therefore, there is a need to develop an alternative method to deliver drugs into cancer cells and overcome drug resistance by avoiding the efflux pumps. One way to increase drug penetration across cell membranes is by utilizing receptor-mediated endocytosis mechanisms. Thus, drugs have been conjugated to peptides, proteins, nanocarriers, carbon nanotubes, and dendrimers. As an example, paclitaxel (PTX), which is widely used to treat breast, ovarian, testicular, and cervical cancers, is known to have poor water solubility.[18] Thus, conjugation to a targeting peptide via a polyethylene glycol (PEG) linker increases solubility and improves selectivity to target cancer cells.

1.2.2 Cell Adhesion Peptides

Cell adhesion peptides have been used to target drugs and radioisotopes for cancer treatments and diagnostics. RGD peptides are cell adhesion molecules that have been extensively explored as carriers in peptide-drug conjugates. Certain cyclic RGD peptides bind selectively to $\alpha_V\beta_3$ and $\alpha_V\beta_5$

integrin receptors, which are upregulated during angiogenesis in tumors. Thus, these selective cyclic RGD peptides have been used to deliver radioisotopes such as ^{18}F, ^{99m}Tc, ^{125}I, or ^{64}Cu as cancer diagnostic agents. For example, ^{18}F-containing galactose was incorporated to RGD-1 peptide (**Table 1.1**) via an amide bond to the D-Lys side chain.[19] The ^{18}F-labeled conjugate binds selectively to upregulated $\alpha_V\beta_3$ integrin receptors on tumor vasculature as observed by positron emission tomography (PET). Thus, the conjugate can be used as imaging tool to detect angiogenesis and tumor metastasis *in vivo*.[19] The levels of $\alpha_V\beta_3$ receptors on human tumor cells have been detected with ^{18}F-labeled conjugates and observed using PET. It was found that the detected levels of $\alpha_V\beta_3$ receptors were similar to those detected using immunohistochemistry.[20] Accumulation of ^{18}F-labeled RGD-1 peptide in human tumors showed intra- and inter-variability of conjugate accumulation due to different levels of $\alpha_V\beta_3$ across different individuals.[19] The various levels of $\alpha_V\beta_3$ found in humans can be used to predict populations of cancer patients most likely to respond to treatments with RGD-anticancer drug conjugates. RGD peptides have been used to selectively deliver the anticancer drugs doxorubicin (DOX)[21] and PTX[22] to cancer cells *in vitro* and *in vivo*. RGD-1-DOX conjugate suppressed the growth of breast cancer xenographs in mice better than DOX alone, suggesting that cyclic RGD peptide improves the targeting of DOX to breast cancer cells *in vivo*.[21]

ALOS4 peptide (**Table 1.1**) is a non-RGD peptide that also binds to $\alpha_V\beta_3$ integrin. The peptide was linked to camptothecin (CPT) and fluorescein isothiocyanate (FITC) via a GABA linker to give ALOS4-CPT and ALOS4-FITC, respectively.[23] FACS analysis showed a strong binding of ALSO4-FITC to WM-266-4, a malignant melanoma cells. *In vivo* studies confirmed that tumor-bearing WM-266-4 cells in mice intravenously administered with ALOS4-FITC showed accumulation of ALOS4-FITC specifically in tumors rather than organs as observed after 24 hours.

Next, ALOS4-CPT enhanced drug cytotoxicity to tumor cells better than CPT and other anticancer drugs. CPT activity has been known to be deactivated by the hydrolytic opening of a vital lactone ring in its structure. In contrast to its free form, the stability of this lactone ring is increased in the ALOS-4-CPT conjugate.[23] At 10 μM, CPT alone kills high percentages of both malignant WM-266-4 and non-malignant HEK-293 tumor cells (human embryonic kidney cells) while ALOS4-CPT kills 70% of malignant WM-266-4 cell compared to 30% of the non-malignant HEK-293 cell. The activity of the conjugate is dose-dependent.[23] These results affirm that ALOS4 selectively targets and delivers conjugates to malignant tumor cells.

1.2.3 Cell-Penetrating Peptides

Generally, most peptides cannot readily cross the cell membranes due to their physicochemical properties; however, cell-penetrating peptides (CPPs with 6–30 amino acids) are capable of crossing membranes and entering the cell's cytoplasm.[24] A detailed mechanism of the cellular uptake of CPPs is not well understood, but it may take place either by direct translocation or by endocytosis. The early CPPs identified were *trans*-activating transcriptional activator (TAT) peptides, derived from human immunodeficiency virus 1 (HIV-1), and antennapedia homeodomain protein of drosophila (pAntp).[25] These long sequences have been reduced to 6–7 amino acid peptides, which maintain similar cell penetrating behavior. CPPs have been used for cellular delivery of small drug molecules (*i.e.*, doxorubicin, methotrexate and taxol), proteins, nucleic acids, and contrasting agents. Apart from the natural CPPs, synthetic and semi-synthetic CPPs, including the chimeric 27-aa transportan, penetratin, and PAF-26, were designed to facilitate drug delivery (**Table 1.1**).

1.2.4 Peptide Hormone for Drug Delivery

Peptide hormones such as octreotide (OCT), gonadotrophin-releasing hormone (GnRH), and epidermal growth factor (EGF) peptides (**Table 1.1**) have been investigated for delivering drugs to cancer cells. GnRH receptors are overexpressed in malignant tumor of ovarian, breast, prostate cancers as part of the paracrine/autocrine regulatory system of malignant tumors.[26-28] OCT and other somatostatin peptides bind to somatostatin receptors (STTRs) especially STTR2, which are upregulated in breast, cervical, colon, lung, ovarian cancers cells.[29] OCT peptide has a long half-life in systemic circulation with good tissue penetration due to its uptake by the STTR2 receptor. OCT has also been used for targeting radiotherapies.[28] PTX-OCT conjugate was designed to improve the biological properties of PTX and overcome the issue of cancer resistance. Ovarian cancer is treated with PTX, but normally through multiple sessions/doses, often causing the emergence of drug resistance.[30] Localization of OCT peptide after delivery has been monitored using FITC-labeled OCT peptide (FITC-OCT), injected into nude mice bearing a xenografted tumor. Localization of FITC-OCT on the xenografted tumor confirmed abnormally high levels of STTR2 receptor expression in tumors. PTX-OCT also suppressed tumor growth in mice xenografts better than in those treated with free PTX, OCT, and mixtures of PTX + OCT.[30] This result demonstrates the selectivity of PTX-OCT to tumor cells on the basis of high expression of STTR2. In addition, the conjugate downregulates the expression of multi drug resistance-1 (MDR1) protein.

GnRH or LHRH peptides effectively deliver anticancer drugs such as DOX and CPT to cancer cells.[31, 32] FITC-labeled GnRH analogues have been used to compare targeting efficiencies of GnRH-1, GnRH-2, and GnRH-3 peptides (**Table 1.1**) in human breast, colon, pancreas, and prostate cancer cells to that in the non-tumor cell line such as Madin-Darby canine kidney

epithelial (MDCK) cells. This study also revealed that human pharynx tumor cells similarly overexpress GnRH receptors on cell surfaces such as human breast, colon and prostate cancer cell lines. In contrast, pancreatic tumor cells (BxPC-3) do not present GnRH-1 receptors on their membranes.[28] As expected, GnRH peptides are internalized by tumor cells via active transport mechanisms. Although different cancer cell lines vary in their uptake properties for three different GnRH peptides, uptake by all tumor cells was significantly higher than in the control MDCK cell-line, thus indicating the role of GnRH receptor upregulation in tumor cells.

1.2.5 pH Low Insertion Peptide (pHLIP)

A pH low insertion peptide (pHLIP; **Table 1.1**) was developed as a pH-dependent cell-penetrating peptide for drug delivery[33]. pHLIP is a water-soluble membrane peptide that interacts weakly with cell membranes at neutral pH; however, when the cell surface is slightly acidic, the pHLIP peptide is inserted into the cell membranes as a stable transmembrane α-helix. Its primary sequence is characterized by acidic residues (*i.e.*, Asp or Glu) that can be protonated at the low extracellular pH observed in tumors. In testing the concept, six pHLIP derivatives were conjugated to monomethyl auristatin F (MMAF) to make pHLIP-MMAF conjugates and the MMAF is attached to the pHLIP C-terminus via a S-S bond that can be cleaved in the cytoplasm.[33] The efficacy of six pHLIP-MMAF conjugates was evaluated *in vitro* against cultured cancer cells to find the lead conjugate. *In vivo*, the lead conjugate showed significant therapeutic efficacy in mouse models without overt toxicities. pHLIP-MMAF was localized in cancer cells and inhibited the proliferation of cancer cells in a pH-selective and concentration-dependent manner.

1.2.6 MMP Peptides

Tumor cells have a high expression of MMPs (MMP-2 and MMP-9) that are important in tumor proliferation and metastasis.[34] One MMP-hexapeptide, PVGLIG, has a high binding affinity

to matrix metalloprotease-2 (MMP-2) enzyme. Conjugated to PTX at the C-terminus of the MMP peptide via an ester bond, PTX-MMP was found to deliver PTX in a tumor-specific manner.[35] Incubation of PTX-MMP with MMP2, as well as with cancer cells (*i.e.*, HT-1080 and U87MG), releases PTX from the conjugate. PTX release was higher in HT-1080 and U87MG cells compared to negative control cells (*i.e.*, Hep-2 and Hep G2), suggesting the involvement of MMPs in both cancer cells.[35] PTX-MMP shows significantly higher cytotoxicity in HT-1080 and U87MG cells compared to PTX alone, with no difference in toxicity between PTX-MMP and PTX on Hep-2 and Hep G2 cells, which have low expression of MMPs. Mice implanted with HT-1080 or U87MG cells have a higher survival rate when treated with PTX-MMP compared to those treated with PBS, PTX, and the MMP hexapeptide.[35] These results support a role for the peptide and MMP-2 in the activity of the PTX-MMP conjugate against tumor cells.

1.2.7 A Combination of Peptides

A combination of two peptides has been used to target drugs to certain cells. Angiopep (ANG) peptide has been used alone or in combination with other peptides (*i.e.*, TAT peptide) to deliver drugs to neuronal cells. ANG peptide (**Table 1.1**) was derived from the ligand of a low-density lipoprotein-related protein 1 (LRP1) receptor that is involved in the uptake and processing of amyloid precursor protein (APP) in the intracellular compartment inside endosomal vesicles.[36] LRP-1 has been shown to mediate transport of various ligands across the BBB.[37] To prove the concept, ANG peptide alone was conjugated to β-secretase inhibitor (SI) (*i.e.*, ANG-SI and ANG-PEG-SI; **Table 1.1**) for endosomal delivery of neuronal cells to inhibit the formation of amyloid-beta (Aβ).[36, 38] Neuroblastoma cells internalize ANG-SI conjugate better than SI peptide alone, suggesting that the uptake is through receptor-mediated endocytosis. Conjugation of ANG to SI peptide alters the recognition of the ANG peptide by LRP1 receptors because the uptake of ANG-

SI is unaffected in the absence of LRP1. This suggests the involvement of another receptor in the uptake of the conjugate.[36]

A combination of ANG and TAT peptides was used to deliver PTX as a conjugate (ANG-TAT-PTX) across the BBB, and this conjugate was developed to treat glioblastoma brain tumor.[37] ANG-TAT-PTX is expected to bind and be internalized by the LRP-1 receptor across the BBB. In previous studies, a conjugate of PTX with angiopep-2 and -3 (ANG1005) has been shown to cross the BBB and was investigated in clinical trials.[39, 40] The cellular uptake of ANG-TAT by U87 glioblastoma cells was higher than that of ANG alone.[37] It is interesting to find that, although ANG-TAT and TAT-ANG were both internalized by U87 glioblastoma cells, only ANG-TAT crossed the BBB.[37] The brain delivery studies were done using Biotin-ANG-TAT and this conjugate was detected in brain tumor tissue. Biotin-ANG-TAT has significantly higher deposition (1.8 times) than Biotin-ANG; in this case, the TAT peptide improved brain tumor uptake. ANG-TAT-PTX-treated mice with implanted U87 glioblastoma cells in the brain have better survival rate than diseased mice treated with ANG-PTX or PTX alone.[37] Therefore, TAT peptide is important in improving the conjugate brain delivery.

A combination of T10 and extracellular signal-regulated kinases (ERK) peptides (**Table 1.1**) was also used to deliver DOX molecule to breast cancer cells to overcome drug resistance.[41] T10 peptide binds to and can be internalized by transferrin receptor (Tfr), which is overexpressed in tumor cells. ERK peptide can prevent activation of ERK by inhibiting phosphorylation and its binding mitogen-activated protein kinase (MEK)**.** T10 peptide was conjugated to ERK peptide via a spacer (GGCG), and the thiol group on the Cys residue was linked to DOX to give T10-ERK-DOX conjugate. The DOX cellular uptake in MCF7/ADR cancer cells was increased when attached to the conjugate. The conjugate reversed the drug resistance by downregulating Pgp

expression and inhibiting ERK phosphorylation. Although T10-DOX delivered DOX to MCF7/ADR cancer cells and suppressed MCF7/ADR xenograft in nude mice, T10-ERK-DOX had better efficacy than T10-DOX in suppressing growth of MCF7/ADR tumor xenografts in nude mice.[42] This indicates that a combination of two peptides with different mechanisms improves the outcome of tumor suppression activity.

The concept of dual peptide targeting was also applied to PEGA peptide (**Table 1.1**) that binds a membrane-bound proline-specific aminopeptidase P (APaseP). APaseP is expressed approximately 100-fold higher in vasculature and malignant lesions in breast cancer than in normal tissues.[43] Thus, PEGA-TAT-TAMRA conjugate was used to evaluate cellular delivery and localization of the peptide in breast cancer cells.[43] The conjugate was internalized by cancer cells *in vitro* and *in vivo* in tumor xenografts. Although conjugation of PEGA to TAT resulted in reduced selectivity for PEGA to APaseP, the overall results of uptake and localization of the dual peptide conjugate showed selective delivery to breast cancer tissue.[43] Thus, this dual peptide has the potential to delivery cytotoxic drugs to tumor cells *in vivo*.

1.3 Peptide-Particle Conjugates for Drug Delivery

Nanoparticles are another emerging technology to improve drug delivery to a specific type of cells. One potential advantage of nanoparticles is that they can be used to store the drug and deliver it in a controlled-release fashion. The drug release can be coupled to the different redox conditions between the extra- and intra-cellular environments of the cell because of elevated concentrations of reductive substances in tumor cells, which differentiate them from normal cells.[44, 45] Certain types of nanoparticles are generated due to self-assembly and micelle formation of the components in water because of their low critical micelle concentration. The micelles normally have high drug encapsulation efficiency. One example is PEGylated chitosan-based glycolipid, which can form a

redox-responsive nanocarrier system called A54-PEG-CSO-ss-SA. The nanoparticles were studded with A54 peptide (**Table 1.1**) conjugated to a PEG moiety. The nanoparticles were loaded with DOX and directed to human hepatoma cells by A54 peptide.[46] The PEG moiety also serves to increase the *in vivo* half-life of nanoparticles by avoiding uptake by the reticuloendothelial (RES) system. *In vitro* and *in vivo* studies of nanoparticles show that DOX can be released via reduction of the disulfide bond depending on the amount of reductive substances in the tumor cells.[46]

Recently, some efforts have been shifted from targeting drugs to specific types of cells to targeting them to subcellular organelles (*e.g.*, the nucleus or mitochondria). In this case, the drug delivery systems are decorated with ligands that are specific for subcellular compartments, including nuclear localization signal (NLS) and the lipophilic triphenylphosphonium (TPP) cation. Both NLS and TPP can penetrate the nucleus because of their high affinity for nuclear pore complexes and can anchor to mitochondria via electrostatic interactions.[47, 48] Previously, drugs conjugated with NLS or TPP failed to reach the nucleus or mitochondria because the design of these conjugates was not favorable for entering cancer cells from the extracellular space.[49, 50] To overcome this problem, a (N-(2-hydroxypropyl) methacrylamide (HPMA) polymeric delivery system was conjugated to G3-C12 peptide (**Table 1.1**), a galectin-3-targeting ligand. The ligand was used for cellular uptake by cancer cells as well as subcellular mitochondria inside the cells.[51] An antibiotic KLA peptide (**Table 1.1**) was also conjugated to HMPA to give a G3-C12-HPMA-KLA delivery system. The *in vitro* studies showed increased receptor-mediated internalization into PC-3 cells with overexpressing galectin-3. Moreover, the specific binding between galectin-3 and the G3-C12 peptide directed HPMA-KLA conjugates to the mitochondria with enhanced cytotoxicity. An *in vivo* study revealed that the G3-C12 peptide significantly enhanced the tumor

accumulation of the polymer conjugate, exhibiting the best therapeutic efficacy and an improved survival rate in animals.[51]

Carboplatin has been used to treat ovarian cancer; however, the uptake of carboplatin by ovarian cancer cells becomes poor because of drug resistance upon multiple treatments of cancer cells. Thus, the poly(amidoamine)-*b*-poly(aspartic acid)-*b*-poly(ethylene glycol) (PAMAM-PAsp-PEG) system was designed to improve carboplatin delivery to ovarian cancer cells (OVCAR-3). The nanoparticles utilize RGD-2 peptide (**Table 1.1**) to direct them to OVCAR-3 cells that have overexpression of cell surface $\alpha_V\beta_3$ and $\alpha_V\beta_5$ integrin receptors. Carboplatin molecules were attached to the polymer via a coordination complex with two carboxylic acid on the poly-aspartic acid tethered to the polymer. The release of carboplatin was pH-dependent, and 88% of carboplatin was released from the polymer over 50 h at pH 5.5, while only 18% of carboplatin was released over 50 h at pH 7.4. To track the cellular uptake and localization of the polymer in OVCAR-3 cells, Cy5-dye was also connected to the particles via PEG linker.[52] The results showed that the particles containing RGD-2 peptide were efficiently internalized by the cells compared to particles without RGD-2 peptide. The targeted particles have significantly higher toxicity to the cells than carboplatin alone. It was proposed that carboplatin was occurring in the lysosome due to pH change and protonation of the carboxylic acid of the Asp residues.[52]

A new drug self-delivery system (DSDS) was designed as nanocarrier for delivering PTX; in this case, PTX was conjugated to octadecanol via a disulfide bond to produce PTX-ODN. The PTX-ODN can self-assemble to form nanoparticles, and Pep-1 (**Table 1.1**) recognized by overexpressed interleukin-13 receptor α2 (IL-13Rα2) was used to direct the particles to glioblastoma multiforme (GBM) and for crossing the BBB and blood-brain-tumor barrier.[53] In this case, the Pep-1-PEG-DSPE conjugate is used to incorporate Pep-1 on the DSDS. The PTX-loaded

nanoparticles were engulfed by IL-13Rα2 receptor-mediated endocytosis into glioblastoma cells and disintegrated in the endosomes to release PTX-ODN component.[53] The disulfide bond of PTX-ODN was reduced in the endosomes by glutathione to release PTX.[53] To follow the uptake and movement of the nanoparticles inside U87MG cells, the particles were labeled with coumarin-6 fluorophore. It was confirmed that the nanoparticles were internalized by U87MG cells in a receptor-mediated manner. *In vivo*, the nanoparticles can be detected in the U87MG glioma brain tumor grafted in nude mice.[53] Brain tumor mice treated with Pep-1-PTX-nanoparticles showed a higher survival population than those treated with vehicle, taxol, and PTX-octadecanol conjugate.[53]

Nanosize particles (PEG-EGFR-PTX) were constructed using branched PEG conjugated to PTX and an epidermal growth factor receptor (EGRF) peptide (**Table 1.1**). The nanoparticles were designed to improve PTX delivery to cancer cells with overexpressing EGFR.[18] The role of PEG was to increase drug water solubility and half-life of the particles. The abilities of PEG-EGFR-PTX, PTX-PEG, and PTX to inhibit cell growth were evaluated in squamous cell carcinoma of the head and neck (SCCHN) cell line. The results showed that the IC_{50}s of PEG-EGFR-PTX, PTX-PEG, and PTX were 21.74, 8.05, and 1.47 nM, respectively.[18] The lower activity of PEG-EGFR-PTX compared to PTX alone may be due to the less efficient uptake of the PEG-EGFR-PTX particles rather than to passive diffusion of PTX. Unfortunately, the toxicities of PEG-EGFR-PTX particles and PTX were not compared between EGFR overexpressing cancer cells and normal cells to prove particle targeting by EGFR peptide. Therefore, it is difficult to evaluate the usefulness of the particles in treating tumors *in vivo*.

A conjugate of peptide in nanobubbles (NBs) was designed to deliver small interfering RNA (siRNA) molecules, which have high specificity for the oncogenic mRNA in cancer cells. siRNA

molecules are known to have unfavorable physicochemical properties (size and anionic charges) for partitioning and crossing the cellular membranes to enter the intracellular space and exert their activity. To overcome this problem, Myc siRNA was conjugated to CPP (**Table 1.1**) to give CPP-Myc siRNA, which is encapsulated in ultrasound sensitive NBs. Ephrin peptide (YSA peptide, **Table 1.1**) was attached to the surface of NBs using 1,2-distearoyl-sn-glycero-3-phosphoethanolamine-N-methoxy-(polyethylene glycol) (DSPE-PEG) to give CPP-siRNA/YSA-NB.[54] YSA peptide selectively binds to overexpressed EphA 2 protein on the cell surface.[54] After cellular uptake, the CPP-Myc siRNA was released from NBs upon exposure to ultrasound that induced apoptosis of MCF-7 breast cancer cells *in vitro*. CPP-Myc siRNA/YSA-NB with ultrasound significantly suppressed tumor growth of MCF-7 xenografts in mice compared to without ultrasound.[54] The CPP-Myc siRNA/YSA-NB+ultrasound was significantly more effective than controls CPP-NC-siRNA/YSA-NB+ultrasound or CPP-siRNA alone, suggesting that YSA and ultrasound improved the efficacy of the CPP-Myc siRNA.

To reduce premature drug release, prodrug nanomedicine was developed to increase stability and solubility and to reduce injection of inactive carriers.[17] Clinical trials of prodrug carriers such as albumin-PTX have shown promise. When formulating prodrug nanomedicine, PEGylation of the drug is often used as carrier because PEGylation is non-toxic and non-immunogenic and can improve the half-life of the drug in circulation.[17] A cleavable linker between the drug and the carrier is also an essential component. The *cis*-asconitic anhydride-DOX (CAD) was conjugated to a PEG group via an amide bond to make a PEG-CAD prodrug. Then, the PEG-CAD prodrug was conjugated to RGD-3 peptide (**Table 1.1**), which selectively binds to neuropilin-1 (NRP-1) receptors. NRP-1 receptors have been shown to be overexpressed in tumor vessels as well as in many human cancer cell lines. The conjugation utilized a thiol-ene reaction to give an acid-labile

prodrug called PEG-CAD-RGD-3. Due to the amphiphilic nature of PEG-CAD-RGD-3, it assembled into nanoparticles in water. During *in vitro* and *in vivo* administration, the release of DOX was triggered in acidic pH, but was restricted in neutral pH environment. Compared to DOX alone, the presence of RGD-3 peptide improved nanomedicine endocytosis and cytotoxicity into tumor cells. In Balb/c mice, PEG-CAD-RGD-3 nanomedicine has shown prolonged accumulation of DOX in tumors.[17]

1.4 Peptide Modulation of Biological Barriers to Improve Drug Delivery

1.4.1 The Blood Brain Barrier (BBB) and the Intestinal Mucosa Barrier (IMB)

Biological barriers such as the intestinal mucosa barrier (IMB) and blood-brain barrier (BBB) are present to protect the body from infections entering into the systemic circulation and the central nervous systems (CNS), respectively.[55] IMB is composed of a single layer of epithelial cells at the luminal side of the gastrointestinal tract followed by the lamina propria and the *muscularis mucosae*. The BBB is comprised of the luminal and abluminal membranes of the brain capillary endothelium as the major route for molecules (drugs and diagnostic agents) to enter the brain.[56] The IMB and BBB function as selective filters to allow needed substances and nutrients to enter the systemic circulation or brain, respectively, while preventing unwanted substances such as toxins from crossing the barriers. The gastrointestinal tract, skin, kidney, and lung barriers are made up of epithelial cells while the BBB microvessels are composed of endothelial cells. The delivery of molecules through the IMB and BBB is normally via the transcellular and paracellular pathways. Passive diffusion of drugs through the transcellular pathway depends on physicochemical properties of the drugs, and the passive diffusion of these drugs is normally regulated by Lipinski's rules of five. In general, peptide and protein drugs cannot cross the transcellular pathways due to their size, hydrophilicity, and hydrogen bonding potential. However,

some hydrophilic small and large molecules (*e.g.*, peptides and proteins) can cross the biological barriers via the transcellular pathway using receptor-mediated transporters.

Alternatively, drug molecules could cross the IMB and BBB via the paracellular pathway, where molecules pass through the intercellular space between the cells.[57, 58] The paracellular space or intercellular junctions are connected by cell-cell adhesion proteins, forming a contiguous membrane connection.[59, 60] Therefore, there is a size limit for molecules to cross the paracellular pathway; normally, only ions and molecules with hydrodynamic radius <11 Å can cross this pathway.[61] This limitation is imposed by the tight junctions that are mediated by cell-cell adhesion proteins such as occludins, claudins, and junction adhesion molecules (JAMs), which act as a fence to prevent free diffusion of molecules **(Figure 1.1)**. Below the tight junctions there are adherens junctions (AJ), which are mediated by nectin and calcium-binding cadherins.[62] Beneath the adherens junctions lie the desmosomes, which are composed of desmoglein and desmocollin proteins; these proteins are also part of the cadherin family of cell-cell adhesion molecules with calcium-dependent binding properties.[63]

Modulation of the intercellular junctions of the IMB and BBB have shown promise in enhancing paracellular permeation of molecules. A hypertonic mannitol solution is used clinically to deliver anticancer drugs to treat terminally ill brain tumor patients.[64-66] This method is called osmotic delivery because the hypertonic solution shrinks the BBB vascular endothelial cells and modulates the intercellular junctions to increase their porosity. Various chemicals as specific and nonspecific junction modulators (*i.e.*, sodium caprate, sodium decanoate, oleic acid, ethyleneglycol-bis-(β-aminoethyl ether)-N, N′-tetraacetic acid (EGTA)) have successfully improved penetration of molecules through *in vitro* models of biological barrier.[61] Due to uncontrolled paracellular opening, many toxic and unwanted side effects were observed with some

of these methods. Thus, much research is focused on designing synthetic peptides that selectively modulate the protein-protein interactions in the intercellular junctions to improve paracellular permeation of delivered molecules.

1.4.2 Peptide Modulation of Tight Junction Proteins

One way to improve delivery of drug molecules via paracellular pathways of IMB and BBB is by modulating the interactions of cell-cell adhesion proteins in the intercellular junctions to increase the porosity of the paracellular pathways.[58, 67] Several peptides derived from occludins have been synthesized and evaluated for this purpose. Occludins are 60 kDa membrane proteins that are involved in maintaining tight junction integrity. They are composed of four transmembrane domains, three cytoplasmic domains, and two extracellular loops of approximately similar size. One of these extracellular loops contains more Tyr and Gly residues.[68] The OCC2 peptide derived from extracellular loop 2 has been shown to modulate the tight junctions of A6 cell monolayers; the peptide lowers the transepithelial electrical resistance (TEER) values of the monolayers.[69] OCC2 also enhances the penetration of paracellular markers such as inulin, dextran 3000, and dextran 40,000 across the A6 cell monolayers, indicating that the peptide increases paracellular porosity. $OP_{90\text{-}135}$ peptide (**Table 1.1**) derived from the first loop of occludin can lower the TEER values of Caco-2 cell monolayers, a model for IMB.[70] The peptide also enhanced the transport of a paracellular marker, ^{14}C-mannitol, across the Caco-2 cell. A smaller $OP_{90\text{-}103}$ peptide (**Table 1.1**) has better modulatory activity than the parent $OP_{90\text{-}135}$ in Caco-2 cell monolayers. In addition, Lip-$OP_{90\text{-}103}$ peptide (**Table 1.1**) that is an N-terminus lipid-alkylated peptide has about 11 times higher modulatory activity than the parent $OP_{90\text{-}103}$.

Besides the occludins, claudins (Cldn-1, -2, -3, and -4) are also responsible for forming tight junctions; claudins have a transmembrane structure similar to that of occludins.[59, 60, 68] They have

a short cytoplasmic N-terminus, two extracellular loops, and a C-terminal cytoplasmic domain. Both occludins and claudins interact via their C-terminus to zonula occludin-1 (ZO-1), ZO-2, and ZO-3 and stabilize the cytoskeleton membranes of the tight junctions. Knocking down the expression of Cldn-1, Cldn-4, occludin, and ZO-1 increases the paracellular permeation of molecules and ions across the cell monolayers.[60] This result confirms their importance in maintaining the tight junctions. A 29-amino acid C1C2 peptide derived from the extracellular loop-1 of claudin-1 can enhance the permeation of small and large paracellular markers (*i.e.*, Lucifer Yellow and FITC-Dextran 10 KDa) across the cell monolayers.[71] *In vivo*, the peptide increases the brain delivery of tetrodoxin and enkephalin peptides, suggesting that the peptide modulates the tight junctions of the BBB. The proposed mechanism of action of C1C2 peptide is via binding to claudins followed by induction of claudin endocytosis into the cytoplasmic domain.[72] Therefore, this internalization lowers the population of claudin in the tight junction to make the tight junctions looser.

1.4.3 Peptide Modulators of Adherens Junction Proteins

Peptides derived from the extracellular domain-1 (EC1) domain of E-cadherin (*i.e.*, HAV and ADT peptides) have been shown to modulate the intercellular junctions of MDCK and Caco-2 cell monolayers.[73, 74] It is proposed that these ADT and HAV peptides modulates the adherens junction in the intracellular junction to make the BBB porous by inhibiting the binding of E-cadherin mediated cell-cell adhesion **(Figure 1.2)** and it has been shown *in vivo* and *in vitro* experiments including bovine brain microvessel endothelial cells (BBMEC).[61, 75] HAV6 and/or ADTC5 peptides (**Table 1.1**) increase the *in vivo* brain delivery of molecules in mice and/or rats; the delivered molecules include paracellular markers (*i.e.*, ^{14}C-mannitol, 25 kDa IRdye800cw-polyethylene glycols or PEG), anticancer drugs (*i.e.*, ^{3}H daunomycin, Glu-CPT), efflux pump

substrates (*i.e.*, rhodamine 800 (R800), ^{3}H daunomycin), magnetic resonance imaging (MRI) enhancing agents (*i.e.*, gadopentetic acid or Gd-DTPA), peptides (*i.e.*, IRdye800cw-cLABL and cIBR) and proteins (*i.e.*, 65 kDa galbumin).[76-79] The brain depositions of radioactive molecules such as ^{14}C-mannitol and ^{3}H-daunomycin were detected and quantified in the brain homogenates using a radioactive counter, while the quantity of brain deposition of R800, IRdye800cw-PEG, and IRdye800cw-cLABL was determined in the intact isolated brain using near IR fluorescence imaging. MRI was used in living animals to detect the brain distribution of Gd-DTPA and galbumin. Finally, the amounts of brain delivered non-labeled Glu-CPT and cIBR peptide in rats were detected using LC-MS/MS. The duration of modulation of the *in vivo* BBB for small molecules was less than 1 h for HAV6 peptide and between 2 and 5 h for ADTC5 peptide.[77, 80] However, the duration of BBB modulation by HAV6 and ADTC5 was short for delivering a large molecule such as 65 kDa galbumin, less than 10 min for HAV6 and from 10–40 min for ADTC4 peptide.[78] The results suggest that the peptides create small pores in the intercellular junctions with a long-time duration compared to a short duration for large pores in the BBB intercellular junctions. The results also indicate that the BBB modulation is reversible.

The mechanism of action of HAV and ADT peptides is hypothesized via their binding to E-cadherin to inhibit cadherin-cadherin interactions in the intercellular junctions of the BBB **(Figure 1.2).** Using nuclear magnetic resonance spectroscopy (NMR) and molecular docking studies, the HAV and ADT peptides were shown to bind at different sites on the EC1 domain of E-cadherin.[81] It is proposed that the HAV6 peptide binds to the EC1 domain and inhibits the binding of the EC1 domain from one E-cadherin to the EC2 domain of another cadherin from the same membranes, which is the *cis*-cadherin interaction. In contrast, ADTC5 peptide binds to the EC1 domain to

prevent the *trans*-EC1 domain from swapping between two E-cadherins from opposite cell membranes or *trans*-cadherin interactions.

1.4.4 Other Peptide Modulators of Tight Junctions

Bocsik *et al*. have shown that C-CPE, AT-1002, PN-78, and PN-159 peptides (**Table 1.1**) could modulate the intercellular junctions of the IMB and BBB in cell culture models.[67] These peptides were not derived from the sequence of proteins form the intercellular junctions of the IMB and/or the BBB. C-CPE and AT-1002 peptides were respectively derived from *clostridium perfringens enterotoxin* (C-CPE) and zonula occludens *toxin* (Zot). Both peptides modulate the penetration of molecules through the paracellular pathways of IMB and BBB *in vitro* and/or *in vitro*.[67, 82] AT-1002 peptide enhances the oral absorption of low molecular weight heparin and calcitonin *in vivo*.[83] PN-78 and PN-159 peptides were discovered using phage display and they increased the paracellular permeation of molecules through the lung epithelial cell monolayer.[84] C-CPE, AT-1002, PN-78, and PN-159 modulate the intercellular junctions of Caco-2 cell and brain endothelial monolayers as models of IMB and BBB, respectively. This junction modulation was reflected in the lowering of *trans*-epithelial/endothelial electrical resistance (TEER) upon peptide treatment. The paracellular transport of fluorescein across the Caco-2 cell monolayers was enhance by C-CPE, AT-1002, PN-159 but not PN-78 peptides. However, all four peptides enhanced the penetration of albumin across the Caco-2 cell monolayers. The paracellular permeation of both fluorescein and albumin across the BBB cell monolayers was increased by AT-1002, PN-78, and PN-159 but not C-CPE. Thus, these peptides can be used to deliver drug molecules across the IMB and the BBB in *in vivo* studies.

1.5 Conclusion

Peptides have been successfully developed as drugs. Now, peptides have been extensively investigated to deliver drugs to specific cells to lower the side effects of the drugs. Similarly, conjugation of peptides to labeled molecules or atoms was shown to be useful for potential diagnostic agents to locate diseased cells within the body using various detection methods such as MRI and PET. Finally, delivery across the intestinal mucosa and the blood-brain barrier can also be enhanced by modulation of the protein-protein interactions in the intercellular junctions of these barriers using peptides. Modulation of the BBB using cadherin peptides can enhance the brain delivery of small-to-large molecules to the brains of living animals. Thus, modulation of the intercellular junctions can be exploited to deliver drug and diagnostic molecules through the IMB and BBB in the clinic in the future.

1.6. Thesis and Chapter Goals

1.6.1. Overall Goals of the Thesis

The overall goals of the thesis were to (a) deliver peptides and proteins to the brain by modulating the BBB using cadherin peptides, (b) develop analytical methods to quantify protein brain depositions, and (c) to design new cyclic peptides for improving BBB modulatory activities that are more successful than the current existing modulating peptides.

1.6.2. Chapter 2

The goal of this project was to show that cadherin peptides (ADT and HAV) can enhance the brain delivery of a large protein, 65 kDa galbumin, and different sized peptides (i.e., cIBR7, cLABL). The study showed that ADTC5 and HAV6 can enhance the brain delivery of galbumin, cIBR7, and cLABL peptides as detected by magnetic resonance imaging (MRI), mass spectrometry, and NIRF imaging methods, respectively. The results also indicated that the durations of the BBB opening for large molecules created by ADTC5 and HAV6 peptides were

short compared to that created by a small marker (e.g., R800 and Gd-DTPA). In addition, a LC-MS/MS method was developed and validated for the detection of a brain-delivered peptide, cIBR7, which could efficiently detect and quantify the amounts of peptide in the brain. Overall, this study found that ADTC5 and HAV6 can increase the brain delivery of different molecules by modulating the BBB in mouse and rat models. Finally, it was concluded that BBB modulation by cadherin peptides depends on (a) the type and dose of the modulator peptide, (b) the timing of delivery between the BBB modulator and the delivered molecule, and (c) the size of the delivered molecules.

1.6.3. Chapter 3

The goal of this project was to evaluate the modulatory activities of HAV6 and ADTC5 for brain delivery of different sizes of proteins such as 15 kDa lysozyme, 65 kDa albumin, 150 kDa IgG mAb, and 220 kDa fibronectin. A novel NIRF method was developed and validated to quantitatively determine the brain deposition of IRdye800CW-conjugated proteins (i.e., lysozyme, albumin, IgG mAb, and fibronectin). ADTC5 showed an improved delivery of lysozyme, albumin, and IgG mAb into the brains of C57BL/6 mice while HAV6 enhanced only the brain delivery of lysozyme. It was found that the cut-off limit for HAV6 peptide is 65 kDa, while ADTC5 can deliver molecules with the size of mAb, or less than 220 kDa. Furthermore, ADTC5 and HAV6 peptides could enhance depositions of delivered proteins in different organs (e.g., kidney and/or liver).

1.6.4. Chapter 4

The goal of this project was to design and synthesize novel cyclic peptides derived from ADTC5 and HAV6 sequences or a combination of them to improve their biological activity and plasma stability for use as BBB modulators. Linear and cyclic ADTHAV peptides were designed

and synthesized from the sequences of ADTC5 and HAV6 peptides using a N-to-C-terminal cyclization method. Cyclic HAVN1 and HAVN2 peptides were derived from the sequence of linear HAV6 peptide to achieve more stability and potency. The cyclic HAVN1 and HAVN2 peptides showed better activity than linear HAV6 peptide for enhancing IRdye-800CW Donkey anti-Goat IgG mAb brain delivery in C57BL/6 mice. Cyclic ADTHAV peptide has a better binding affinity to the EC1 domain of cadherin than ADTC5 peptide, as determined by surface plasmon resonance (SPR). Linear and cyclic ADTHAV peptides as well as ADTC5 peptide significantly enhanced the delivery of IgG mAb compared to control in C57BL/6 mice. It seemed that cyclic ADTHAV improved brain delivery of IgG mAb more than did linear ADTHAV ($p = 0.07$).

1.7 Figures and Legends

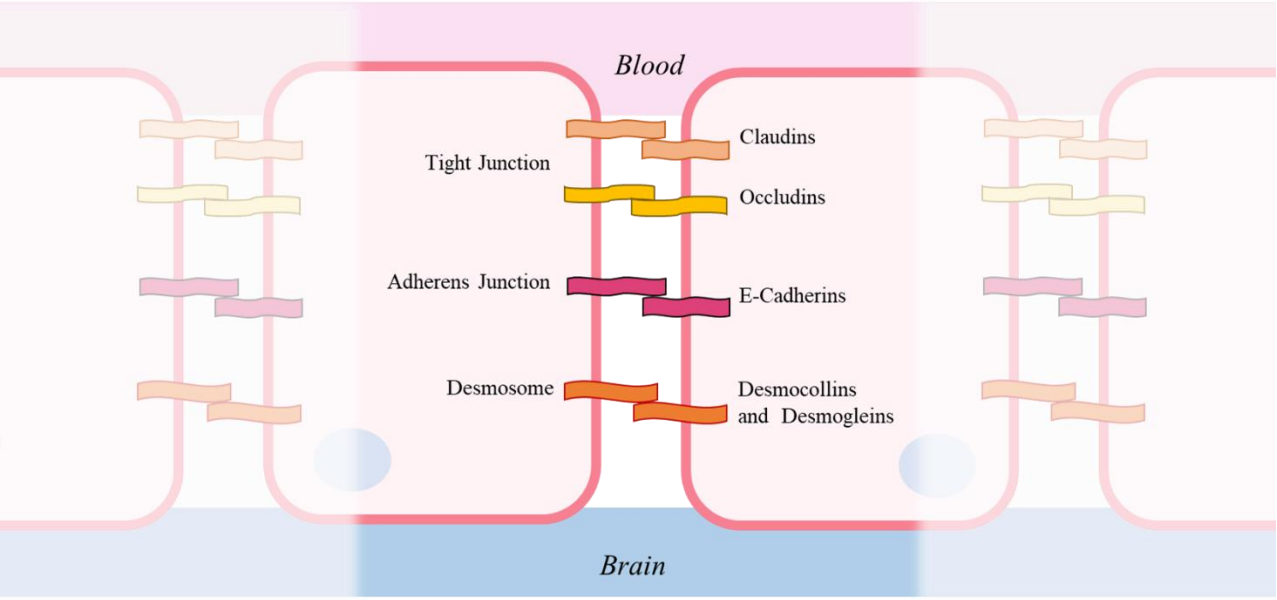

Figure 1.1 Schematic of cell adhesion proteins at intracellular junction in the blood-brain barrier (BBB). It consist of tight junction (TJ), adherens junction, and desmosomes. The TJ are mediated by occludins, claudins, junctional adhesion molecules (JAM), and zonula occludins-1, -2 and -3. Adherens junctions that are below the tight junctions are mediated by cadherins and nectins. Desmosomes are mediated by desmocollins and desmogleins.

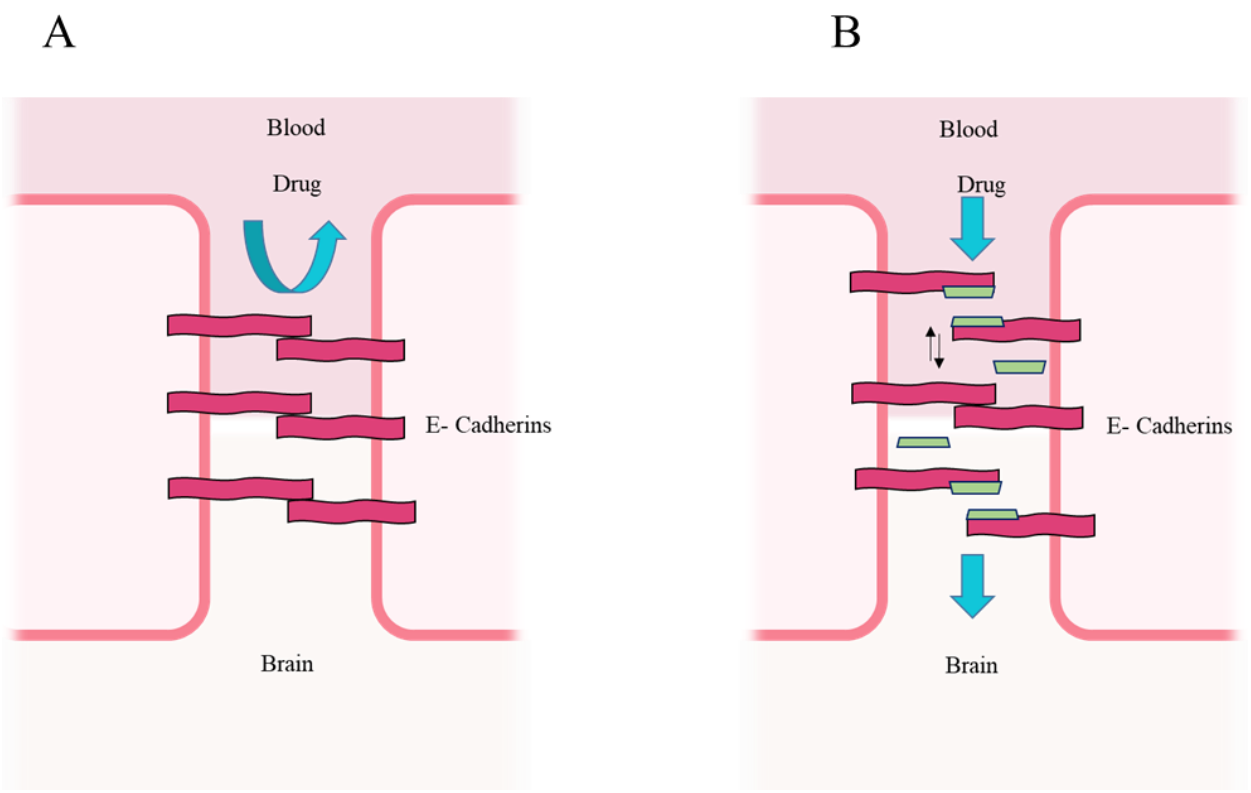

Figure 1.2 Schematic of the proposed modulation for the intracellular junction in the blood-brain barrier (BBB). (A) In normal condition, the E-cadherins are tightly attached together preventing the passage of drugs from the blood side to the brain side. (B) Once the peptide is in blood, these ADT or/and HAV peptides inhibit the cell-cell adhesion in an equilibrium and dynamic fashion to allow the drug to pass through the intracellular junction and reseal back to its original position after the clearance of the peptide.

1.8 References:

1. Kaspar, A. A.; Reichert, J. M. Future directions for peptide therapeutics development. *Drug Discov Today* **2013,** *18*, (17-18), 807-817.
2. Uhlig, T.; Kyprianou, T.; Martinelli, F. G.; Oppici, C. A.; Heiligers, D.; Hills, D.; Calvo, X. R.; Verhaert, P. The emergence of peptides in the pharmaceutical business: From exploration to exploitation. *EuPA Open Proteomics* **2014,** *4*, 58-69.
3. Fosgerau, K.; Hoffmann, T. Peptide therapeutics: current status and future directions. *Drug Discov Today* **2015,** *20*, (1), 122-8.
4. Bell, A. F.; Erickson, E. N.; Carter, C. S. Beyond labor: the role of natural and synthetic oxytocin in the transition to motherhood. *J Midwifery Womens Health* **2014,** *59*, (1), 35-42: quiz 108.
5. Tella, S. H.; Gallagher, J. C. Prevention and treatment of postmenopausal osteoporosis. *J Steroid Biochem Mol Biol* **2014,** *142*, 155-70.
6. Broder, M. S.; Beenhouwer, D.; Strosberg, J. R.; Neary, M. P.; Cherepanov, D. Gastrointestinal neuroendocrine tumors treated with high dose octreotide-LAR: a systematic literature review. *World J Gastroenterol* **2015,** *21*, (6), 1945-55.
7. Knop, F. K.; Bronden, A.; Vilsboll, T. Exenatide: pharmacokinetics, clinical use, and future directions. *Expert Opin Pharmacother* **2017,** *18*, (6), 555-571.
8. Ruoslahti, E.; Pierschbacher, M. D. New perspectives in cell adhesion: RGD and integrins. *Science* **1987,** *238*, (4826), 491-7.
9. Ruoslahti, E. Cell adhesion and tumor metastasis. *Princess Takamatsu Symp* **1994,** *24*, 99-105.
10. Dunehoo, A. L.; Anderson, M.; Majumdar, S.; Kobayashi, N.; Berkland, C.; Siahaan, T. J. Cell adhesion molecules for targeted drug delivery. *J Pharm Sci* **2006,** *95*, (9), 1856-72.

11. Mas-Moruno, C.; Rechenmacher, F.; Kessler, H. Cilengitide: the first anti-angiogenic small molecule drug candidate design, synthesis and clinical evaluation. *Anticancer Agents Med Chem* **2010,** *10*, (10), 753-68.

12. Yusuf-Makagiansar, H.; Anderson, M. E.; Yakovleva, T. V.; Murray, J. S.; Siahaan, T. J. Inhibition of LFA-1/ICAM-1 and VLA-4/VCAM-1 as a therapeutic approach to inflammation and autoimmune diseases. *Med Res Rev* **2002,** *22*, (2), 146-67.

13. Majumdar, S.; Anderson, M. E.; Xu, C. R.; Yakovleva, T. V.; Gu, L. C.; Malefyt, T. R.; Siahaan, T. J. Methotrexate (MTX)-cIBR conjugate for targeting MTX to leukocytes: conjugate stability and in vivo efficacy in suppressing rheumatoid arthritis. *J Pharm Sci* **2012,** *101*, (9), 3275-91.

14. Hamann, P. R.; Hinman, L. M.; Beyer, C. F.; Lindh, D.; Upeslacis, J.; Flowers, D. A.; Bernstein, I. An anti-CD33 antibody-calicheamicin conjugate for treatment of acute myeloid leukemia. Choice of linker. *Bioconjug Chem* **2002,** *13*, (1), 40-6.

15. Buyuktimkin, B.; Stewart Jr., J.; Tabanor, K.; Kiptoo, P.; Siahaan, T. J., Chapter 20: Protein and peptide conjugates for targeting therapeutics and diagnostics to specific cells. In *Drug Delivery: Principles and Applications*, 2nd ed.; Wang, B.; Hu, L.; Siahaan, T. J., Eds. Wiley: Hoboken, New Jersey, 2016; pp 475-497.

16. Leal, M.; Sapra, P.; Hurvitz, S. A.; Senter, P.; Wahl, A.; Schutten, M.; Shah, D. K.; Haddish-Berhane, N.; Kabbarah, O. Antibody-drug conjugates: an emerging modality for the treatment of cancer. *Annals of the New York Academy of Sciences* **2014,** *1321*, 41-54.

17. Song, H.; Zhang, J.; Wang, W.; Huang, P.; Zhang, Y.; Liu, J.; Li, C.; Kong, D. Acid-responsive PEGylated doxorubicin prodrug nanoparticles for neuropilin-1 receptor-mediated targeted drug delivery. *Colloids Surf B Biointerfaces* **2015,** *136*, 365-74.

18. Majumdar, D.; Rahman, M. A.; Chen, Z. G.; Shin, D. M. Anticancer activity of drug conjugates in head and neck cancer cells. *Front Biosci (Elite Ed)* **2016,** *8*, 358-69.

19. Haubner, R.; Weber, W. A.; Beer, A. J.; Vabuliene, E.; Reim, D.; Sarbia, M.; Becker, K. F.; Goebel, M.; Hein, R.; Wester, H. J.; Kessler, H.; Schwaiger, M. Noninvasive visualization of the activated alphavbeta3 integrin in cancer patients by positron emission tomography and [18F]Galacto-RGD. *PLoS Med* **2005,** *2*, (3), e70.

20. Beer, A. J.; Haubner, R.; Sarbia, M.; Goebel, M.; Luderschmidt, S.; Grosu, A. L.; Schnell, O.; Niemeyer, M.; Kessler, H.; Wester, H. J.; Weber, W. A.; Schwaiger, M. Positron emission tomography using [18F]Galacto-RGD identifies the level of integrin alpha(v)beta3 expression in man. *Clin Cancer Res* **2006,** *12*, (13), 3942-9.

21. Arap, W.; Pasqualini, R.; Ruoslahti, E. Cancer treatment by targeted drug delivery to tumor vasculature in a mouse model. *Science* **1998,** *279*, (5349), 377-80.

22. Chen, X.; Plasencia, C.; Hou, Y.; Neamati, N. Synthesis and biological evaluation of dimeric RGD peptide-paclitaxel conjugate as a model for integrin-targeted drug delivery. *J Med Chem* **2005,** *48*, (4), 1098-106.

23. Redko, B.; Tuchinsky, H.; Segal, T.; Tobi, D.; Luboshits, G.; Ashur-Fabian, O.; Pinhasov, A.; Gerlitz, G.; Gellerman, G. Toward the development of a novel non-RGD cyclic peptide drug conjugate for treatment of human metastatic melanoma. *Oncotarget* **2016,** 10.18632/oncotarget.12748.

24. Vives, E. Present and future of cell-penetrating peptide mediated delivery systems: "is the Trojan horse too wild to go only to Troy?". *Journal of controlled release : official journal of the Controlled Release Society* **2005,** *109*, (1-3), 77-85.

25. Zou, L.; Peng, Q.; Wang, P.; Zhou, B. Progress in Research and Application of HIV-1 TAT-Derived Cell-Penetrating Peptide. *J Membr Biol* **2017,** *250*, (2), 115-122.

26. Bajusz, S.; Janaky, T.; Csernus, V. J.; Bokser, L.; Fekete, M.; Srkalovic, G.; Redding, T. W.; Schally, A. V. Highly potent analogues of luteinizing hormone-releasing hormone containing D-phenylalanine nitrogen mustard in position 6. *Proc Natl Acad Sci U S A* **1989,** *86*, (16), 6318-22.

27. Limonta, P.; Moretti, R. M.; Montagnani Marelli, M.; Motta, M. The biology of gonadotropin hormone-releasing hormone: role in the control of tumor growth and progression in humans. *Front Neuroendocrinol* **2003,** *24*, (4), 279-95.

28. Muranyi, J.; Gyulavari, P.; Varga, A.; Bokonyi, G.; Tanai, H.; Vantus, T.; Pap, D.; Ludanyi, K.; Mezo, G.; Keri, G. Synthesis, characterization and systematic comparison of FITC-labelled GnRH-I, -II and -III analogues on various tumour cells. *J Pept Sci* **2016,** *22*, (8), 552-60.

29. Hejna, M.; Schmidinger, M.; Raderer, M. The clinical role of somatostatin analogues as antineoplastic agents: much ado about nothing? *Ann Oncol* **2002,** *13*, (5), 653-68.

30. Chen, X.; Zhang, X. Y.; Shen, Y.; Fan, L. L.; Ren, M. L.; Wu, Y. P. Synthetic paclitaxel-octreotide conjugate reversing the resistance of A2780/Taxol to paclitaxel in xenografted tumor in nude mice. *Oncotarget* **2016,** *7*, (50), 83451-83461.

31. Nagy, A.; Schally, A. V.; Armatis, P.; Szepeshazi, K.; Halmos, G.; Kovacs, M.; Zarandi, M.; Groot, K.; Miyazaki, M.; Jungwirth, A.; Horvath, J. Cytotoxic analogs of luteinizing hormone-releasing hormone containing doxorubicin or 2-pyrrolinodoxorubicin, a derivative 500-1000 times more potent. *Proc Natl Acad Sci U S A* **1996,** *93*, (14), 7269-73.

32. Dharap, S. S.; Qiu, B.; Williams, G. C.; Sinko, P.; Stein, S.; Minko, T. Molecular targeting of drug delivery systems to ovarian cancer by BH3 and LHRH peptides. *Journal of controlled release : official journal of the Controlled Release Society* **2003,** *91*, (1-2), 61-73.

33. Burns, K. E.; Hensley, H.; Robinson, M. K.; Thevenin, D. Therapeutic Efficacy of a Family of pHLIP-MMAF Conjugates in Cancer Cells and Mouse Models. *Mol Pharm* **2017,** 10.1021/acs.molpharmaceut.6b00847.

34. Paez Pereda, M.; Ledda, M. F.; Goldberg, V.; Chervin, A.; Carrizo, G.; Molina, H.; Muller, A.; Renner, U.; Podhajcer, O.; Arzt, E.; Stalla, G. K. High levels of matrix metalloproteinases regulate proliferation and hormone secretion in pituitary cells. *The Journal of clinical endocrinology and metabolism* **2000,** *85*, (1), 263-9.

35. Huang, C.; Yi, X.; Kong, D.; Chen, L.; Min, G. Controlled release strategy of paclitaxel by conjugating to matrix metalloproteinases-2 sensitive peptide. *Oncotarget; Vol 7, No 32* **2016**.

36. Kim, J. A.; Casalini, T.; Brambilla, D.; Leroux, J. C. Presumed LRP1-targeting transport peptide delivers beta-secretase inhibitor to neurons in vitro with limited efficiency. *Sci Rep* **2016,** *6*, 34297.

37. Li, Y.; Zheng, X.; Gong, M.; Zhang, J. Delivery of a peptide-drug conjugate targeting the blood brain barrier improved the efficacy of paclitaxel against glioma. *Oncotarget* **2016,** *7*, (48), 79401-79407.

38. Barve, A.; Jain, A.; Liu, H.; Jin, W.; Cheng, K. An enzyme-responsive conjugate improves the delivery of a PI3K inhibitor to prostate cancer. *Nanomedicine* **2016,** *12*, (8), 2373-2381.

39. Regina, A.; Demeule, M.; Che, C.; Lavallee, I.; Poirier, J.; Gabathuler, R.; Beliveau, R.; Castaigne, J. P. Antitumour activity of ANG1005, a conjugate between paclitaxel and the new brain delivery vector Angiopep-2. *Br J Pharmacol* **2008,** *155*, (2), 185-97.

40. Thomas, F. C.; Taskar, K.; Rudraraju, V.; Goda, S.; Thorsheim, H. R.; Gaasch, J. A.; Mittapalli, R. K.; Palmieri, D.; Steeg, P. S.; Lockman, P. R.; Smith, Q. R. Uptake of ANG1005, a novel paclitaxel derivative, through the blood-brain barrier into brain and experimental brain metastases of breast cancer. *Pharm Res* **2009,** *26*, (11), 2486-94.

41. Sheng, Y.; You, Y.; Chen, Y. Dual-targeting hybrid peptide-conjugated doxorubicin for drug resistance reversal in breast cancer. *Int J Pharm* **2016,** *512*, (1), 1-13.

42. Sheng, Y.; Xu, J.; You, Y.; Xu, F.; Chen, Y. Acid-Sensitive Peptide-Conjugated Doxorubicin Mediates the Lysosomal Pathway of Apoptosis and Reverses Drug Resistance in Breast Cancer. *Mol Pharm* **2015,** *12*, (7), 2217-28.

43. Cordova, A.; Woodrick, J.; Grindrod, S.; Zhang, L.; Saygideger-Kont, Y.; Wang, K.; DeVito, S.; Daniele, S. G.; Paige, M.; Brown, M. L. Aminopeptidase P Mediated Targeting for Breast Tissue Specific Conjugate Delivery. *Bioconjug Chem* **2016,** *27*, (9), 1981-90.

44. McEligot, A. J.; Yang, S.; Meyskens, F. L., Jr. Redox regulation by intrinsic species and extrinsic nutrients in normal and cancer cells. *Annual review of nutrition* **2005,** *25*, 261-95.

45. Jones, D. P. Redox sensing: orthogonal control in cell cycle and apoptosis signalling. *Journal of internal medicine* **2010,** *268*, (5), 432-48.

46. Liu, N.; Tan, Y.; Hu, Y.; Meng, T.; Wen, L.; Liu, J.; Cheng, B.; Yuan, H.; Huang, X.; Hu, F. A54 Peptide Modified and Redox-Responsive Glucolipid Conjugate Micelles for Intracellular Delivery of Doxorubicin in Hepatocarcinoma Therapy. *ACS Appl Mater Interfaces* **2016,** *8*, (48), 33148-33156.

47. Smith, R. A. J.; Porteous, C. M.; Gane, A. M.; Murphy, M. P. Delivery of bioactive molecules to mitochondria in vivo. *Proceedings of the National Academy of Sciences* **2003,** *100*, (9), 5407-5412.

48. Kang, B.; Mackey, M. A.; El-Sayed, M. A. Nuclear Targeting of Gold Nanoparticles in Cancer Cells Induces DNA Damage, Causing Cytokinesis Arrest and Apoptosis. *Journal of the American Chemical Society* **2010,** *132*, (5), 1517-1519.

49. Jensen, K. D.; Nori, A.; Tijerina, M.; Kopeckova, P.; Kopecek, J. Cytoplasmic delivery and nuclear targeting of synthetic macromolecules. *Journal of controlled release : official journal of the Controlled Release Society* **2003,** *87*, (1-3), 89-105.

50. Callahan, J.; Kopecek, J. Semitelechelic HPMA copolymers functionalized with triphenylphosphonium as drug carriers for membrane transduction and mitochondrial localization. *Biomacromolecules* **2006,** *7*, (8), 2347-56.

51. Sun, W.; Li, L.; Yang, Q. Q.; Zhang, Z. R.; Huang, Y. Two birds, one stone: dual targeting of the cancer cell surface and subcellular mitochondria by the galectin-3-binding peptide G3-C12. *Acta pharmacologica Sinica* **2017,** 10.1038/aps.2016.137.

52. Wang, Y.; Wang, L.; Chen, G.; Gong, S. Carboplatin-Complexed and cRGD-Conjugated Unimolecular Nanoparticles for Targeted Ovarian Cancer Therapy. *Macromol Biosci* **2016,** 10.1002/mabi.201600292.

53. Jiang, Y.; Wang, X.; Liu, X.; Lv, W.; Zhang, H.; Zhang, M.; Li, X.; Xin, H.; Xu, Q. Enhanced Antiglioma Efficacy of Ultrahigh Loading Capacity Paclitaxel Prodrug Conjugate Self-Assembled Targeted Nanoparticles. *ACS Appl Mater Interfaces* **2017,** *9*, (1), 211-217.

54. Xie, X.; Yang, Y.; Lin, W.; Liu, H.; Liu, H.; Yang, Y.; Chen, Y.; Fu, X.; Deng, J. Cell-penetrating peptide-siRNA conjugate loaded YSA-modified nanobubbles for ultrasound triggered siRNA delivery. *Colloids Surf B Biointerfaces* **2015,** *136*, 641-50.

55. Deli, M. A. Potential use of tight junction modulators to reversibly open membranous barriers and improve drug delivery. *Biochimica Et Biophysica Acta-Biomembranes* **2009,** *1788*, (4), 892-910.

56. Pardridge, W. M. Drug transport across the blood-brain barrier. *Journal of Cerebral Blood Flow and Metabolism* **2012,** *32*, (11), 1959-1972.

57. O'Donnell, M. J.; Maddrell, S. H. Paracellular and transcellular routes for water and solute movements across insect epithelia. *J Exp Biol* **1983,** *106*, 231-53.

58. Laksitorini, M.; Prasasty, V. D.; Kiptoo, P. K.; Siahaan, T. J. Pathways and progress in improving drug delivery through the intestinal mucosa and blood-brain barriers. *Ther Deliv* **2014,** *5*, (10), 1143-63.

59. Anderson, J. M.; Van Itallie, C. M. Physiology and function of the tight junction. *Cold Spring Harb Perspect Biol* **2009,** *1*, (2), a002584.

60. Van Itallie, C. M.; Anderson, J. M. Architecture of tight junctions and principles of molecular composition. *Semin Cell Dev Biol* **2014,** *36*, 157-65.

61. Lutz, K. L.; Siahaan, T. J. Molecular structure of the apical junction complex and its contribution to the paracellular barrier. *J Pharm Sci* **1997,** *86*, (9), 977-84.

62. Zheng, K.; Trivedi, M.; Siahaan, T. J. Structure and function of the intercellular junctions: barrier of paracellular drug delivery. *Curr Pharm Des* **2006,** *12*, (22), 2813-24.

63. Garrod, D.; Chidgey, M. Desmosome structure, composition and function. *Biochim Biophys Acta* **2008,** *1778*, (3), 572-87.

64. Neuwelt, E. A.; Maravilla, K. R.; Frenkel, E. P.; Rapaport, S. I.; Hill, S. A.; Barnett, P. A. Osmotic blood-brain barrier disruption. Computerized tomographic monitoring of chemotherapeutic agent delivery. *The Journal of clinical investigation* **1979,** *64*, (2), 684-8.

65. Neuwelt, E. A.; Hill, S. A.; Frenkel, E. P. Osmotic blood-brain barrier modification and combination chemotherapy: concurrent tumor regression in areas of barrier opening and progression in brain regions distant to barrier opening. *Neurosurgery* **1984,** *15*, (3), 362-6.

66. Neuwelt, E. A.; Specht, H. D.; Barnett, P. A.; Dahlborg, S. A.; Miley, A.; Larson, S. M.; Brown, P.; Eckerman, K. F.; Hellstrom, K. E.; Hellstrom, I. Increased delivery of tumor-specific monoclonal antibodies to brain after osmotic blood-brain barrier modification in patients with melanoma metastatic to the central nervous system. *Neurosurgery* **1987,** *20*, (6), 885-95.

67. Bocsik, A.; Walter, F. R.; Gyebrovszki, A.; Fulop, L.; Blasig, I.; Dabrowski, S.; Otvos, F.; Toth, A.; Rakhely, G.; Veszelka, S.; Vastag, M.; Szabo-Revesz, P.; Deli, M. A. Reversible Opening of Intercellular Junctions of Intestinal Epithelial and Brain Endothelial Cells With Tight Junction Modulator Peptides. *J Pharm Sci* **2016,** *105*, (2), 754-65.

68. Gonzalez-Mariscal, L.; Betanzos, A.; Nava, P.; Jaramillo, B. E. Tight junction proteins. *Progress in biophysics and molecular biology* **2003,** *81*, (1), 1–44.

69. Wong, V.; Gumbiner, B. M. A synthetic peptide corresponding to the extracellular domain of occludin perturbs the tight junction permeability barrier. *Journal of Cell Biology* **1997,** *136*, (2), 399-409.

70. Tavelin, S.; Hashimoto, K.; Malkinson, J.; Lazorova, L.; Toth, I.; Artursson, P. A new principle for tight junction modulation based on occludin peptides. *Mol Pharmacol* **2003,** *64*, (6), 1530-40.

71. Zwanziger, D.; Hackel, D.; Staat, C.; Bocker, A.; Brack, A.; Beyermann, M.; Rittner, H.; Blasig, I. E. A peptidomimetic tight junction modulator to improve regional analgesia. *Mol Pharm* **2012,** *9*, (6), 1785-94.

72. Staat, C.; Coisne, C.; Dabrowski, S.; Stamatovic, S. M.; Andjelkovic, A. V.; Wolburg, H.; Engelhardt, B.; Blasig, I. E. Mode of action of claudin peptidomimetics in the transient opening of cellular tight junction barriers. *Biomaterials* **2015,** *54*, 9-20.

73. Yusuf-Makagiansar, H.; Makagiansar, I. T.; Hu, Y.; Siahaan, T. J. Synergistic inhibitory activity of alpha- and beta-LFA-1 peptides on LFA-1/ICAM-1 interaction. *Peptides* **2001,** *22*, (12), 1955-62.

74. Sinaga, E.; Jois, S. D.; Avery, M.; Makagiansar, I. T.; Tambunan, U. S.; Audus, K. L.; Siahaan, T. J. Increasing paracellular porosity by E-cadherin peptides: discovery of bulge and groove regions in the EC1-domain of E-cadherin. *Pharm Res* **2002,** *19*, (8), 1170-9.

75. Pal, D.; Audus, K. L.; Siahaan, T. J. Modulation of cellular adhesion in bovine brain microvessel endothelial cells by a decapeptide. *Brain Res* **1997,** *747*, (1), 103-13.

76. Kiptoo, P.; Sinaga, E.; Calcagno, A. M.; Zhao, H.; Kobayashi, N.; Tambunan, U. S.; Siahaan, T. J. Enhancement of drug absorption through the blood-brain barrier and inhibition of intercellular tight junction resealing by E-cadherin peptides. *Mol Pharm* **2011,** *8*, (1), 239-49.

77. On, N. H.; Kiptoo, P.; Siahaan, T. J.; Miller, D. W. Modulation of blood-brain barrier permeability in mice using synthetic E-cadherin peptide. *Mol Pharm* **2014,** *11*, (3), 974-81.

78. Ulapane, K. R. O., N.; Kiptoo, P.; Williams, T. D.; Miller, D. W.; Siahaa, T. J. Improving brain delivery of biomolecules via BBB Modulation in Mouse and Rat: Detection using MRI, NIRF, and Mass Spectrometry. *Nanotheranostics* **2017,** *1*, (1), In Press.

79. Alaofi, A.; On, N.; Kiptoo, P.; Williams, T. D.; Miller, D. W.; Siahaan, T. J. Comparison of Linear and Cyclic His-Ala-Val Peptides in Modulating the Blood-Brain Barrier

Permeability: Impact on Delivery of Molecules to the Brain. *J Pharm Sci* **2016,** *105*, (2), 797-807.

80. Laksitorini, M. D.; Kiptoo, P. K.; On, N. H.; Thliveris, J. A.; Miller, D. W.; Siahaan, T. J. Modulation of intercellular junctions by cyclic-ADT peptides as a method to reversibly increase blood-brain barrier permeability. *J Pharm Sci* **2015,** *104*, (3), 1065-75.
81. Alaofi, A.; Farokhi, E.; Prasasty, V. D.; Anbanandam, A.; Kuczera, K.; Siahaan, T. J. Probing the interaction between cHAVc3 peptide and the EC1 domain of E-cadherin using NMR and molecular dynamics simulations. *J Biomol Struct Dyn* **2017,** *35*, (1), 92-104.
82. Sonoda, N.; Furuse, M.; Sasaki, H.; Yonemura, S.; Katahira, J.; Horiguchi, Y.; Tsukita, S. Clostridium perfringens enterotoxin fragment removes specific claudins from tight junction strands: Evidence for direct involvement of claudins in tight junction barrier. *J Cell Biol* **1999,** *147*, (1), 195-204.
83. Motlekar, N. A.; Fasano, A.; Wachtel, M. S.; Youan, B. B. Zonula occludens toxin synthetic peptide derivative AT1002 enhances in vitro and in vivo intestinal absorption of low molecular weight heparin. *J Drug Target* **2006,** *14*, (5), 321-9.
84. Herman, R. E.; Makienko, E. G.; Prieve, M. G.; Fuller, M.; Houston, M. E., Jr.; Johnson, P. H. Phage display screening of epithelial cell monolayers treated with EGTA: identification of peptide FDFWITP that modulates tight junction activity. *J Biomol Screen* **2007,** *12*, (8), 1092-101.

CHAPTER 2

Improving Brain Delivery of Biomolecules via BBB Modulation in Mouse and Rat: Detection using MRI, NIRF, and Mass Spectrometry

2.1. Introduction

There is an urgent need to develop new and alternative methods to deliver molecules to the brain for diagnosis and treatment of brain diseases (*i.e.*, Parkinson's, Alzheimer's, multiple sclerosis, brain tumors).[1, 2] Furthermore, approaches that can safely deliver molecules to the brain can also provide opportunities to probe brain functions at the cellular and molecular levels using selected imaging and cellular signaling molecules. The protective function of the BBB selectively restricts molecules from entering the brain; however, under pathological conditions, the BBB can also restrict the accumulation of drugs to the brain. Numerous invasive methods have been developed to directly deliver or sample molecules to or from the brain, respectively; these methods include (a) brain microdialysis,[3], (b) intracerebral implantation,[4] and (c) intraventricular delivery.[5] However, these methods can be problematic for patients, and these invasive approaches can cause damage in the surrounding brain tissues. Alternatively, various non-invasive approaches have been developed to improve brain delivery of molecules, including the use of (a) prodrug technology, (b) efflux pump inhibitors, (c) receptor-mediated transport, (d) osmotic agents, and (e) BBB modulators; however, in general, the success of these methods has been limited.[1, 2, 6, 7]

One way to deliver drug and diagnostic molecules to the brain is via the transcellular pathway, allowing the molecule to diffuse through the membranes of the BBB endothelial cells. Traditionally, changing the physicochemical properties of the drug was done to improve its brain delivery via the transcellular pathway. However, changing the drug structure may alter its biological activity. As an alternative, several prodrug methods have been developed to transiently change the physicochemical properties of the drug, permitting greater transcellular BBB penetration.[1] Although the physicochemical properties of the drug can be changed to improve its membrane partition for transcellular passive diffusion, the presence of efflux pumps on the BBB

can prevent the drug molecule from crossing the BBB cell membranes. Inhibitors have been designed to block the activity of efflux pumps in allowing the drug to cross the BBB.[1] Receptor-mediated transcytosis has also been explored for improving brain delivery of molecules. For example, the high expression of transferrin receptors on the luminal side of brain capillary endothelial cells has been exploited as a carrier of drugs/macromolecules across the BBB, and has shown promise in pre-clinical animal models.[2, 8]

Table 2.1. Peptide Names and Peptide Sequences

Peptide	Sequence	Peptide Origin
HAV6	Ac-SHAVSS-NH_2	EC1 of E-cadherin
HAV4	Ac-SHAVAS-NH_2	Ala5 mutant of HAV6
cHAVc3	Cyclo(1,6)Ac-CSHAVC-NH_2	EC1 of E-cadherin
ADTC5	Cyclo(1,7)Ac-CDTPPVC-NH_2	EC1 of E-cadherin
cLABL	Cyclo(1,12)PenITDGEATDSGC	I-domain of LFA-1
cIBR7	Cyclo(1,8)CPRGGSVC	D1 of ICAM-1
IS	Cyclo(1,8)CPRGGSIC	Ile7 mutant of cIBR7

An alternative approach to deliver molecules across the BBB is via the paracellular pathway by increasing the porosity of the intercellular junctions. Under normal conditions, the penetration of molecules through this pathway is limited by the presence of the tight intercellular junctions. Therefore, modulation of these junctions is needed to improve paracellular passive diffusion of molecules. One successful method for enhancing paracellular delivery across the BBB that has been used in the clinic to deliver anticancer drugs to brain tumor patients is hyperosmotic agents

such as mannitol. In this case, administration of osmotic agents is used to produce a hypertonic environment within the brain vasculature, causing shrinkage of endothelial cells of the BBB and allowing opening of the tight junctions for molecules to cross via paracellular pathways.[9] The positive results from the osmotic method have stimulated investigation of other methods to transiently modulate the integrity of the BBB to enhance molecule delivery via the paracellular pathway. Several molecules have been developed to modulate the intercellular junctions of the BBB, including bradykinin derivatives and inhibitors of cell-cell adhesion proteins (*i.e.*, occludins, claudins, cadherins).[10-13]

Our group have designed and utilized cadherin peptides called HAV (His-Ala-Val)[14] and ADT (Ala-Asp-Thr)[15] peptides derived from the extracellular domain-1 (EC1) of E-cadherin (**Table 2.1.**) to modulate the intercellular junctions of the BBB and improve paracellular penetration of functional biomolecules (*i.e.*, peptides and proteins). Previously, HAV and ADT peptides have been shown to enhance the *in vivo* brain delivery of small-to-large marker molecules (*e.g.*, ^{14}C-mannitol, gadopentetic acid, and 25 kDa polyethylene glycols (PEG)) in mice and rats.[16-20] However, the utility of HAV and ADT peptides in enhancing *in vivo* brain delivery of proteins and peptides has not yet been evaluated. Thus, the aim of this work was to evaluate the ability of cadherin peptides to enhance brain delivery of galbumin, IRdye800cw-cLABL peptide, and unlabeled cIBR7 peptide.

In this study, four different cadherin peptides (HAV4, HAV6, cHAVc3, ADTC5) were evaluated in their effectiveness for delivering a large protein, galbumin, a gadolinium-labeled albumin magnetic resonance imaging contrast agent, into the brains of Balb/c mice. Both the extent and duration of BBB modulation by HAV6 or ADTC5 peptides was evaluated. Galbumin is a gadolinium-labeled albumin that can be detected using magnetic resonance imaging (MRI) due to

the increase in T_1 relaxation rate ($1/T_1$) to produce a positive image contrast in the brain.[21] Due to its physicochemical properties (*i.e.*, size, hydrogen binding potential, and hydrophilicity), galbumin cannot cross the BBB via the transcellular or paracellular pathways. Therefore, it is a good model molecule to test the activity of cadherin peptides to enhance brain delivery of protein via the paracellular pathway due to the increase in BBB paracellular porosity.

Secondly, the brain delivery of IRdye800cw-cLABL peptide was accomplished using ADTC5 peptide in Balb/c mice. cLABL peptide was derived from the I-domain sequence of lymphocyte function-associated antigen-1 (LFA-1) receptors found on the surface of T cells. The cLABL peptide binds to and is internalized by intercellular adhesion molecule-1 (ICAM-1) on the surface of vascular endothelial and immune cells.[22, 23] Because ICAM-1 is upregulated during inflammation, the hypothesis is that labeled cLABL peptide can be used to detect changes in ICAM-1 expression in the brain during neuroinflammation. In this study, the brain deposition of cLABL was quantified using near-infrared fluorescence (NIRF) imaging. Although this peptide is smaller than galbumin, it has unfavorable physiochemical properties for crossing the BBB via the transcellular and paracellular pathways, thus, it is also a good model of peptide delivery to the brain.

Finally, this study was carried out to evaluate the brain delivery of unlabeled cIBR7 peptide using ADTC5 peptide in Sprague-Dawley rats. The aim is to develop a method to extract and detect the unlabeled cIBR7 peptide in the brain to confirm our findings using labeled molecules. Sprague-Dawley rats were used to evaluate the applicability of ADTC5 peptide to enhance delivery of molecules into rat brains *in vivo* because ADTC5 has not been used in rat model previously. cIBR7 peptide was derived from ICAM-1 sequence and it binds to the I-domain of LFA-1 receptor on immune cells (*i.e.*, T cells); therefore, brain delivery of cIBR7 peptide can

detect the presence of immune cells in the brain during the neuroinflammation process.[24-26] Most of our studies to deliver molecules to the brain have been carried out using labeled molecules, and their brain deposition was detected using radioactivity, NIRF imaging, and magnetic resonance imaging (MRI). One possible caveat of using labeled molecules is that the labeled molecule may degrade during delivery. Thus, the detected quantity of the molecule may be due to a combination of the intact molecule and its degraded fragments containing the label. Therefore, unlabeled cIBR7 peptide was delivered using ADTC5 peptide, and brain depositions of cIBR7 and ADTC5 peptides were quantified using tandem mass spectrometry (LC-MS/MS).

2.2 Materials and Methods

2.2.1 Chemicals, Reagents, and Animals

Ketamine hydrochloride and xylazine were purchased from MWI Veterinary Supply Co. (Boise, ID) and Lloyd Inc. (Shenandoah, IA), respectively. IRdye800cw-NHS ester was purchased from LiCOR Inc. (Lincoln, NE). Amino acids for peptide synthesis were purchased from Protein Technologies Inc. (Tucson, AZ). Galbumin was purchased from BioPal Inc. (Worcester, MA). All other reagents and chemicals were purchased from Sigma Aldrich Chemical Company (St. Louis, MO). All protocols involving the use of animals were approved by the Institutional Animal Care and Use Committee (IACUC) at The University of Kansas or the University of Manitoba. The animals were maintained in the Animal Care Unit with free access to food and water.

2.2.2 Peptide Synthesis and Purification

The synthesis of peptides (**Table 2.1**) was accomplished using a solid-phase peptide synthesizer. After peptide cleavage from the resin using TFA, the crude peptides were precipitated in cold diethyl ether. In most cases, the crude precipitate showed high concentration of the desired peptide. After purification with semi-preparative HPLC, the isolated peptides had high purity

(>96%) as determined by analytical HPLC with a C18 column. The formation of a disulfide bond in the cyclic peptide (*i.e.*, cIBR7, ADTC5, cHAVc3, IS) was accomplished by stirring the precursor linear peptide in bicarbonate buffer solution under air oxidation at pH 9.0 in high dilution. The cyclization reaction produced primarily the desired monomer with minor oligomer side-products; the monomer was isolated from the mixture using semi-preparative HPLC. Because cIBR7, IS, and ADTC5 peptides were quantified in the brain by mass spectrometry, their exact mass data are presented in **Table 2.2**.

Table 2.2. Mass Spectrometry Identification of ADTC5, cIBR7 and IS

Peptide	Exact Mass (g/mol)	Accurate Mass (g/mol)	Mass Error (ppm)
ADTC5	772.293	772.298	6.5
cIBR7	775.315	775.316	1.3
IS	789.331	789.336	6.3

To synthesize IRdye800cw-cLABL, cLABL peptide (0.86 mg, 0.71 μmol, MW = 1197.2 g/mol) and IRdye800cw-NHS ester (5.0 mg, 4.2 μmol, MW = 1166.2 g/mol with 3 Na^+) were mixed in 1.0 mL of 0.5 M potassium phosphate buffer at pH 8.5 followed by stirring overnight in the dark. The reaction progress was monitored by analytical HPLC with a C18 column. After the reaction was completed, IRdye800cw-cLABL (MW = 2248.4 with 3 Na^+ and 2182.4 without Na^+ ions) was purified using HPLC with a C18 semi-preparative column. The identity of the pure product was determined using mass spectrometry to give 2182.69 amu for IRdye800cw-cLABL without Na^+ ions.

2.2.3 In Vivo Delivery of Galbumin in Balb/c Mice and Quantification using MRI

The effects of cadherin peptides (*i.e.*, HAV4, HAV6, ADTC5, cHAVc3) to enhance brain delivery of 65 kDa galbumin were determined in Balb/c mice. A Bruker Biospect MR spectrometer equipped with 7 tesla/21 cm magnets and 2.5 × 2.5 cm^2 field of view was used to quantify brain depositions of galbumin. After anesthesia, Balb/c mice were placed in the MRI magnet followed by simultaneous delivery of galbumin (0.6 μmol/kg) with the peptide (0.010 mmol/kg). The brain was scanned with a series of T1- and T2-weighted images before initial delivery of galbumin to determine the brain background images and structural coordinates.[17] Every 3 minutes, T1-weighted images of the brain were collected for up to 51 min following the injection of galbumin with peptide. The galbumin brain deposition was determined using the intensity of the contrast agent from manually outlined regions of interest (ROI) within the coronal brain slices using Marevisi 3.5 software (Institute for Biodiagnostics, National Research Council, Ottawa, Ontario, Canada). Paravision 3.0 software package was used to quantify the increase in image intensity of galbumin in the brain using the following formula for percent change:

[(Post-Gd-DTPA T1-weighted images – Pre-Gd-DTPA T1-weighted images) ÷ Pre-Gd-DTPA T1-weighted images] × 100.

2.2.4 In Vivo Delivery of IRdyeR800cw-cLABL into the Brains of Balb/c Mice and NIRF Detection

The effect of ADTC5 in enhancing BBB penetration of IRdyeR800cw-cLABL in Balb/c mice was quantified using NIRF imaging as described previously.[17] Briefly, IRdye800cw-cLABL (10 μg/mouse) along with ADTC5 (0.01 mmol/kg) was delivered into Balb/c mice via tail vein injection. After 20 min, the mice were sacrificed, followed by cardiac perfusion with 10% formaldehyde solution.[17] The brains were removed and 1-mm coronal slices prepared for *ex vivo*

quantitative analysis using an Odyssey NIRF imaging system (Licor, Lincoln, NE). The depositions of IRdyeR800cw-cLABL peptide in the brain were quantified by integrating the fluorescence intensities at the ROI. The integrated fluorescence intensities were normalized to the fluorescence from the blood sample at the same time point. The data were presented as the relative fluorescence units/mm^3 of tissue divided by relative fluorescence units/μL blood.

2.2.5 In vivo Delivery of cIBR7 into the Rat Brain and LC-MS/MS Detection

ADTC5 peptide was used to deliver cIBR7 in male Sprague–Dawley rats (300–400 g). Rats were anaesthetized with a combination of ketamine (100 mg/kg) and xylazine (5 mg/kg) delivered intraperitoneally. A heat lamp was used to maintain the animal's body temperature during the experiment. The jugular vein of the rat was cannulated with a polyethylene catheter (PE 50) containing heparinized saline (100 IU/mL) through which cIBR7 (40 mg/kg) and ADTC5 (30 mg/kg) were administered over 10 min. Then, the rats were sacrificed and a heart-cut was performed followed by perfusion of the brain with saline to remove leftover peptide in the microvessels of endothelial cells of the BBB. The whole brain tissue was isolated and rinsed with saline followed by storage at –80 °C. In the meantime, blood was collected in tubes containing anticoagulants and centrifuged at 12000 rpm for 10 min. Plasma was obtained and stored at –80 °C until further processing. Control studies were done following the same procedure but with the administration of only cIBR7 (without ADTC5). Samples were extracted and analyzed using LC-MS/MS.

2.2.6 Capillary Depletion Method

Parallel capillary depletion experiments were performed as described by Triguero *et al*.[27] to ensure that there is no trapping of the delivered molecules in the microvessel endothelial cells. Brain homogenates from rat brains dosed with cIBR7 and ADTC5 were mixed together and divided into two sets. One set of homogenates (580 µL) was extracted using the optimized extraction procedure (see below). The other set of brain homogenates was extracted after capillary depletion was performed to remove cerebral vasculature contaminants. In this method, 580 µL of 26% dextran solution was added to 580 µL of brain homogenate with IS. The mixture was centrifuged at 5,400 *g* for 15 min, and the supernatant was extracted with 1 mL acetonitrile using the optimized extraction procedure described below.

2.3 LC-MS/MS Method Development and Peptide Extraction and Detection Procedures

Instrumentation and Chromatographic Conditions for Quantitative LCMS/MS Analysis.

The LC-MS/MS system consisted of an Acquity UPLC system (Waters Corp., Milford, MA) coupled to an electrospray (ESI) ion source and a Quattro Ultima triple quadrupole mass analyzer (Micromass Ltd., Manchester, UK). Separation was performed at room temperature on a Luna UPLC C_{18} (2.1 mm × 50 mm, 5 µm particle size, 100 Å; Phenomenex, Inc., Torrance, CA) using a binary gradient mobile phase consisting of solvents (A) H_2O:formic acid (99.92:0.08) and (B) acetonitrile:formic acid (99.92:0.08). The gradient was carried out as follows: 1% B (initial–0.5 min), 1–7% B (3.5 min), 7–18% B (1 min), 18–50% B (1 min), 50–80% B (1 min), 80% B (2 min), 80–100% B (1 min) and 100% B (1 min). A 20-µL sample was injected into the mobile phase flowing at a rate of 0.350 mL/min. Mass spectrometric analysis was conducted in positive ion mode using multiple reaction monitoring (MRM). Nitrogen was used as the desolvation gas and argon gas was used for collision-induced dissociation (CID). Cone voltages for the analytes and

collision energies were set at 35–55 V and 35–120 V, respectively. MRM chromatograms were quantified using MassLynx v 4.1 software (Micromass) for the integration of relevant peak areas.

Preparation of Stock, Standard, and IS Solutions.

ADTC5, cIBR7, and internal standard (IS) were dissolved in nanopure water to prepare (1 mg/mL) stock solutions, which were stored at –20 °C and later diluted for the required working standard solutions. Calibrations of standard brain homogenate samples were prepared as follows. The working standard solutions (10 µL) and IS (10 µL, target concentration of 200 ng/mL) were spiked into 580 µL of blank brain homogenates from untreated rats. These were recovered using the extraction procedure given below to yield a linear range from 50 to 500 ng/mL (50, 100, 175, 250, 350, 500 ng/ml) for the calibration curves. Quality control (QC) samples were prepared in the same way.

Sample Preparation.

Extraction of peptides from brain tissue: The whole brain was homogenized with 0.25% acetic acid using a PowerGen 700 tissue homogenizer. 590 µL aliquots of rat brain homogenate were spiked with 10 µL of IS (target concentration, 200 ng/mL). The homogenate was vortexed for 1 min followed by addition of 1 mL acetonitrile; the mixture was then vigorously vortexed again for 1 min followed by centrifugation at 12000 rpm. The supernatant was isolated, transferred to a clean tube, and evaporated to dryness using a Savant SpeedVac concentrator. The dry extract was reconstituted in 100 µL of water, vortexed for 30 s, and centrifuged for 10 min at 12000 rpm to remove residual precipitated proteins.

Extraction of peptides from plasma: 100 µL of rat plasma was spiked with 10 µL of IS (target concentration 200 ng/mL). The mixture was vortexed for 1 min followed by addition of 250 µL of

acetonitrile. The mixture was vigorously vortexed again for 1 min, followed by centrifugation at 12000 rpm. The supernatant was isolated, transferred to a clean tube, and evaporated to dryness using a Savant SpeedVac concentrator. The dry extract was reconstituted in 100 μL of water, vortexed for 30 s, and centrifuged for 10 min at 12000 rpm to remove residual precipitated proteins.

Extraction Recovery.

Recovery and matrix effects of cIBR7 and ADTC5 were tested in the spiked rat brain homogenates at three concentrations 50, 250 and 500 ng/mL. Extraction recovery of cIBR7 and ADTC5 from brain tissue homogenate was determined by the ratios of peak areas in the post-extraction spiked samples and in pre-extraction spiked samples.

Accuracy, Precision, and Stability.

The intra-day as well as inter-day accuracy and precision were calculated by analyzing replicates of spiked brain homogenates at three concentrations 50, 250 and 500 ng/mL. The stability of the cIBR7 and ADTC5 peptides in spiked brain homogenates was evaluated under different temperature and storage conditions. Three sets of samples were subjected to (a) room temperature for 10 h, (b) −20 °C for 24 h followed by unassisted thawing at room temperature, and (c) three freeze-thaw cycles between −20 °C and room temperature over a 24-h period. The total chromatogram time for one sample was 11 min, and the total duration for a set of samples for the experiment per day was less than 8 h. All stability studies were conducted using 50, 250, and 500 ng/mL of cIBR7 and ADTC5 with three determinations for each concentration of peptide.

2.3.1 Statistical Analysis

For brain delivery of peptides and galbumin, the differences in the brains treated with or without BBB modulators were compared using ANOVA with Student–Newman–Keuls for determining the statistical significance. A *p*-value of less than 0.05 was used as a criterion for statistical significance.

2.4 Results

2.4.1 In Vivo Brain Delivery of Galbumin in Balb/c Mice as Detected by MRI

The activity of cadherin peptides (*i.e.*, HAV6, HAV4, cHAVc3, and ADTC5) to enhance the brain delivery of galbumin into the brain of Balb/c mice was evaluated. The HAV6, cHAVc3, and ADTC5 treatment groups showed a significant increase in the brain deposition of galbumin in the posterior, midbrain, anterior regions compared to those of vehicle (**Figures 2.1A–D**). The enhanced brain delivery of galbumin was observed as early as 3 min after the i.v. injection (**Figures 2.1B–D**). In contrast, the HAV4 treatment group did not show an enhancement of galbumin brain deposition. From the AUC (**Figure 2.1D**), the levels galbumin enhancement were in the following order: posterior > midbrain > anterior.

To evaluate the duration of BBB opening for large macromolecules, galbumin was delivered 10 or 40 min after administration of HAV6 and ADTC5 peptides in a pretreatment experiment. Time-dependent galbumin brain depositions are shown in Figures **2.2A–D** for 10-min pretreatment and in **Figures 2.2A** and **2.2E–G** for 40-min pretreatment. The galbumin AUCs were also shown on immediate as well as 10- and 40-min pretreatment experiments (**Figure 2.3**). As previously shown, immediate delivery of galbumin with the HAV6 or ADTC5 peptide produced significant enhancements of galbumin brain deposition in all brain regions. After 10-min pretreatment with ADTC5, that there was still significant enhancement of brain deposition of galbumin while no

enhancement was observed with HAV6 pretreatment. Using 40-min pretreatment, there was no observed galbumin enhancement produced by ADTC5 or HAV6.

2.4.2 In Vivo Brain Delivery of R800cw-cLABL in Balb/c Mice as Detected by NIRF Imaging

The brain delivery of a 12-amino acid peptide, IRdye800cw-cLABL (MW = 2182.4 g/mol), was accomplished via i.v. administration in the presence and absence of ADTC5 (**Figure 2.4**). Twenty minutes after i.v. administration, the mice were sacrificed. NIRF imaging was used to detect peptide brain deposition. The labeled cLABL peptide delivered with ADTC5 has qualitatively higher brain fluorescence than that without ADTC5 (**Figures 2.4A–B**). Quantitatively, the brain-to-plasma ratio was used to determine the effect of ADTC5; the brain deposition of cLABL with ADTC5 was about 3.5-fold higher than that without ADTC5 (**Figure 2.4C**, bottom panel).

2.4.3 LC-MS/MS Method Development for Quantification of cIBR7 in Rat Brain

For calculating the amounts of peptides in the rat brains, liquid chromatography and tandem mass spectroscopy conditions were optimized to achieve the best separation and quantification of cIBR7, ADTC5, and the IS peptides in the rat brain extracts. The standard solution for each peptide was infused into the mobile phase using a syringe; the dominant peaks were observed with mass-to-charge ratios of m/z 776.5, 773.5, and 395.9 for cIBR7, ADTC5, and IS, respectively. MRM was used for each precursor ion to produce three respective transitions, including m/z 776.5 → m/z 70.2 for cIBR7; m/z 773.5 → m/z 294.1 for ADTC5 and m/z 395.9 → m/z 86 for IS using optimized collision energies of 120 V, 35 V, and 35 V, respectively.

2.4.4 Validation of Mass Spectrometric Method

Selectivity.

Selectivity of the method was evaluated by analyzing chromatograms of blank brain homogenate samples and blank brain homogenates spiked with cIBR7, ADTC5, and IS. The results showed no endogenous interferences at the retention times of the three analytes (**Figure 2.5**). The retention times for cIBR7, IS, and ADTC5 were 2.88 min, 3.80 min, and 6.10 min, respectively.

Linearity, Accuracy, and Precision.

Calibration curves for cIBR7 and ADTC5 were prepared in concentrations ranging from 50 to 500 ng/mL to determine the lowest limit of detection (LLOD) and intra-day and inter-day accuracy and precision (**Table 2.3.**). In this case, the peak area ratios of cIBR7-to-IS and ADTC5-to-IS were plotted separately. Good linearity was observed for both cIBR7 and ADTC5 with $R^2 \geq 0.99$. The LLOD for cIBR7 and ADTC5 were 15 ng/mL and 10 ng/mL, respectively. Intra-day and inter-day accuracy and precision were determined by analyzing samples at three concentration levels for %RSD and %RE (**Table 2.3.**). The %RSD and %RE values were less than 15% for intra-day and inter-day for both analytes.

Table 2.3. Precision and Accuracy for cIBR7 and ADTC5 (n=3)

Analytes	**Concentration (ng/mL)**	**Intra-day**		**Inter-day**	
		%RSD	**%RE**	**%RSD**	**%RE**
cIBR7	50	10.1	14.1	9.6	11.2
	250	9.9	4.1	9.1	–1.9
	500	8.5	2.3	6.4	3.3
ADTC5	50	7.4	6.6	12.4	3.7
	250	14.6	–3.3	6.7	2.1
	500	10.5	2.5	7.1	4.2

Stability and Extraction Recovery.

The potential instability of cIBR7 and ADTC5 during the experiments was determined in three different peptide concentrations, temperatures, and storage conditions (**Table 2.4.**). The variability of each peptide in the brain extract was calculated to be less than 15% (%RSD) (**Table 2.4.**). The extraction recoveries of cIBR7 and ADTC5 from the brain homogenates were calculated by comparing the extracted and spiked samples. At three concentrations, the calculated mean recoveries for cIBR7 and ADTC5 were 90% and 92%, respectively (**Table 2.5.**).

Table 2.4. Stability of cIBR7 and ADTC5 in brain extract (n=3)

Analyte	**Concentration (ng/mL)**	**%RSD**		
		Room Temp.	**–20 °C**	**Three freeze thaw cycles**
cIBR7	50	7.79	13.54	9.72
	250	9.48	1.90	5.72
	500	8.73	8.96	6.34
ADTC5	50	12.18	9.18	13.12
	250	10.61	0.45	11.01
	500	6.95	7.16	8.97

Table 2.5. Extraction recovery of cIBR7 and ADTC5 from rat brain homogenate		
Analytes	**Concentration (ng/mL)**	**Extraction Recovery (%)**
cIBR7	50	89
	250	90
	500	92
ADTC5	50	90
	250	92
	500	94

2.4.5 In Vivo Brain Delivery of cIBR7 in Sprague-Dawley Rats

The brain delivery of cIBR7 was evaluated in Sprague-Dawley rats following bolus i.v. injection of cIBR7 either alone or in combination with the cadherin peptide ADTC5. The amount of cIBR7 in the brain in the presence of ADTC5 was significantly higher (approximately four times) than that without ADTC5 (p = 0.013, **Figure 2.6**). In the presence of ADTC5, the average total amount of cIBR7 was 855 ± 171 ng/g brain while it was 213 ± 53 ng/g brain in the absence of ADTC5. Brain accumulation of cIBR7 was also determined in brain homogenates following capillary depletion to remove any cIBR7 within the brain vasculature. In this case, the ratios of cIBR7-to-IS without and with vasculature depletion were 0.133 and 0.128, respectively. This suggests that there is no difference between the two methods.

2.5. Discussion

The delivery of peptides and proteins including antibodies (MW~150 kDa) or Fab-fragment of antibodies (MW~50 kDa) into the brain for diagnosis and treatment of brain diseases had been a topic of great interest. However, success in delivering them to the brain has been very limited because they have physicochemical properties (*e.g.*, size, hydrogen-bonding potential, and conformation) that prevent them from partitioning into cell membranes to cross the BBB.[1] There is clearly a need to develop methods to deliver peptides and proteins into the brain. The ability to deliver functional peptides and proteins, including antibodies, into the brains of normal and diseased animals (*i.e.*, mice and rats) would provide advantages in treating various brain pathologies and studying brain functions at the cellular level. Previously, cadherin peptides have been shown to improve *in vivo* delivery of small-to-large marker molecules, including 25 kDa IRdye-800cw PEG, into the brains of mice and/or rats.[16-18, 20] In *in vivo* Balb/c mice, HAV6 peptide also enhances the delivery of IRdye-800cw PEG in the lung, kidney, and small intestine.[17] It should be noted that the PEG molecule has physicochemical properties different from those of peptides and proteins in that they have a variety of functional groups as well as secondary or tertiary structures.

The first aim was to determine brain delivery of a large protein, 65 kDa galbumin, using several known cadherin peptides (*i.e.*, HAV6, HAV4, cHAVc3, or ADTC5) in Balb/c mice. Galbumin is a conjugate between albumin and Gd-complex; thus, it can be detected and quantified in the brains of living animals using MRI. Compared to vehicle control, ADTC5, HAV6, and cHAVc3 peptides significantly enhanced the delivery of galbumin into all three regions of the brain (*i.e.*, posterior, midbrain, and anterior). The enhancement was immediate— within 3 min after administration of the modulator peptide with galbumin (**Figure 2.1B–D**). Our hypothesis is that cadherin peptides

open the intercellular junctions to create small, medium, and large pores in the paracellular pathways of the BBB as soon as the peptide is injected.[18] It is interesting to find that HAV4 did not enhance galbumin brain delivery (**Figure 2.1D**); however, HAV4 did enhance brain delivery of Gd-DTPA.[20] This suggests that HAV4 creates small pores but is unable to create the large pores in the intercellular junctions of the BBB required for delivery of macromolecules to the brain. Overall, ADTC5, HAV6, and cHAVc3 can effectively enhance the brain delivery of a protein as large as 65 kDa in Balb/c mice.

The duration of the BBB opening created by HAV6 and ADTC5 peptides to allow large molecules to enter the brain is an important parameter for avoiding unwanted side effects of this method. The opening of BBB paracellular pathways for brain delivery should be tightly controlled to avoid BBB permeation of unwanted large molecules and immune cells (*e.g.*, macrophages, T cells, and B cells) entering the brain. Therefore, the time-dependent effect of pretreatment using HAV6 or ADTC5 on the BBB permeation of galbumin was investigated. As expected, immediate treatment with HAV6 or ADTC5 peptide along with galbumin showed enhanced brain deposition of galbumin (**Figure 2.3A**). In contrast, ADTC5 but not HAV6 enhanced the brain delivery of galbumin when a 10-min peptide pretreatment experiment was conducted (**Figure 2.3B**). This indicates that the duration of the BBB opening provided by HAV6 peptide for a large molecule is less than 10 min and shorter than that produced by ADTC5. In contrast, the BBB opening for a large molecule by ADTC5 lasts longer than 10 min. After 40-min pretreatment, there was no enhancement of galbumin deposition in the brain by either peptide. This suggests that the duration of BBB opening for ADTC5 was longer than 10 min but shorter than 40 min. Overall, for both HAV6 and ADTC5, the BBB opening for large molecular weight molecules was reversible and short.

In previous studies, HAV6, HAV4, cHAVc3, and ADTC5 peptides significantly enhanced the brain delivery of a small molecular weight vasculature marker, Gd-DTPA (MW = 547.575 g/mol), in a dose-dependent manner.[17, 18, 20] To determine the duration of BBB opening created by cadherin peptides for a small molecule, pretreatment studies were carried out using Gd-DTPA and detected by MRI. Following a 1-h pretreatment with peptide, linear HAV6 and HAV4 peptides did not aid the penetration of Gd-DTPA through the BBB, suggesting that the BBB opening created by these linear peptides lasts less than 1 h. In contrast, cyclic ADTC5 and cHAVc3 peptides create a BBB opening for Gd-DTPA delivery of more than 2 h but less than 4 h.[18, 20] Therefore, cyclic ADTC5 and cHAVc3 peptides created a longer lasting BBB opening than did linear HAV6 and HAV4 peptides. The data suggest that both HAV6 and ADTC5 peptides create a longer duration of BBB opening for a small molecule (*i.e.,* Gd-DTPA) than a large molecule (*i.e.,* galbumin). To explain the observations in the pretreatment studies, it is proposed that cadherin peptides modulate the BBB by immediately creating small, medium, and large pores in the intercellular junctions. However, the large pores quickly collapse to medium and small pores and, finally, the medium pores collapse to small pores in the intercellular junctions of the BBB.

To evaluate brain delivery of peptides, a 12-amino acid residue peptide, IRdye800cw-cLABL peptide, was delivered with ADTC5 in Balb/c mice. The peptide brain deposition was detected using NIRF imaging, which has an advantage in its ease of quantifying the molecule. The administration of ADTC5 peptide significantly enhanced brain delivery of cLABL peptide compared to control. The data suggest that the mechanism of transport of cLABL peptide was via passive diffusion through the paracellular pathway of the BBB. Although cLABL peptide could bind to and be internalized by ICAM-1 on the surface of BBB endothelial microvessels, the brain deposition of this peptide when delivered with vehicle was very low, suggesting that ICAM-1

receptor-mediated endocytosis was not involved (**Figure 2.4**). cLABL peptide was selected because it binds to ICAM-1 protein on the surface of epithelial, endothelial, and immune cells. ICAM-1 is upregulated during inflammation;[22, 23] thus, it can be used as a target protein for labeled cLABL to detect upregulation of ICAM-1 during neuroinflammation. cLABL peptide is derived from the binding region of the I-domain of LFA-1 to the domain-1 (D1) of ICAM-1.[28] It binds to ICAM-1 and inhibits LFA-1/ICAM-1-mediated T-cell adhesion to epithelial cells.[29] In addition, it is also internalized by ICAM-1 in activated Molt-3 T cells.[23]

The final aim is to develop a method to detect and quantify an intact peptide in the brain without the use of any radioactive, MRI, or NIRF label. cIBR7 peptide was selected for brain delivery using ADTC5 peptide in Sprague-Dawley rats; ADTC5 has not been evaluated in modulating the BBB of in rats *in vivo*. Previously, ADTC5 peptide was shown to enhance brain delivery of ^{14}C-mannitol in an *in situ* rat brain perfusion model.[18]. In addition, HAV6 peptide has been shown to enhance brain delivery of an MRI contrast agent, Gd-DTPA, in *in situ* brain perfusion and *in vivo* in Sprague-Dawley rats.[16] These results suggest that ADTC5 could also enhance the brain delivery of cIBR in rats. To detect the brain deposition of cIBR7, an extraction as well as a sensitive and selective LC-MS/MS method were developed to detect and quantify the delivered peptide in the rat brain. cIBR7 peptide was delivered in the presence of ADTC5 or control by injection via the jugular vein. After 10 min, the rat was sacrificed and the BBB was perfused with saline to remove potential residual peptides in the vascular endothelial cells to ensure accurate measurement of the analyte concentration in the brain. ADTC5 significantly enhanced the brain delivery of unlabeled cIBR7 peptide by as much as 4-fold (**Figure 2.6**, $p = 0.013$), and 855 ± 171 or 213 ± 53 ng/g brain of cIBR7 was detected when delivered using ADTC5 or vehicle, respectively. In summary, this study showed that ADTC5 enhanced the brain delivery of intact cIBR7 in Sprague-Dawley rats,

and that the extraction and LC-MS/MS detection methods were sensitive to quantified cIBR7 brain deposition.

cIBR7 peptide was selected because it binds to LFA-1 receptors on the surface of T cells and inhibits T-cell adhesion to Caco-2 cell monolayers.[25] cIBR7 is a smaller analog of the parent cIBR peptide, which is derived from the D1 of ICAM-1. cIBR peptide has been shown to bind to the I-domain of LFA-1 receptor.[25, 26, 30] cIBR7 and cIBR peptides can be internalized by LFA-1 into the cytoplasmic domain of immune cells (*i.e.*, T cells, H-60 leukemic cells);[24, 31] therefore, labeled cIBR and cIBR7 peptides have the potential to detect LFA-1-expressing immune cells in the brain.

It is interesting to find that the ADTC5 peptide was also detected in a lower amount (about 23 ng/g brain) than cIBR7 (855 ng/g brain) in the brain although they were administered at almost similar dosage levels (*i.e.*, 40 mg/kg cIBR7 and 30 mg/kg ADTC5). There are several potential reasons for this difference. First, ADTC5 could bind to cadherins in the adherens junctions of the BBB to lower the amount of free ADTC5 that would be available to penetrate the BBB. The half-lives ($t_{1/2}$) of plasma stabilities of ADTC5 and cIBR7 were 5.7 h and 2.8 h, respectively, suggesting that the low amount of ADTC5 in the brain was not due to its instability in plasma. Another alternative explanation is that cIBR7 and ADTC5 have vastly different pharmacokinetic and pharmacodynamic profiles; thus, further studies are needed to understand the difference in their brain depositions.

This study developed and validated an extraction as well as a sensitive LC-MS/MS method to quantify the intact cIBR7, ADTC5, and IS in rat brains after *in vivo* studies. The results showed that cIBR7 peptide could be detected confidently as an intact molecule in the brain. The optimized extraction was very efficient, and it recovered higher than 90% of the intact cIBR7 and ADTC5 peptides from the brain (**Table 2.5.**). The recoveries of cIBR7 and ADTC5 peptides from the brain

were accomplished by optimizing the homogenization medium, composition of extraction solvent, and the reconstitution solvent mixture. In addition, this study also confirmed our previous observation on brain delivery of labeled molecules (*i.e.*, radioactive, IRdye, and Gd-DTPA). It also suggests that the detected labeled molecules could reasonably represent the intact molecules in the brain and are not due to detection of the label or molecular fragments of the parent molecules.

IS peptide was designed as a reference molecule for the LC-MS/MS analysis to maximize the precision of peptide quantification in the brain and it has similar physicochemical properties as cIBR7 peptide. It was also used to account for errors and losses during sample handling and ionization during LC-MS/MS experiments. IS peptide was designed to have physicochemical properties similar to those of cIBR7 peptide. In this case, the Val6 residue in cIBR7 peptide was replaced with the Ile6 residue, and this simple change in IS provided a longer retention time (3.8 min) for IS compared to cIBR7 peptide (2.88 min) in the C18 column of LC-MS/MS (**Figure 2.5**). The ADTC5 peptide was eluted at 6.10 min, which is 3.8 min later than IS peptide; therefore, all three peptides were well separated in the column. All three peptides (cIBR7, IS, ADTC5) were readily water soluble and, thus, no other additives or co-solvents were need for peptide reconstitution during the study.

To improve the sensitivity of analyte detection, mass spectrometry (MS) parameters were initially optimized using a direct infusion of each analyte to the instrument, and the MRM of several stable transitions were optimized for each analyte. The best transition with the highest intensity was selected for each analyte. Then, the method validations for QC samples were carried out to determine selectivity, linearity, accuracy, precision, sensitivity, and stability over a range of concentrations in the calibration curve at 50–500 ng/mL following FDA guidelines.[32] The results showed that the LC-MS/MS method was selective for all three analytes with no interferences. A

good linearity was achieved over a concentration range of 50–500 ng/mL for cIBR7 and ADTC5. Intra-day and inter-day precision and accuracy variability for both cIBR7 and ADTC5 were less than 15% (R.S.D and R.E) (**Table 2.3.**), suggesting that the MS method is accurate and precise. Variability (%R.S.D) for stability for both peptides was less than 15%, suggesting that the analytes are stable in brain extract under different conditions. Thus, the developed LC-MS/MS method was very sensitive and reliable for detecting the amount of delivered peptides in the brain.

The hypothesis for the mechanism of action of cadherin peptides is that they bind in equilibrium fashion to the extracellular domain of E-cadherins to inhibit E-cadherin homophilic physical interactions (*i.e.*, *trans* and/or *cis* interactions) among cadherins in the intercellular junctions in an equilibrium fashion.[33] The physical nature of this inhibition is not expected to change the expression of E-cadherin on the cell surface. Incubation of MDCK cell monolayers (2–4 h) with HAV6 peptide increased the total expression of E-cadherin in response to peptide modulation of the intercellular junction.[14] However, it is still not clear whether the same phenomenon occurs in the BBB. Although E-cadherin is found on the epithelial cells and VE-cadherin (cadherin-5) is found in the peripheral vascular endothelium,[34] we found that proteins from bovine brain microvessel endothelial cells (BBMEC) react only with anti-E-cadherin antibody and not with anti-cadherin-5 and anti-N-cadherin.[35] Abbruscato and Davis indicated that BBMEC monolayers also expressed E-cadherin.[36] Vorbrodt *et al*. showed VE-cadherin in the rat endothelial BBB and a weak reaction with anti-E-cadherin;[37] however, Vorbordt *et al.*[38] and Rubin *et al.*[34] suggested that VE-cadherin might not be associated with BBB function. Fluorescence-labeled HAV decapeptide and anti-E-cadherin mAb can bind to the intercellular junctions of the BBMEC monolayers as punctate structures as observed by fluorescence microscopy.[35] This labeled HAV peptide can also bind to single cells of BBMEC as detected by flow cytometry.[35]

HAV peptides and anti-E-cadherin mAb also inhibit cadherin-mediated homotypic single cell aggregation of BBMEC.[39] Taken together, these results suggest that there is a potential role of E-cadherin in the BBB. At this point, it is not clear whether these peptides also bind to VE-cadherin.

To test whether cadherin peptides can bind to E-cadherin, the ^{15}N-labeled extracellular-1 (EC1) domain of E-cadherin was expressed and was titrated with cadherin peptides (*i.e.*, ADTC5, HAV6, and cHAVc3). These cadherin peptides caused changes in chemical shifts of several amino acids on the EC1 as observed using heteronuclear single quantum correlation (HSQC) NMR spectroscopy experiments.[33] A combination of NMR spectroscopy and molecular docking experiments indicated that HAV6 and cHAVc3 peptides have a different binding site than that of ADTC5 peptide. The binding site of HAV6 and cHAVc3 is at residues Y36, I38, F77, S78, and I94 on the EC1 domain;[33] in contrast, ADTC5 binds to residues I4, P5, P6, S8, and P10 on the N-terminal β sheet of the EC1 domain. To put these results into perspective, the X-ray structure of C-cadherin was used to explain the potential mechanism of action of HAV- or ADT-peptides. C-cadherin could form *cis*- and *trans*-interactions. The *cis*-interactions are formed via the EC1 domain of one molecule to the EC2 domain of a neighboring molecule on the same cell membranes.[40] In contrast, the *trans*-interactions are formed by domain swapping of two N-termini of one EC1 domain from two opposing cell membranes. In the *trans*-interaction, the Trp residue at the N-terminus of one EC1 binds to a hydrophobic binding pocket of another EC1 domain from the opposing cell.[40] Using a combination of the X-ray structure of C-cadherin and our NMR binding and molecular docking studies, we hypothesize that HAV peptides block the EC1-EC2 *cis*-interactions of two cadherins from the same cell membranes to create greater porosity of the intercellular junctions of the BBB.[33] In contrast, ADTC5 binds to the domain-swapping region of two EC1 domains for *trans*-interactions of E-cadherin from the opposing cell membranes. In

summary, the results suggest that HAV6 peptide disrupts the intercellular junctions of the BBB via inhibition of *cis*-cadherin interactions while ADTC5 modulates the BBB opening by inhibiting the *trans*-cadherin interactions.

2.6 Conclusion

This study has shown that cadherin peptides enhance the delivery of functional molecules such as a 65 kDa galbumin and peptides (*i.e.*, cIBR7, cLABL). Both ADTC5 and HAV6 peptides create a short opening of the BBB for delivering a large molecule (*i.e.*, galbumin) compared to a small molecule (*e.g.*, Gd-DTPA). The intact cIBR7 peptide can be efficiently detected and quantified in the brain using LC-MS/MS. ADTC5 has been shown to modulate the BBB and enhance the brain delivery of molecules in mouse and rat models. The results suggest that there is compatibility of quantifying molecules in the brain using MRI, NIRF, and LC-MS/MS. Finally, BBB modulation by cadherin peptides depends on (a) the type and dose of modulator peptide, (b) the timing of delivery between BBB modulator and the delivered molecule, and (c) the size of the delivered molecules. These results further support potential uses of cadherin peptides in delivering molecules to the brains of animal models of brain diseases for treatment, diagnosis, and evaluation of mechanisms of progression of brain diseases.

2.7 Figures and Legends

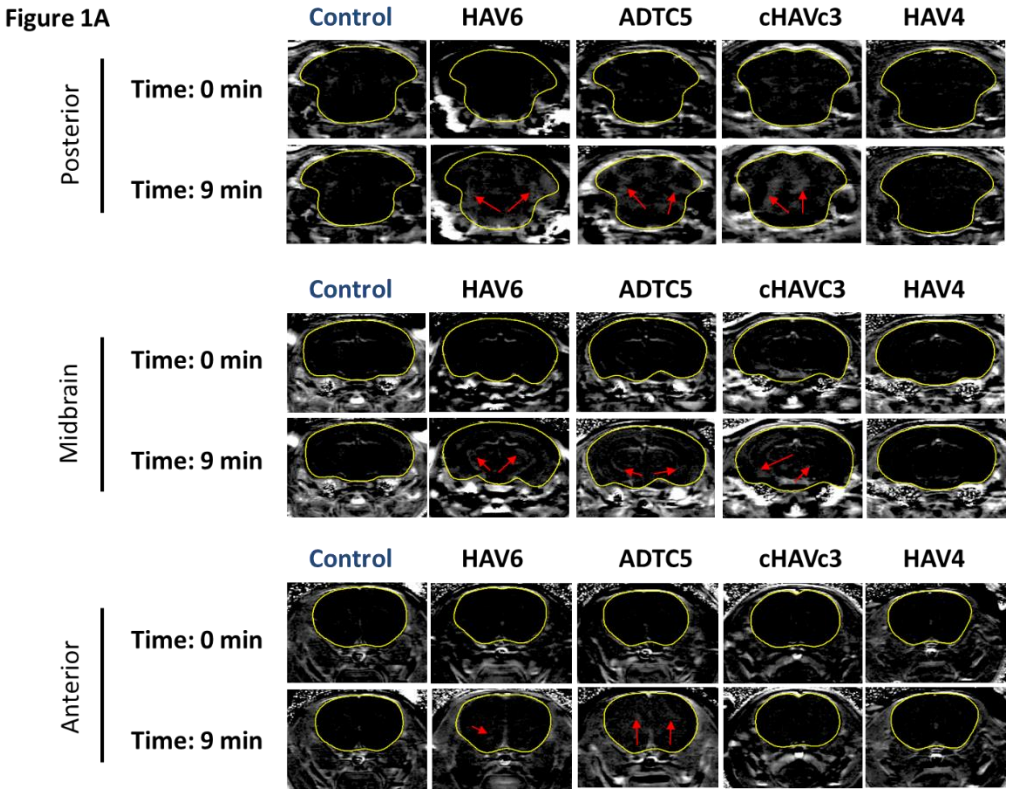

Figure 1B

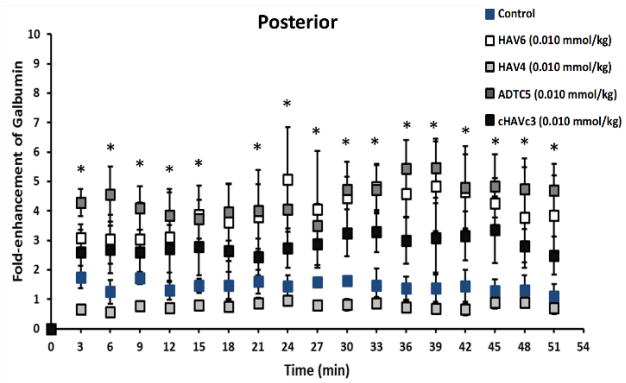

Figure 1C

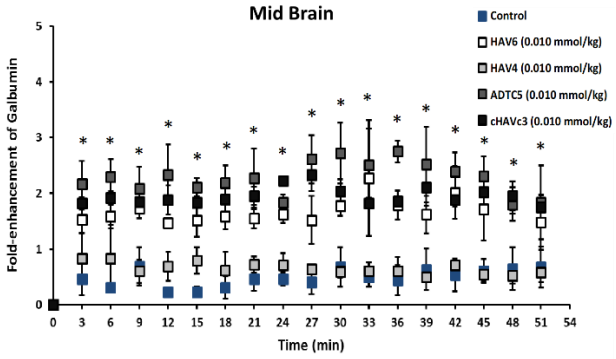

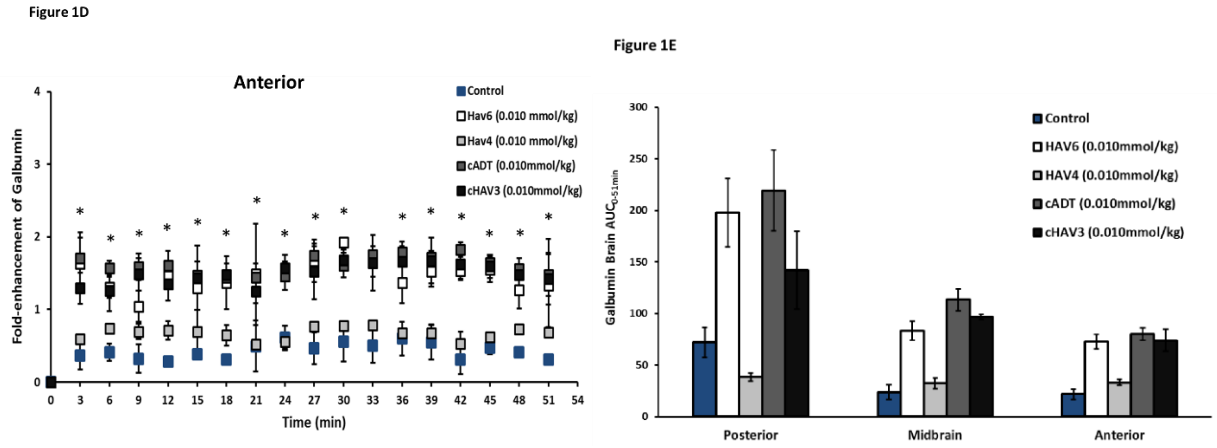

Figure 2.1 The effects of cadherin peptides (HAV6, HAV4, ADTC5, and cHAVc3) on enhancing brain delivery of 65 kDa galbumin as monitored MRI. **(A)** T1-weighted MR images of brain depositions of galbumin at 0 and 9 min time points when delivered with and without peptide. The depositions of galbumin were observed in the posterior, midbrain, and anterior regions as gray spots (see red arrows). **(B–D)** The time-dependent brain depositions of galbumin in the **(B)** posterior, **(C)** midbrain, and **(D)** anterior regions as monitored by MRI every 3 min over a 51-min imaging session. **(E)** The AUC of galbumin brain depositions when delivered with peptides or control vehicle. Star (*) represents statistical significant with $p < 0.05$ as evaluated using ANOVA with Student–Newman–Keuls post hoc comparison of the means (n = 3).

Figure 2A

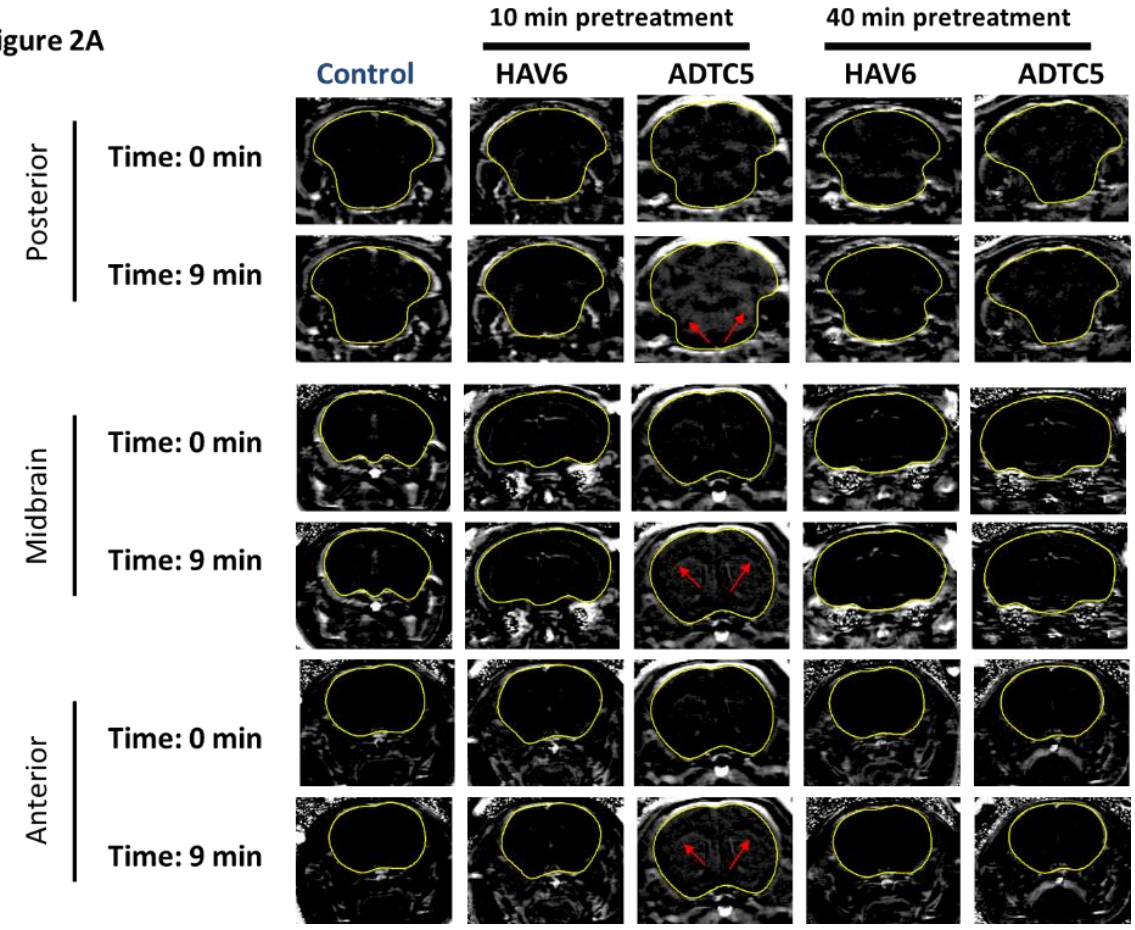
10 min pretreatment
40 min pretreatment
Control
HAV6
ADTC5
HAV6
ADTC5
Posterior
Time: 0 min
Time: 9 min
Midbrain
Time: 0 min
Time: 9 min
Anterior
Time: 0 min
Time: 9 min

Figure 2B

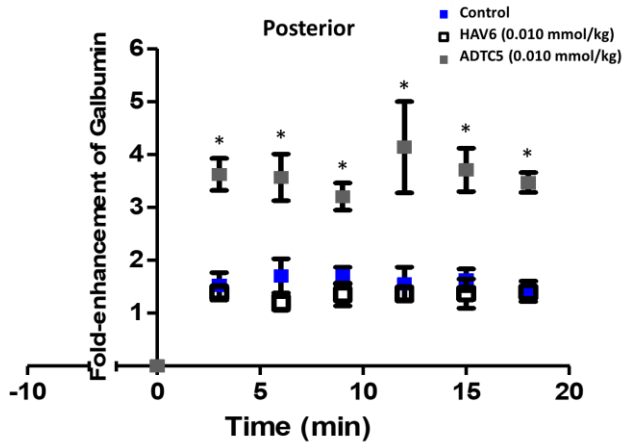

Figure 2C

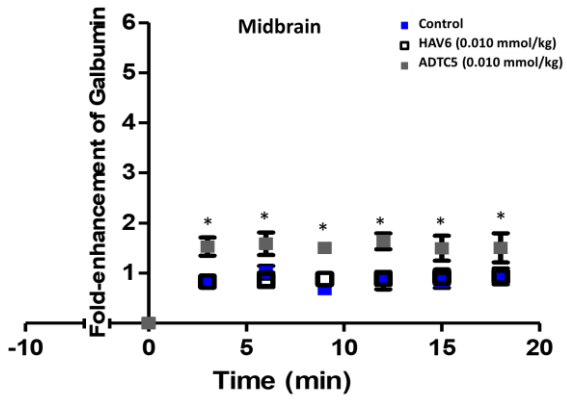

Figure 2D

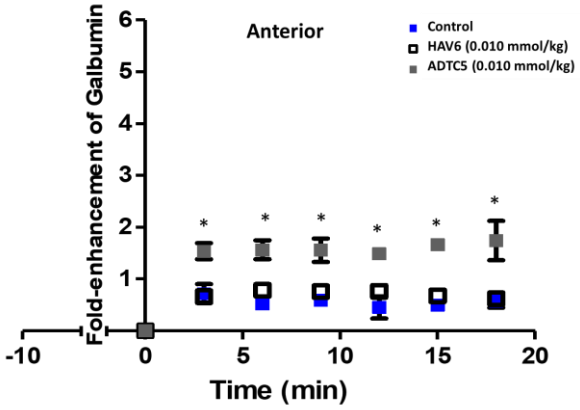

Figure 2E

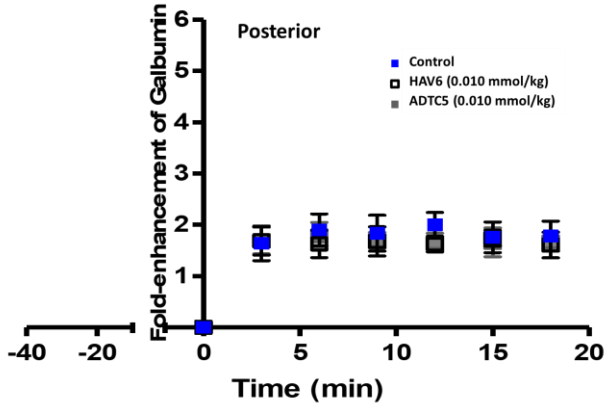

Figure 2F

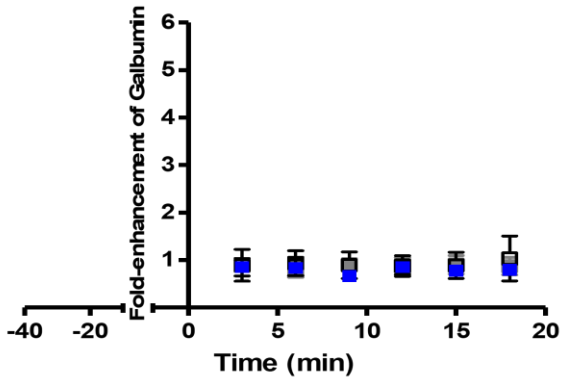

Figure 2G

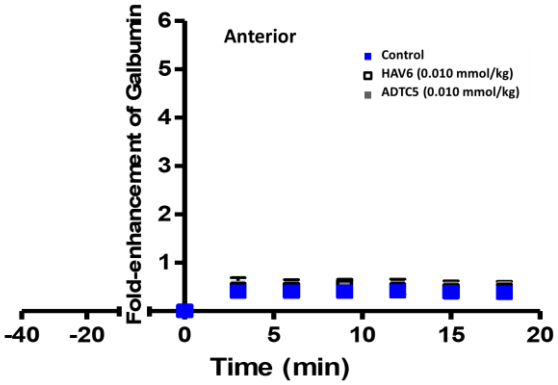

Figure 2.2 Comparison of 10-min and 40-min pretreatment with HAV6 or ADTC5 peptide on the brain depositions of galbumin. **(A)** T1-weighted MR image comparisons of brain depositions of galbumin after 10-min and 40-min pretreatment with HAV6 and ADTC5. The brain depositions of galbumin were observed as gray spots (see red arrows) in the posterior, midbrain, and anterior regions at 0 and 9 min time points using MRI. **(B–D)** Time-dependent brain depositions of galbumin observed at the **(B)** posterior, **(C)** midbrain, and **(D)** anterior regions when delivered 10 min after HAV6 or ADTC5 administration. **(E–G)** Time-dependent brain depositions of galbumin observed at the **(E)** posterior, **(F)** midbrain, and **(G)** anterior regions when delivered 40 min after HAV6 or ADTC5 administration. Star (*) represents statistical significance with $p < 0.05$ as evaluated using ANOVA with Student–Newman–Keuls post hoc comparison of the means (n = 3).

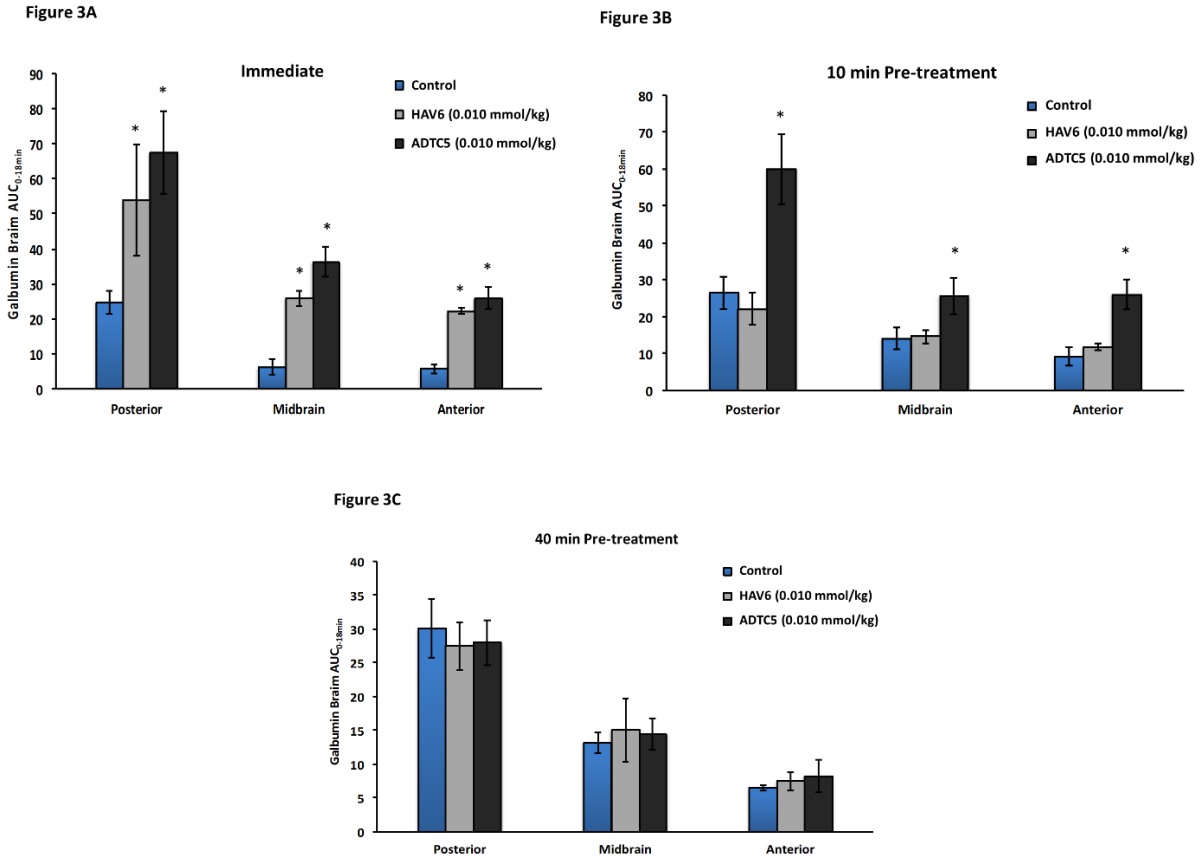

Figure 2.3 Comparisons of the AUC of galbumin brain deposition upon **(A)** immediate, (**B**) 10-min, and **(C)** 40-min pretreatment with HAV6 and ADTC5 peptides. **(A)** Immediate delivery with HAV6 or ADTC5 peptide significantly enhanced brain deposition of galbumin in posterior, midbrain, and anterior regions. **(B)** With 10-min pretreatment, ADTC5 still significantly enhanced the delivery of galbumin while HAV6 did not. **(C)** With 40-min pretreatment, there was no enhancement in galbumin accumulation in the brain with either ADTC5 or HAV6 peptide. Star (*) represents statistical significant with $p < 0.05$ as evaluated using ANOVA with Student–Newman–Keuls post hoc comparison of the means (n = 3).

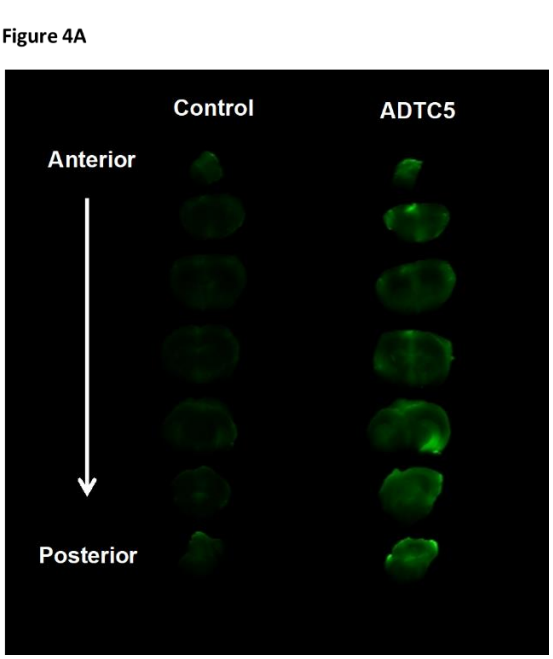

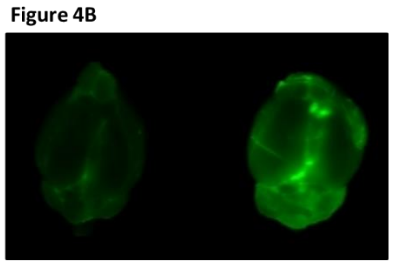

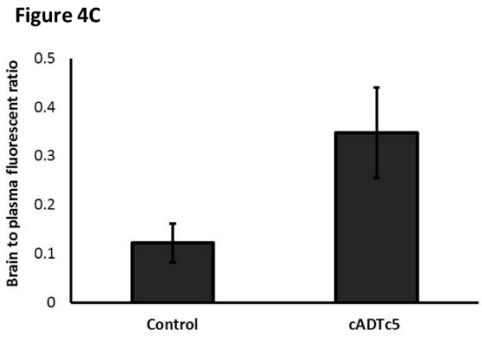

Figure 2.4 The effect of ADTC5 peptide on increasing the brain deposition of IRdye800cw-cLABL peptide after i.v. administration in Balb/c mice as detected by NIRF imaging. **(A)** The images of brain depositions of IRdye800cw-cLABL in different slices of the brain from anterior to posterior regions when delivered with vehicle (left) and ADTC5 (right). **(B)** The additive representation of brain depositions of IRdye800cw-cLABL when delivered with vehicle (left) or ADTC5 (right). **(C)** Comparison of brain-to-plasma ratios of IRdye800cw-cLABL peptide when administered with vehicle (control) and ADTC5. Star (*) indicates statistical significance with $p < 0.05$; ADTC5-treated group, n = 4; control group, n =3. The error bars represent SD.

Figure 5

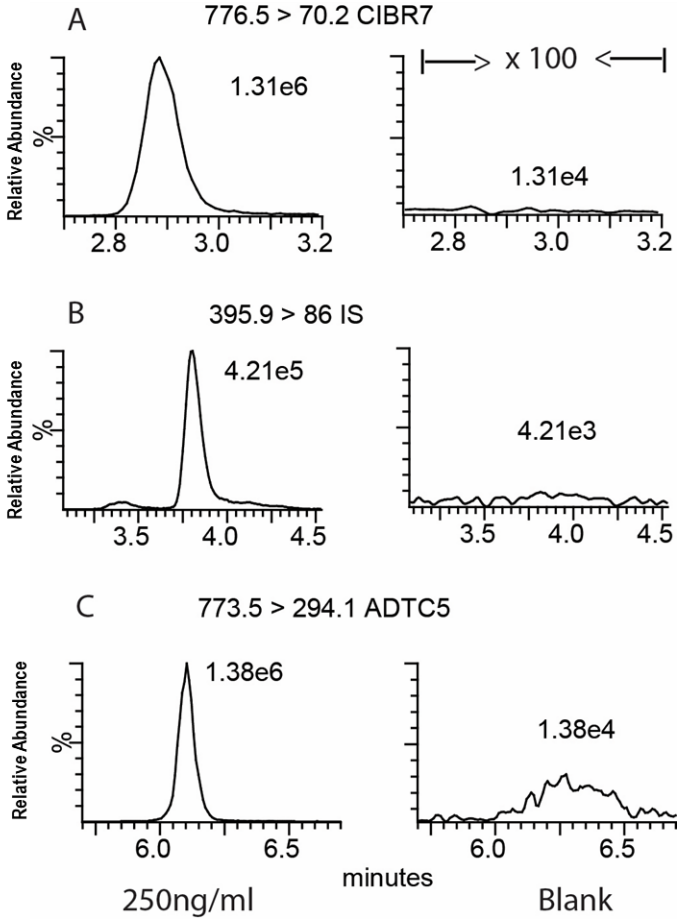

Figure 2.5 MRM chromatograms of brain extracts with **(A)** cIBR7 peptide (left) and blank (right), **(B)** IS peptide (left) and blank (right), and **(C)** ADTC5 peptide (left) and blank (right). The peptide separation was done using a Luna UPLC C_{18} column with 2.1 mm × 50 mm dimensions, particle size 5 μm, and pore size 100 Å (Phenomenex, Inc., Torrance, CA). The elution was done using a binary gradient mobile phase consisting of solvent A: H_2O:formic acid (99.92:0.08) and solvent B: acetonitrile:formic acid (99.92:0.08).

Figure 6

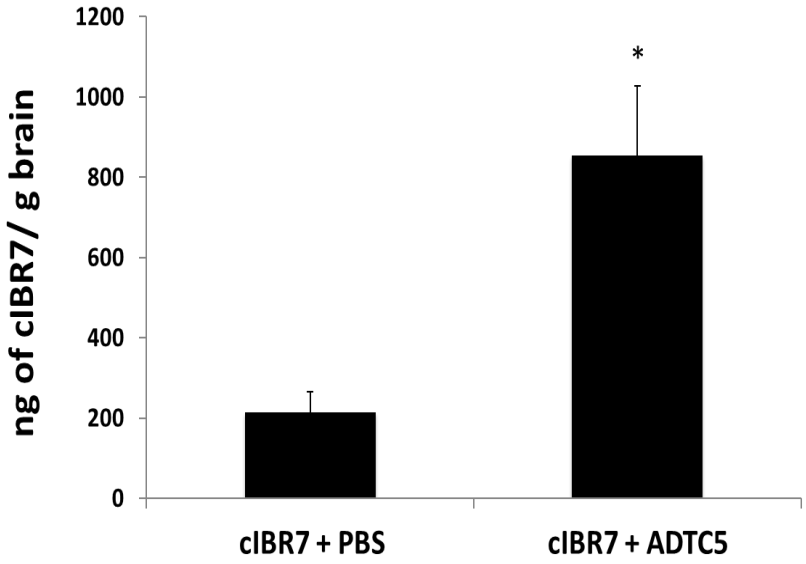

Figure 2.6 The effect of ADTC5 peptide on enhancing brain delivery of cIBR7 peptide in rats as detected by LC-MS/MS. cIBR7 (40 mg/kg) was delivered in the presence or absence of ADTC5 (30 mg/kg). The rats were sacrificed after 10 minutes, and the whole brains were collected for analysis. The total amount of cIBR7 in rat brains after *in vivo* delivery via i.v. administration was significantly higher in the presence of ADTC5 compared to control with PBS treatment. Star (*) indicates a significant difference from the control study with $p < 0.05$. Error bars show the mean ± SE from ADTC5-treated group (n = 5) and PBS-treated group (n = 4).

2.8 References

1. Laksitorini, M.; Prasasty, V. D.; Kiptoo, P. K.; Siahaan, T. J. Pathways and progress in improving drug delivery through the intestinal mucosa and blood-brain barriers. *Ther Deliv* **2014,** *5*, (10), 1143-63.
2. Pardridge, W. M. Blood-brain barrier delivery. *Drug Discovery Today* **2007,** *12*, (1-2), 54-61.
3. Shannon, R. J.; Carpenter, K. L. H.; Guilfoyle, M. R.; Helmy, A.; Hutchinson, P. J. Cerebral microdialysis in clinical studies of drugs: pharmacokinetic applications. *Journal of Pharmacokinetics and Pharmacodynamics* **2013,** *40*, (3), 343-358.
4. Grathwohl, S. A.; Jucker, M. Replacement of osmotic minipumps to extend the intracerebral infusion time of compounds into the mouse brain. *Biotechniques* **2013,** *55*, (2), 75-8.
5. Huang, Z.; Cheng, C.; Jiang, L.; Yu, Z.; Cao, F.; Zhong, J.; Guo, Z.; Sun, X. Intraventricular apolipoprotein ApoJ infusion acts protectively in Traumatic Brain Injury. *J Neurochem* **2016,** *136*, (5), 1017-25.
6. Chen, Y.; Liu, L. Modern methods for delivery of drugs across the blood-brain barrier. *Adv Drug Deliv Rev* **2012,** *64*, (7), 640-65.
7. Oberoi, R. K.; Parrish, K. E.; Sio, T. T.; Mittapalli, R. K.; Elmquist, W. F.; Sarkaria, J. N. Strategies to improve delivery of anticancer drugs across the blood-brain barrier to treat glioblastoma. *Neuro-Oncology* **2016,** *18*, (1), 27-36.
8. Pardridge, W. M. Blood-brain barrier drug delivery of IgG fusion proteins with a transferrin receptor monoclonal antibody. *Expert Opinion on Drug Delivery* **2015,** *12*, (2), 207-222.

9. Neuwelt, E. A.; Hill, S. A.; Frenkel, E. P. Osmotic blood-brain barrier modification and combination chemotherapy: concurrent tumor regression in areas of barrier opening and progression in brain regions distant to barrier opening. *Neurosurgery* **1984,** *15*, (3), 362-6.

10. Deli, M. A. Potential use of tight junction modulators to reversibly open membranous barriers and improve drug delivery. *Biochimica Et Biophysica Acta-Biomembranes* **2009,** *1788*, (4), 892-910.

11. Wong, V.; Gumbiner, B. M. A synthetic peptide corresponding to the extracellular domain of occludin perturbs the tight junction permeability barrier. *Journal of Cell Biology* **1997,** *136*, (2), 399-409.

12. Zwanziger, D.; Hackel, D.; Staat, C.; Bocker, A.; Brack, A.; Beyermann, M.; Rittner, H.; Blasig, I. E. A peptidomimetic tight junction modulator to improve regional analgesia. *Mol Pharm* **2012,** *9*, (6), 1785-94.

13. Raymond, J. J.; Robertson, D. M.; Dinsdale, H. B. Pharmacological modification of bradykinin induced breakdown of the blood-brain barrier. *Can J Neurol Sci* **1986,** *13*, (3), 214-20.

14. Makagiansar, I. T.; Avery, M.; Hu, Y.; Audus, K. L.; Siahaan, T. J. Improving the selectivity of HAV-peptides in modulating E-cadherin-E-cadherin interactions in the intercellular junction of MDCK cell monolayers. *Pharm Res* **2001,** *18*, (4), 446-53.

15. Sinaga, E.; Jois, S. D.; Avery, M.; Makagiansar, I. T.; Tambunan, U. S.; Audus, K. L.; Siahaan, T. J. Increasing paracellular porosity by E-cadherin peptides: discovery of bulge and groove regions in the EC1-domain of E-cadherin. *Pharm Res* **2002,** *19*, (8), 1170-9.

16. Tabanor, K.; Lee, P.; Kiptoo, P.; Choi, I. Y.; Sherry, E. B.; Eagle, C. S.; Williams, T. D.; Siahaan, T. J. Brain Delivery of Drug and MRI Contrast Agent: Detection and Quantitative

Determination of Brain Deposition of CPT-Glu Using LC-MS/MS and Gd-DTPA Using Magnetic Resonance Imaging. *Mol Pharm* **2016,** 10.1021/acs.molpharmaceut.5b00607.

17. On, N. H.; Kiptoo, P.; Siahaan, T. J.; Miller, D. W. Modulation of blood-brain barrier permeability in mice using synthetic E-cadherin peptide. *Mol Pharm* **2014,** *11*, (3), 974-81.
18. Laksitorini, M. D.; Kiptoo, P. K.; On, N. H.; Thliveris, J. A.; Miller, D. W.; Siahaan, T. J. Modulation of intercellular junctions by cyclic-ADT peptides as a method to reversibly increase blood-brain barrier permeability. *J Pharm Sci* **2015,** *104*, (3), 1065-75.
19. Kiptoo, P.; Sinaga, E.; Calcagno, A. M.; Zhao, H.; Kobayashi, N.; Tambunan, U. S.; Siahaan, T. J. Enhancement of drug absorption through the blood-brain barrier and inhibition of intercellular tight junction resealing by E-cadherin peptides. *Mol Pharm* **2011,** *8*, (1), 239-49.
20. Alaofi, A.; On, N.; Kiptoo, P.; Williams, T. D.; Miller, D. W.; Siahaan, T. J. Comparison of Linear and Cyclic His-Ala-Val Peptides in Modulating the Blood-Brain Barrier Permeability: Impact on Delivery of Molecules to the Brain. *J Pharm Sci* **2016,** *105*, (2), 797-807.
21. Osting, S.; Bennett, A.; Power, S.; Wackett, J.; Hurley, S. A.; Alexander, A. L.; Agbandje-Mckena, M.; Burger, C. Differential effects of two MRI contrast agents on the integrity and distribution of rAAV2 and rAAV5 in the rat striatum. *Mol Ther Methods Clin Dev* **2014,** *1*, 4.
22. Xu, C. R.; Yusuf-Makagiansar, H.; Hu, Y.; Jois, S. D.; Siahaan, T. J. Structural and ICAM-1-docking properties of a cyclic peptide from the I-domain of LFA-1: an inhibitor of ICAM-1/LFA- 1-mediated T-cell adhesion. *J Biomol Struct Dyn* **2002,** *19*, (5), 789-99.

23. Yusuf-Makagiansar, H.; Siahaan, T. J. Binding and internalization of an LFA-1-derived cyclic peptide by ICAM receptors on activated lymphocyte: a potential ligand for drug targeting to ICAM-1-expressing cells. *Pharm Res* **2001,** *18*, (3), 329-35.

24. Anderson, M. E.; Siahaan, T. J. Mechanism of binding and internalization of ICAM-1-derived cyclic peptides by LFA-1 on the surface of T cells: a potential method for targeted drug delivery. *Pharm Res* **2003,** *20*, (10), 1523-32.

25. Anderson, M. E.; Yakovleva, T.; Hu, Y.; Siahaan, T. J. Inhibition of ICAM-1/LFA-1-mediated heterotypic T-cell adhesion to epithelial cells: design of ICAM-1 cyclic peptides. *Bioorg Med Chem Lett* **2004,** *14*, (6), 1399-402.

26. Zimmerman, T.; Oyarzabal, J.; Sebastian, E. S.; Majumdar, S.; Tejo, B. A.; Siahaan, T. J.; Blanco, F. J. ICAM-1 peptide inhibitors of T-cell adhesion bind to the allosteric site of LFA-1. An NMR characterization. *Chem Biol Drug Des* **2007,** *70*, (4), 347-53.

27. Triguero, D.; Buciak, J.; Pardridge, W. M. Capillary depletion method for quantification of blood-brain barrier transport of circulating peptides and plasma proteins. *J Neurochem* **1990,** *54*, (6), 1882-8.

28. Bella, J.; Kolatkar, P. R.; Marlor, C. W.; Greve, J. M.; Rossmann, M. G. The structure of the two amino-terminal domains of human ICAM-1 suggests how it functions as a rhinovirus receptor and as an LFA-1 integrin ligand. *Proc Natl Acad Sci U S A* **1998,** *95*, (8), 4140-5.

29. Yusuf-Makagiansar, H.; Makagiansar, I. T.; Siahaan, T. J. Inhibition of the adherence of T-lymphocytes to epithelial cells by a cyclic peptide derived from inserted domain of lymphocyte function-associated antigen-1. *Inflammation* **2001,** *25*, (3), 203-14.

30. Anderson, M. E.; Tejo, B. A.; Yakovleva, T.; Siahaan, T. J. Characterization of binding properties of ICAM-1 peptides to LFA-1: inhibitors of T-cell adhesion. *Chem Biol Drug Des* **2006,** *68*, (1), 20-8.

31. Majumdar, S.; Kobayashi, N.; Krise, J. P.; Siahaan, T. J. Mechanism of internalization of an ICAM-1-derived peptide by human leukemic cell line HL-60: influence of physicochemical properties on targeted drug delivery. *Mol Pharm* **2007,** *4*, (5), 749-58.

32. Services, D. o. H. a. H.; Administration, F. a. D.; (CDER), C. f. D. E. a. R.; (CBER), C. f. B. E. a. R. Analytical Procedures and Methods Validation for Drugs and Biologics: Guidance for Industry. *Pharmaceutical Quality/CMC* **2015,** *July*, 1–15.

33. Alaofi, A.; Farokhi, E.; Prasasty, V. D.; Anbanandam, A.; Kuczera, K.; Siahaan, T. J. Probing the interaction between cHAVc3 peptide and the EC1 domain of E-cadherin using NMR and molecular dynamics simulations. *J Biomol Struct Dyn* **2016,** 10.1080/07391102.2015.1133321, 1-13.

34. Rubin, L. L.; Staddon, J. M. The cell biology of the blood-brain barrier. *Annu Rev Neurosci* **1999,** *22*, 11-28.

35. Pal, D.; Audus, K. L.; Siahaan, T. J. Modulation of cellular adhesion in bovine brain microvessel endothelial cells by a decapeptide. *Brain Res* **1997,** *747*, (1), 103-13.

36. Abbruscato, T. J.; Davis, T. P. Protein expression of brain endothelial cell E-cadherin after hypoxia/aglycemia: influence of astrocyte contact. *Brain Res* **1999,** *842*, (2), 277-86.

37. Vorbrodt, A. W.; Dobrogowska, D. H. Molecular anatomy of interendothelial junctions in human blood-brain barrier microvessels. *Folia Histochem Cytobiol* **2004,** *42*, (2), 67-75.

38. Vorbrodt, A. W.; Dobrogowska, D. H. Molecular anatomy of intercellular junctions in brain endothelial and epithelial barriers: electron microscopist's view. *Brain Research Reviews* **2003,** *42*, (3), 221-242.

39. Lutz, K. L.; Siahaan, T. J. Modulation of the cellular junction protein E-cadherin in bovine brain microvessel endothelial cells by cadherin peptides. *Drug Delivery* **1997,** *4*, (3), 187-193.

40. Boggon, T. J.; Murray, J.; Chappuis-Flament, S.; Wong, E.; Gumbiner, B. M.; Shapiro, L. C-cadherin ectodomain structure and implications for cell adhesion mechanisms. *Science* **2002,** *296*, (5571), 1308-13.

CHAPTER 3

In Vivo Brain Delivery and Brain Deposition of Proteins of Various Sizes

3.1 Introduction

Currently, protein drugs are a successful class of therapeutics for treating a wide variety of diseases such as cancers, infectious agents, genetic disorders, and autoimmune diseases (*e.g.*, type-1 diabetes (T1D), rheumatoid arthritis (RA), and multiple sclerosis (MS)). Protein therapeutics are normally developed with a specific and known mechanism of action and have reduced toxicity compared to small molecule drugs.[1] Some proteins such as brain-derived neurotrophic factor (BDNF),[2] nerve growth factor (NGF),[3] and insulin-like growth factor 1 (IGF-1)[4] have been investigated for inducing neuroregeneration in brain diseases such as MS and Alzheimer's (AD). Unfortunately, previous attempts to deliver proteins via the systemic circulation have met with only limited success due to the presence of the blood-brain barrier (BBB), which prevents them from entering the brain.[5-7] Monoclonal antibodies (mAbs), the fastest growing type of drugs, have also been investigated to treat brain diseases.[8] Several mAbs such as anti-Nogo-A,[9] anti-LINGO-1,[10] sHIgM22,[11] and VX15/2503[12] have been evaluated in clinical trials for inducing remyelination in MS patients; however, the clinical trials for most of these molecules were terminated due to their lack of efficacy in MS patients. A similar fate befell amyloid beta (Aβ) mAbs, which failed to effectively treat AD patients. Although many reasons could contribute to these failures, one potential problem is their inability to cross the BBB effectively from the blood into the brain.

The BBB is a selective barrier between the blood stream and the brain that prevents unwanted molecules from entering the brain. Many drug molecules cannot readily cross the BBB because the molecules need to have appropriate physicochemical properties for crossing the BBB. Most molecules that can passively cross the BBB can be predicted using the Lipinski's rule of five.[13] Because proteins do not satisfy this rule, BBB passive diffusion of proteins is very limited unless the protein has its own transporter on the endothelial microvessels for its transcytosis across into the brain. Therefore, there is a need to develop methods to improve protein delivery into the brain

in a non-invasive manner. Currently, many invasive ways such as intracerebral ventricular (ICV) delivery have been used to directly administer protein drugs into the brain in critical brain diseases. One of the limitations of the direct delivery method is the potential increase in brain infection and inflammation due to exposure to the outside environment. Currently, many non-invasive methods are being developed for enhancing brain drug delivery utilizing prodrug technology, receptor-mediated transcytosis mechanisms,[7] microbubble enhanced diagnostic ultrasound (MEUS) system,[14] intranasal delivery,[15] and BBB modulation.[16, 17] A BBB modulation method called "osmotic BBB delivery" has been successfully used to deliver antitumor drugs for treating brain tumor patients.[18] The osmotic BBB delivery method utilizes a hypertonic mannitol solution to disrupt the intercellular junctions of the BBB by shrinking the microvessel endothelial cells to allow anticancer drugs to passively penetrate the paracellular pathway of the BBB. Thus, the clinical success of the osmotic method provides impetus to investigate other ways to modulate the intercellular junctions of the BBB to improve brain delivery.

One way to modulate the BBB intercellular junctions in a controlled and selective way is by inhibiting cadherin-cadherin interactions that mediate cell-cell adhesion. Thus, we designed cadherin peptides such as HAV6 and ADTC5 to inhibit cadherin-cadherin interactions in a dynamic and equilibrium fashion to increase the porosity of the paracellular pathways reversibly and allow molecules to cross the BBB from the blood stream into the brain. HAV6 peptide can enhance the *in vivo* brain delivery of small molecules (*e.g.*, ^{14}C-mannitol, ^{3}H daunomycin, and gadopentetic acid (Gd-DTPA), and IRdye R800), and large molecules (*e.g.*, 25 kDa IRdye800CW-polyethylene glycol and 65 kDa galbumin).[19-23] Similarly, ADTC5 peptide enhances brain delivery of ^{14}C-mannitol, Gd-DTPA, 8–12 amino acid peptides, and galbumin.[17, 22]

In this study, the modulatory activities of HAV6 and ADTC5 were compared for brain delivery of different sizes of proteins such as 15 kDa lysozyme, 65 kDa albumin, 150 kDa IgG mAb, and 220 kDa fibronectin. To accomplish this, the proteins were conjugated with IRdye800CW on lysine residues and the protein brain depositions were determined quantitatively using NIRF imaging. The quantification method was developed and validated using standard curves of homogenized brain containing the IRdye800CW-conjugate protein. The method of validation to generate quantitative data for delivered protein was carried out by determining the stability, accuracy, precision, and linear dynamic range of the quantitation method. This study provides the difference between the effectiveness of HAV6 and ADTC5 for delivering different sizes of proteins as well as the size limit of the protein that each peptide can deliver through the BBB. The effects of each peptide on depositions of each protein in different organs, including liver, kidney, heart, spleen and lungs, were also determined.

3.2 Materials and Methods

3.2.1 Chemicals, Reagents, and Animals.

Gyros Protein Technologies, Inc. (Tucson, AZ) was used as a vendor to purchase amino acids and coupling reagents for the automated peptide synthesizer. IRdye-800CW-NHS ester and IRdye-800CW Donkey anti-Goat IgG were purchased from LI-COR, Inc. (Lincoln, NE). Sigma Aldrich Chemical Company (St. Louis, MO) and Fisher Scientific, Inc. (Hampton, NH) were used as suppliers or proteins and reagents in this study. Protocols used for all animal studies have been approved by the Institutional Animal Care and Use Committee (IACUC) at The University of Kansas. All animals were cared by the Animal Care Unit personnel at The University of Kansas under the supervision of Veterinarians.

Table 3.1. BBB Modulator Peptides			
Peptide	**Sequence**	**Mass (Da)**	**Exact Mass**
ADTC5	Cyclo(1,7)Ac-CDTPPVC-NH_2	772	795.2778 (Na^+ Adduct)
HAV6	Ac-SHAVSS-NH_2	627	650.2869 (Na^+ Adduct)

3.2.2 Peptide Synthesis and Purification.

The synthesis of the linear and cyclic peptides (**Table 3.1**) were accomplished using a Tribute solid-phase peptide synthesizer from Gyros Protein Technologies, Inc. (Tucson, AZ). After peptide cleavage from the resin using TFA, the crude product was precipitated in cold diethyl ether. The formation of a disulfide bond in the cyclic ADTC5 peptide was accomplished by stirring the precursor linear peptide in bicarbonate buffer solution under air oxidation at pH 9.0 in high dilution. The cyclization reaction produced a high yield of the desired monomer with minor amounts of dimer and oligomer as side-products. The monomer was isolated from the mixture using a semi-preparative C18 column Waters XBridge C18 (19 mm × 250 mm, 5 μm particle size; Waters Corporation, Milford, MA)) in HPLC. The purity of each isolated fraction was determined by analytical HPLC using C18 column (Luna C18 (4.6 mm × 250 mm, 5 μm particle size, 100 Å; Phenomenex, Inc., Torrance, CA)). The identity of each peptide was confirmed by mass spectrometry.

3.2.3 Conjugation of Proteins with IRdye-800CW-NHS Ester.

Lysozyme, albumin, and fibronectin used in this study were conjugated with IRdye-800CW according to the manufacturer's instructions. Briefly, dyes were reacted with 1 mg/mL of protein in PBS with 10% potassium phosphate buffer, pH 9 (v/v) for 2 h at 25 °C. The resulting conjugates were purified using a spin column called Zeba Spin Desalting Column with 7 kDa molecular weight cut-off (Fisher Scientific, Inc. (Hampton, NH)). The purity of each conjugate was determined using SDS-PAGE, and the conjugate band was scanned (Excitation = 778 nm;

Emission = 794 nm) with an Odyssey CLx NIR scanner to ensure that there was no free IRdye-800CW in the protein conjugate solution. Once any free dye was removed, the degree of labeling was determined using a UV spectrophotometer (Varian Cary 100, Agilent) to measure the fluorophore absorption and the protein absorbance at 280 nm, corrected for the fluorophore.

The protein concentration is calculated using the formula,

$$Protein\ Conc.\left(\frac{mg}{mL}\right) = \frac{A_{280} - (0.03 \times A_{780})}{\varepsilon_{Protein}} \times MW_{Protein} \times Dilution\ Factor$$

in which 0.03 is a correction factor for the absorbance of the IRDye-800CW at 280 nm (equal to 3.0% of its absorbance at 780 nm). $\varepsilon_{Protein}$ is the molar extinction coefficient of the protein and $MW_{Protein}$ is the molecular weight of the protein.

3.2.4 NIRF Method to Quantify Protein Amount in the Brain.

Preparation of Stock and Standard Curves.

The stock solution for IRDye800CW protein (*i.e.*, lysozyme, 70 µg/mL) was prepared and stored at –80 °C. The stock solution was later diluted with PBS to make the required standard solutions. To produce a standard calibration curve, 200 μL of blank brain homogenates was spiked with 10 μL standard solutions of various concentrations to yield a linear range from 0.5 to 50 ng/mL. The same method was employed for the sample's quality control (QC).

Accuracy and Precision.

For precision studies, IRDye-800CW-lysozyme was used. The intra-day and inter-day, accuracy and precision were calculated by analyzing replicates of spiked brain homogenates at three concentrations between 0.5 and 50 ng/mL.

Evaluation of Method Stability.

To evaluate the stability of the quantitative method, IRDye-800CW-labeled lysozyme was used in spiked brain homogenates under various temperature and storage conditions. Three sets of

samples were subjected to (a) room temperature for 6 h, (b) −20 °C for 24 h followed by unassisted thawing at room temperature, and (c) three freeze-thaw cycles between −20 °C and room temperature over a 24-h period. All stability studies were conducted at 0.5 to 50 ng/mL with three determinations for each.

3.2.5 Brain Delivery IRdye800CW-labeled IgG mAb using ADTC5 in SJL/elite Mice.

For initial evaluation of whether a cadherin peptide can deliver proteins into the brain, IRdye800CW donkey-anti-goat IgG mAb was administered via i.v. with and without ADTC5 peptide in 5–8-week-old SJL/elite mice. Two groups of healthy SJL/elite mice were injected with (a) a mixture of IgG mAb (26.8 nmol/kg) and ADTC5 peptide (13 μmol/kg) (n = 5) and (b) IgG mAb alone (26.8 nmol/kg) (n = 4). After 15 min in the systemic circulation, the mice were euthanized using CO_2 inhalation followed by brain perfusion using PBS to remove the remaining protein in the BBB microvasculature. Next, the brains were isolated followed by NIRF imaging using Licor Odyssey CLx (Licor, Lincoln, NE). Eight optical sections were taken at 0.5 mm increments beginning from the bottom surface of the brain to a depth of 4 mm. The optical sections were summed to yield a fluorescence intensity value per each brain**.**

3.2.6 Comparison of HAV6 and ADTC5 in Delivering Various Sizes of Proteins into C57BL/6 Mice.

The BBB modulatory activities of ADTC5 and HAV6 to enhance brain delivery of IRdyeR800CW-labeled lysozyme, albumin, IgG mAb, and fibronectin were compared in C57BL mice. The proteins with or without 13 μmol/kg HAV6 or ADTC5 were administered via tail vein injection. For lysozyme, the delivered doses were 21.6 and 54 nmol/kg. For albumin, IgG mAb, and fibronectin, the dose used was 21.6 nmol/kg. After 15 min, the mice were sacrificed followed by cardiac perfusion with PBS with 0.5% Tween-20. The brain and other organs such as lung,

heart, spleen, liver and kidney were harvested and rinsed with PBS. Protein depositions in the brain and other organs were quantified by NIRF imaging using an Odyssey CLx NIRF scanner.

A second quantification method was done using brain homogenates. In this case, the brains were homogenized in 2.0 mL PBS by mechanical disruption and 200 μL of homogenized brain (n = 8) was aliquoted to a 96-well plate followed by quantification using the Odyssey CLx scanner. The signal intensity was compared to calibration curve and normalized to brain weight and homogenate volume.

3.2.7 Capillary Depletion Method.

Parallel capillary depletion experiments were performed as described by Triguero *et al.*[24] to ensure that there was no trapping of the delivered molecules in the BBB microvessel endothelial cells. Brain homogenates dosed with IRdye800CW-labeled protein were mixed together and divided into two sets. A 500 μL set of homogenates was mixed with 500 μL of PBS while another set of 500 μL homogenates was mixed with 500 μL of 26% dextran solution. Both sets were centrifuged at 5,400 g for 15 min at 4 °C and 200 μL of supernatant was collected for analysis using the Odyssey CLx scanner.

3.2.8 Statistical Analysis.

For brain delivery of various sized molecules, the differences in the brains treated with or without BBB modulators were compared using ANOVA with Student–Newman-Keuls for determining the statistical significance. A *p*-value of less than 0.05 was used as a criterion for statistical significance.

3.3 Results

3.3.1 Peptide Synthesis and Purification.

The Fmoc solid-phase synthesis method was used to make linear precursor to ADTC5 and HAV6 peptides. ADTC5 was cyclized using air oxidation in a high dilution solution at pH 9.0 to give mostly the desired cyclic monomer. A semi-preparative HPLC with C18 column was used to purify both ADTC5 and HAV6 peptides with >96% purity of each peptide as determined by C18 column in analytical HPLC. The mass spectra for both purified peptides show exact masses of 650.2869 Da for sodium adduct of HAV6 and 795.2778 Da for sodium adduct of ADTC5 **(Table 3.1).**

3.3.2 Synthesis and Purification of IRdye800CW-labeled Proteins.

To make IRdye800CW-labeled lysozyme, albumin, or fibronectin, IRdye800CW-NHS was reacted to free amino groups of the respective protein to form stable conjugates. To purify the protein conjugates, the excess of IRdye800CW-NHS was removed from the reaction mixture using a Pierce Zeba desalting spin column with a cut-off molecular weight of 7 kDa. The purified conjugates were evaluated with SDS-PAGE scanned with an Odyssey CLx NIR imager. Lysozyme and albumin conjugates showed a single band while fibronectin had a faint lower fragment band; all proteins have the appropriate mass without unreacted IRdye (**Figure 3.1**). The final protein concentrations for lysozyme, albumin, and fibronectin were determined to be 1.35, 1.68, 2.30 mg/mL, respectively.

3.3.3 Initial Brain Delivery of IRDye800CW-IgG mAb by ADTC5 in SJL/Elite Mice.

In this study, IgG mAb was administered via i.v. in SJL/elite mice in the absence or presence of ADTC5 peptide. Prior to injection, IgG mAb identity was evaluated using SDS-PAGE gel and showed a major band at ~150 kDa with very light bands for ~100 kDa heavy and ~50 kDa light chains (data not shown). There was no observation of the band for IRDye800CW alone. After delivery, the brain scans of mice treated with IgG mAb alone showed very low NIRF image in eight different levels of brain scans (n = 4) (**Figure 3.2A**). In contrast, the mouse brains

administered IgG mAb with ADTC5 showed strong NIRF signals on eight different brain scan levels (n = 5) (**Figure 3.2A**). Quantitative accumulation of NIRF signals from all scan levels indicated that the brains from mice treated with IgG mAb + ADTC5 had a significantly higher signal intensity than those of mice treated with IgG mAb alone (**Figure 3.2B**). In summary, ADTC5 increases the brain delivery of IgG mAb in C57BL/6 mice**.**

3.3.4 Method Development and Validation of NIRF Quantification

Linearity, Accuracy, and Precision.

The lowest limit of detection (LLOD) and intra-day as well as inter-day precision and accuracy were determined using a calibration curve generated with concentrations from 0.5 to 50 ng/mL (**Table 3.2**). The calibration curve was generated by plotting concentrations of standard *vs.* NIRF intensity from the Odyssey CLx imaging system (**Figure 3.3**). The resulting standard curve has good linearity with $R^2 \geq 0.98$ and LLOD of 0.3 ng/mL. Intra-day and inter-day accuracy as well as precision were determined by analyzing samples at three different concentrations to obtain %RSD and %RE (**Table 3.2**). The acceptable analytical method was determined when the %RSD and %RE values were less than 15%.

Table 3.2. Precision and Accuracy

Concentration (ng/mL)	Intra-day		Inter-day	
	%RSD	%RE	%RSD	%RE
0.5	15.1	7.1	10.5	6.4
5.0	4.6	-2.8	3.4	5.8
50.0	2.8	5.4	3.8	1.6

Stability Assay.

The stability of the analyte during evaluation was investigated using IRDye800CW-lysozyme in three concentrations at two temperatures and a freeze-thaw condition (**Table 3.3**). In different analyte concentrations in the brain extracts, the %RSA was less than 15% at room temperature for 6 h. The RSD was higher than 15% under the other two conditions (a) −20 °C for 24 h followed by unassisted thawing at room temperature and (b) after three freeze-thaw cycles between −20 °C and room temperature over a 24-h period.

Table 3.3. Stability of Protein			
Concentration (ng/mL)	**%RSD**		
	Room Temp. (6 h)	**–20 °C (24 h)**	**Three freeze-thaw cycles**
0.5	7.7	16.2	23.1
5.0	5.4	18.5	8.5
50.0	3.7	25.1	18.4

Table 3.4. Quantitative Amounts of Proteins in the Brain		
Protein	**Group**	**pmol/g brain**
Lysozyme	Control	0 ± 0
	HAV6	8.3 ± 2.5
	ADTC5	37.8 ± 7.1
Albumin	Control	11.8 ± 1.0
	HAV6	15.5 ± 3.1
	ADTC5	40.7 ± 7.4
IgG mAb	Control	4.0 ± 0.4
	HAV6	3.4 ± 0.5
	ADTC5	13.3 ± 0.7

3.3.5 Comparison of HAV6 and ADTC5 in Enhancing Brain Delivery of Various Proteins.

In this study, the activities of HAV6 and ADTC5 peptides to deliver various sized proteins (*i.e.*, lysozyme, albumin, IgG mAb, and fibronectin) in C57BL/6 mice were compared in a quantitative manner. The intensities of lysozymes at various concentrations in the brain homogenates are shown in **Figure 3.2A**. **Figure 3.2A** also shows the examples of NIRF scans of brain homogenates from animals treated with lysozyme alone, lysozyme + HAV6, and lysozyme + ADTC5. The resulting calibration curve generated from 0.5 to 50 ng/mL of lysozyme produced a linear curve with $R^2 \geq 0.99$ (**Figure 3.2B**). Similar calibration curves were generated for albumin and IgG mAb. The amount of protein in the brain was determined by interpolation of NIRF intensity of the brain homogenate into the standard curve.

3.3.6 Brain Delivery of 15 kDa Lysozyme and Peripheral Organ Distributions.

The first delivery of lysozyme was carried out at a dose of 21.6 nmol/kg with 13 μmol/kg of HAV6 or ADTC5 peptide, and no significant improvement was observed in the brain compared to lysozyme alone (data not shown). Next, the dose of lysozyme was increased to 54 nmol/kg with 13 μmol/kg of HAV6 or ADTC5 peptide (**Figure 3.4**). Through visual observation, the NIRF brain images of mice treated with HAV6 + lysozyme and ADTC5 + lysozyme appeared to show higher intensity than those treated with lysozyme alone (**Figure 3.4A**). The NIRF intensity of the ADTC5 group was higher than that of HAV6 group. Quantitatively, the average amount of lysozyme in the ADTC5 group (37.8 ± 7.1 pmol/g brain) was significantly higher than that in the HAV6 group (8.3 ± 2.5 pmol/g brain, p <0.05) (**Figure 3.4B**, **Table 3.4**). The lysozyme amounts in the brains of both peptide groups were higher than that of control group, which was below the detection limits. The results suggest that ADTC5 is a better BBB modulator than HAV6. To ensure that the brain perfusion procedure eliminated any residual molecule in the BBB microvessels, the brain capillary depletion was carried out using the brain homogenates. The capillary depleted samples were

compared to non-depleted samples. The difference between the capillary depleted and non-depleted samples was less than 1.9%, indicating the that the perfusion method was satisfactory in removing almost all the labeled protein from the brain capillaries.

The effects of HAV6 and ADTC5 in lysozyme distributions in kidney, lung, heart, spleen, and liver were also determined (**Figures 3.4C & D**). Visually, the most intense NIRF images were in the kidney in all three groups, with the highest image intensity on ADTC5 group. Quantitative data confirmed that lysozyme deposition in the kidney was the highest in the ADTC5-treated group, followed by the HAV6-treated group and control. It is not surprising that the lysozyme undergoes glomerular filtration in the kidney because of its molecular weight being lower than 65 kDa.

3.3.7 Brain Delivery of 65 kDa Albumin and Peripheral Organ Distributions.

To evaluate molecules larger than lysozyme, 65 kDa albumin was delivered using HAV6 and ADTC5 in C57BL/6 mice compared to control (*i.e.*, albumin alone) (**Figures 3.5A, B**). The calibration curve was generated with 0.5 to 500 ng/mL labeled albumin in brain homogenates to generate a good linearity with $R^2 \geq 0.98$. The mice treated with albumin + ADTC5 showed a significantly higher albumin deposition (40.7 ± 7.4 pmol/g brain) compared to albumin alone (11.8 ± 1.0 pmol/g; $p < 0.05$). Although it was not significant, the HAV6 group showed a trend of enhanced brain with brain deposition of 15.5 ± 3.1 pmol/g compared to control (11.8 ± 1.0 μmol/g brain ($p = 0.20$)). These data also showed that ADTC5 was a better BBB modulator than HAV6 in delivering albumin.

The effects of HAV6 and ADTC5 peptides in the distribution of albumin in different organs were evaluated using NIRF quantitative imaging (**Figures 3.5C**, **D**). The data indicated that HAV6 ($p = 0.04$) and ADTC5 ($p = 0.04$) significantly enhanced the distributions of albumin into the liver compared to control. There was no significant difference in albumin depositions between the liver ADTC5 group and the HAV6 group ($p = 0.15$). Although the deposition in spleen is lower than in

liver, the HAV5 and ADTC5 groups both enhanced the deposition of albumin in the spleen compared to control.

3.3.8 Brain Delivery of 150 kDa IgG mAb and Peripheral Organ Distributions.

Because many mAbs have been utilized as therapeutics, there is high interest in improving their brain delivery. For quantitative determinations, a calibration curve for mAb was prepared with concentrations ranging from 10 to 200 ng/mL of IRDye800CW-IgG mAb spiked into blank brain homogenates. The calibration curve showed good linearity with $R^2 \geq 0.99$. As in the previous study in SJL/elite, NIRF imaging signals from mAb in the brains of ADTC5+mAb-treated mice were higher than those of mAb-treated mice in C57BL/6 mice (**Figure 3.6A**). The amounts of mAb in the brains of mice treated with ADTC5+mAb (13.3 ± 0.7 pmol/g) were significantly higher compared to those of HAV6+mAb (3.42 ± 0.5 pmol/g; $p < 0.05$) and mAb alone (4.0 ± 0.4 pmol/g; $p < 0.05$) (**Figure 3.6B**). HAV6 peptide was not able to deliver mAb ($p > 0.05$) compared to control mAb (**Figure 3.6B**). The enhancement of mAb brain deposition by ADTC5 is about three times that of control. ADTC5 showed a trend to enhance the distribution of mAb into liver compared to HAV6- ($p = 0.06$) and control-treated animals ($p = 0.06$) (**Figures 3.6C, D**). The distributions of mAb in HAV6- and control-treated animals were about the same ($p = 0.54$).

3.3.9 Brain Delivery of 220 kDa Fibronectin and Peripheral Organ Distributions.

To find the larger limit of pore sizes made by ADTC5 peptide, the brain delivery of fibronectin (220 kDa) was evaluated in the presence and absence of ADTC5 (**Figure 3.7A, B**). HAV6 was not investigated for delivering 220 kDa fibronectin because it cannot deliver 150 kDa mAb. ADTC5 did not enhance brain delivery of 220 kDa fibronectin because the NIRF signals for the ADTC5 + fibronectin group ($35.498 \pm 3.001 \times 10^3$A.U.) was not different than that of fibronectin alone group ($33.026 \pm 2.080 \times 10^3$ A.U.) (**Figure 3.7A, B**). The distributions of fibronectin were mostly in the

liver, and ADTC5 did not influence the distribution of fibronectin in other organs (**Figure 3.7C, D**).

3.4 Discussion

Proteins have been successfully used to treat many diseases, and some proteins such as mAbs have been evaluated to treat brain diseases such as brain tumors (*e.g.,* glioblastoma) as well as neurodegenerative diseases, including Alzheimer's, multiple sclerosis (MS), and Parkinson's. Unfortunately, many proteins, including mAbs that were developed to treat brain diseases, have failed in clinical trials. One of the reasons is the inefficiency of proteins to cross the BBB sufficiently to exude their activities in the brain. The BBB plays a vital role in restricting unwanted molecules from reaching the brain for regulating the internal environment of the brain.[25] Various approaches have been investigated to deliver drugs to the brain following systemic administration. Our approach is to use cadherin peptides to modulate cadherin-cadherin interactions to create larger pores in the intercellular junctions to allow proteins to enter the brain in a non-invasive manner. In an initial proof-of-concept, ADTC5 peptide was used to deliver IRDye800CW-IgG mAb in SJL/elite mice. The brains of animals treated with ADTC5+IgG mAb had high NIRF intensities while very low NIRF intensities were observed in the brains of animals treated with IgG mAb alone (**Figure 3.2**). With the initial data, the next step was to compare the effectiveness of HAV6 and ADTC5 peptides in enhancing the brain delivery of various sized proteins such as 15 kDa lysozyme, 65 kDa albumin, 150 kDa IgG mAb, and 220 kDa fibronectin. It was proposed that each peptide has different BBB modulatory activities in delivering different sizes of proteins. In addition, each peptide creates a maximum pore size opening in the paracellular pathway so there is a cut-off size of proteins that can pass through the BBB. Thus, it was necessary to develop a rapid method to quantitatively determine the amount of protein delivered into the brain. Finally,

the effects of each peptide on the distributions of i.v. administered proteins in organs other than the brain were evaluated.

Prior to evaluating the delivery of various sized proteins, 150 kDa IR800-IRdye-IgG mAb was administered via i.v. tail-vein injection to SJL/elite mice in the presence (n = 5) and absence (n = 4) of ADTC5 peptide (13 μmol/kg) and allowed to circulate for 15 min (**Figure 3.2**). The brains of mice administered mAb alone (n = 4) showed very low background-intensity NIRF (**Figure 3.2 A**, left images), suggesting that little or no mAb entered the brain. The brains of mice administered mAb + ADTC5 showed high NIRF intensity, suggesting that ADTC5 enhanced mAb brain delivery (**Figure 3.2A**, right images). The mean pixel NIRF intensity was significantly higher (4.7 times higher) in mAb + ADTC5-treated mice compared to those from mice injected with mAb alone (**Figure 3.2B**). Because IgG mAb can be delivered to the brain, a NIRF quantitative method was developed to determine the amounts of delivered proteins in the brain per gram of brain (pmol/g brain).

To develop a simple, rapid, and quantitative method to determine the amount delivered protein in the brain, NIRF imaging method was used in this study. Calibration curves were developed for each delivered protein. Homogenized brain samples were spiked with different concentrations of standard labeled proteins, and fluorescence intensities were determined using with the Odyssey CLx scanner (**Figure 3.3A**). Good linearity for the calibration curve was achieved with $R^2 \geq 0.98$. The amount of delivered protein in the brain in pmol/g brain can be determined by interpolating the NIRF intensity from the brain homogenate into the calibration curve (**Figure 3.3B**). To validate the NIRF method, QC samples of IRDye800CW-lysozyme were analyzed to determine the stability, accuracy, and precision over the range of the calibration curve following FDA guidelines. Intra-day and inter-day precision and accuracy variability were found to be less than 15% (R.S.D

and R.E) (**Table 3.2**), suggesting that the NIRF method was accurate and precise. The stability of the labeled protein in brain homogenates was evaluated under different conditions; only the brain homogenates that were kept at room temperature for 6 h showed %R.S.D. values under 15%. It was found that the other conditions for the analytes were not stable in brain extracts, including −20 °C for 24 h followed by unassisted thawing at room temperature as well as after three freeze-thaw cycles between −20 °C and room temperature over a 24-h period. Therefore, all the analyses were done within the time frame of 6 h. With a linear calibration curve and lower %RSD and %RE values for precision and accuracy, the developed NIRF imaging method was very sensitive and reliable for detecting and quantifying the delivered labeled proteins.

To carry out the *in vivo* brain delivery experiments, the protein was administered via i.v. with and without BBB modulators (*i.e.*, HAV6 or ADTC5) followed by allowing the delivered protein to remain in the systemic circulation for 15 min. The animal was then euthanized, followed by perfusion of the brain capillaries to eliminate the remaining protein in the blood vessels. The brain was isolated and homogenized followed by transferring the homogenates into a 96-well plate. The intensity of NIRF from the protein in the homogenate was detected by scanning with the Odyssey CLx scanner and the intensity was normalized by weight of the brain. Previously, the NIRF method has been used to quantify study IRDye800CW mAb distribution *ex vivo* in tissues. The method was deemed to be accurate and sensitive when compared to a commonly used reference method called gamma ray quantification.[26] Comparison of NIRF and gamma ray quantification data sets using the Bland-Altman method concluded that the results from quantification using NIRF are the same as those using the gamma ray method.[26]

Comparison between the activities of ADTC5 and HAV6 in modulating the BBB provides insight into the paracellular pore size openings and potential use of each peptide in delivering

various sized proteins into the brain. In this study, ADTC5 peptide can effectively improve the delivery of lysozyme, albumin, and IgG mAb into the brains compared to control; however, ADTC5 cannot enhance the delivery of 220 kDa fibronectin. Using a 15-min circulation time, the results suggest that ADTC5 created pores large enough to allow proteins with the largest size between 150 and 220 kDa to penetrate the BBB. Using the same experimental conditions, HAV6 significantly enhanced the brain delivery of lysozyme but not albumin and IgG mAb, indicating that the pore-size opening in the BBB paracellular pathways was smaller than that crated by ADTC5. In summary, the modulatory activity of ADTC5 is distinctly different than that of HAV6; thus, this difference can be used to deliver selected groups of proteins, depending on the therapeutic need.

Although lysozyme is smaller than albumin and IgG mAb, no observable lysozyme was found in the brains when delivered with a dose of 21.6 nmol/kg along with HAV6 or ADTC5 at 13 μmol/kg (data not shown). In contrast, the lysozyme was observed in the brain when it was delivered at a higher dose (54 nmol/kg) along with HAV6 or ADTC5 at 13 μmol/kg (**Figure 3.4**). The depositions of lysozyme were significantly higher in the brain when delivered with ADTC5 compared to HAV6 peptide (**Figure 3.4A, B**). In addition, the amounts of lysozyme in the brains were slightly lower than albumin when delivered using HAV6 or ADTC5, although the administered dose of lysozyme was higher than that of albumin (**Table 3.4**). One of the explanations for the need of a higher dose of lysozyme is the rapid clearance of lysozyme in the kidney because of glomerular filtration. The depositions of lysozyme in the kidney were higher than in other organs (*i.e.,* heart, lung, spleen, and liver) (**Figures 3.4C, D**). It is interesting to find that ADTC5-treated mice have significantly enhanced deposition of lysozyme in the kidney compared to control, suggesting that ADTC5 affected cadherin interactions in the kidney. In

contrast, HAV6 did not significantly enhance the amount of lysozyme in the kidney compared to control. Previously, low molecular weight proteins (LMWP) have been shown to be suitable carriers for specific renal drug delivery due to their high accumulation in kidney. They are freely filtered in the glomerulus and subsequently accumulate specifically in the proximal tubular cells, utilizing receptor-mediated endocytosis.[27, 28] Conjugation of the antihypertensive drug captopril and the analgesic drug naproxen to lysozyme resulted in a 6–to–60-fold enriched accumulation in the kidney.[29] Taken together, the results suggest that the brain delivery of lysozyme or other proteins is influenced by its kidney clearance, resulting in a decrease in systemic concentration for penetration into the brain.

Albumin has been explored as a drug carrier where several strategies have been developed including various forms of physical and covalent binding (*e.g.*, albumin-drug and peptide conjugate) as well as drug encapsulation in albumin nanoparticles.[15, 30-32] Falcone *et al.* showed an improved brain uptake of radioactive-labeled albumin in CD1 mice when administered via intranasal delivery;[15] however, there is no clear mechanism for the way that albumin can be transported into the brain. The paracellular brain delivery of albumin using ADTC5 and HAV6 was compared and quantified by NIRF imaging. It showed a significantly higher brain deposition of albumin in the presence of ADTC5 compared to control and HAV6 peptide (**Figure 3.5A, B**). In contrast, the HAV6-treated group did not have significantly higher brain deposition of albumin compared to a control group (*i.e.*, albumin alone). Although, using the current conditions, HAV6 peptide did not enhance the delivery of albumin, our previous data showed that HAV6 peptide could significantly enhance the delivery of 65 kDa galbumin (a gadolinium complex conjugated to albumin) into the brain compared to control as detected using magnetic resonance imaging (MRI) in living mice.[22] In the MRI study, the dose of HAV6 peptide (10 μmol/kg) was similar to

the current study dose, but the dose of galbumin in the MRI study was 27 times higher (600 nmol/kg) than the dose (21.6 nmol/kg) in the current study.[22] The circulation time of the MRI study was 51 min compared to 15 min in the current study. Therefore, the high dose of galbumin provides a more pronounce amount of galbumin in the brain as detected by MRI. The MRI studies suggested that ADTC5 was a better enhancer of galbumin brain delivery than HAV6, and this previous finding was confirmed by the current findings when ADTC5 was compared to HAV6 in delivering IRdye800CW-albumin (**Table 3.4**). ADTC5 significantly enhanced brain deposition of albumin while HAV6 did not (**Figure 3.5A, B**). In summary, the data indicated that ADTC5 is a better modulator for large proteins compared to HAV6 peptide, and the dose of delivered molecules influences the transport of molecule across the BBB. The results also suggest that both peptides created different populations of small, medium, and large pore sizes, but ADTC5 created a higher population of large pores than did HAV6 peptide. Thus, ADTC5 allows larger molecules to penetrate the BBB compared to HAV6.

The enhancement of IgG mAb brain delivery using ADTC5 or HAV6 was evaluated. Due to their size, passive diffusion of IgG mAb across the BBB was very minimal and normally antibody brain concentrations are 1,000 times lower than in the bloodstream. Here, brain delivery of IgG mAb was significantly improved by ADTC5 in C57BL/6 mice but not by HAV6 (**Figure 3.5A, B**; **Table 3.4**). The results support a proposal that each peptide has a limit of size cut-off for delivering various sized proteins. In the future, the effects of circulation time and multiple injections of proteins will be explored in the future to determine the optimal delivery protocol for mAbs or other proteins. This method can also be used to rapidly screen the modulatory activity of new peptides in improving brain protein delivery.

The data from mice treated with both peptides suggest that there is a cut-off size for each peptide in delivering molecules to the brain. ADTC5 peptide did not enhance the delivery of fibronectin (220 kDa), suggesting that the molecular size cut-off for ADTC5 is 220 kDa. The molecular cut-off is important to limit the number of unwanted molecules or proteins from penetrating the BBB and potentially generating side effects. Another important characteristic for BBB modulation is the duration of the BBB modulation created by HAV6 and ADTC5 peptides to prevent long-term opening that would allow unwanted large molecules to enter the brain. Previously, ADTC5 and HAV6 have been shown to modulate the BBB immediately, allowing delivered molecules to enter the brain within 3 min.[17, 20, 22] The modulation of the BBB by HAV6 within the span of less than 1 h would allow a small molecule such as Gd-DTPA (547 Da) to enter the brain.[20] In contrast, HAV6 did not allow 65 kDa galbumin to enter the brain after a 10-min delay between delivery of HAV6 and galbumin.[22] Pretreatment of mice with ADTC5 produced a longer opening (between 2 and 4 h) than with HAV6 for a small molecule such as Gd-DTPA.[17] However, with large molecules (*e.g.,* galbumin, 65 kDa), ADTC5 showed an enhancement only after a 10-min delay of pretreatment with peptide but no enhancement after a 40-min pretreatment.[22] The duration of paracellular pathways opening of the BBB created by ADTC5 is longer for all types of molecules compared to HAV6.[22] For ADTC5 peptide, the BBB opening lasted for a smaller time frame for a large molecule than for a small molecule. More importantly, the BBB seals back to its original position after the clearance of the peptide, which is a crucial parameter in delivering selected proteins into the brain.[17, 22] Our previous studies using transmission electron microscopy showed that after modulation of the BBB with cadherin peptides (i.e., ADTC5) there are no detectable differences in the morphology of brain microvessel endothelial cells compared to that of unmodulated control.[17] We also found that vesicular activity

appeared to be similar in both vehicle and peptide-treated mice.[17] Taken together, these results suggest that each peptide creates different mechanism of modulatory activity that translate to generation of various pore sizes in the intercellular junctions. One hypothesis is that each peptide creates sub-populations of small, medium, and large pores in the intercellular junctions and the large pores collapse to medium and small pores and the medium pores collapse to small pores in a time-dependent manner. It is proposed that the large pores collapse faster than medium pores; this will be tested in the future.

Evaluations of ADTC5 and HAV6 peptides in other organs are necessary to assess their applicability as drug delivery enhancers because cadherin-mediated cell-cell adhesion is present in other organs (*i.e.*, kidney, lung, spleen, liver, and heart). Modulation of cadherin-cadherin interactions in other organs may lead to increased permeability to other parts of the body, which can lead to off-target site delivery as well as side effects in the host. Therefore, it is necessary to find out the effects of each peptide on the deposition of delivered proteins in other organs. The results could also be utilized to design better and selective BBB modulators that will not affect other organs. As mentioned previously, 15 kDa lysozyme is highly accumulated in the kidney compared to other organs (*i.e.*, heart, spleen, lungs, and liver) for all three groups (*i.e.*, control, HAV6-, and ADTC5-treated groups). ADTC5-treated groups had significantly higher lysozyme kidney deposition compared to control while HAV6-treated groups did not. ADTC5-treated groups for all other proteins larger than lysozyme have higher deposition in the liver compared to control but lower deposition in kidney, spleen, lung, and heart. For HAV6-treated groups, only albumin has higher deposition in the liver compared to control, and there were no significant differences in other organs. There was no enhancement of fibronectin deposition in the liver of ADTC5-treated groups. In summary, ADTC5 has influenced in depositions of delivered proteins in kidney or liver

while HAV6 has influence in protein deposition in kidney and liver for lysozyme and albumin, respectively.

The BBB modulatory activities of ADTC5 and HAV6 peptide were due their binding to cadherin and inhibiting cadherin-cadherin interactions in the intercellular junctions of the BBB. Both HAV6 and ADTC5 peptides bind to the EC1 domain of E-cadherin at different binding sites as determined using heteronuclear single quantum correlation (HSQC) NMR spectroscopy and molecular docking experiments. ADTC5 binds to I4, P5, P6, S8, and P10 residues on the N-terminal β sheet of the EC1 domain while HAV6 binds to the Y36, I38, F77, S78, and I94 residues of the EC1 domain.[33] Using the X-ray structure of C-cadherin as a model, it is proposed that HAV6 peptide binds to the EC1 domain and blocks the EC1-EC2 *cis*-cadherin derived from two cadherins on the same cell membranes.[34, 35] In contrast, ADTC5 bind to the domain-swapping region of EC1 and inhibits EC1-EC1 *trans*-cadherin interactions from the opposite cells.[33] Because ADTC5 blocks *trans*-cadherin interactions, its effects on the intercellular junctions presumably are more pronounced than those of HAV6, which inhibits *cis*-cadherin interactions. Experimentally, our data for all proteins indicate that ADTC5 has higher modulatory activity and longer duration of BBB modulation than HAV6, and these observations could partly be explained by their binding mechanisms.

3.5 Conclusion

ADTC5 can deliver 15 kDa lysozyme, 65 kDa albumin, and 150 kDa mAb IgG but not 220 kDa into the brain of C57BL/6 mice while HAV6 can enhance only brain delivery of lysozyme. Each peptide creates cut-off size of proteins that can be delivered into the brain. HAV6 peptide only allows molecule less than 65 kDa to enter the brain while ADTC5 can deliver molecules of less than 220 kDa to enter the brain. ADTC5 and HAV6 peptides could enhance the depositions

of delivered proteins in the kidney and liver. Finally, the NIRF imaging method is a very useful and rapid method to quantitively determine the amounts of delivery of proteins in the brain.

3.6. Figures and Legends

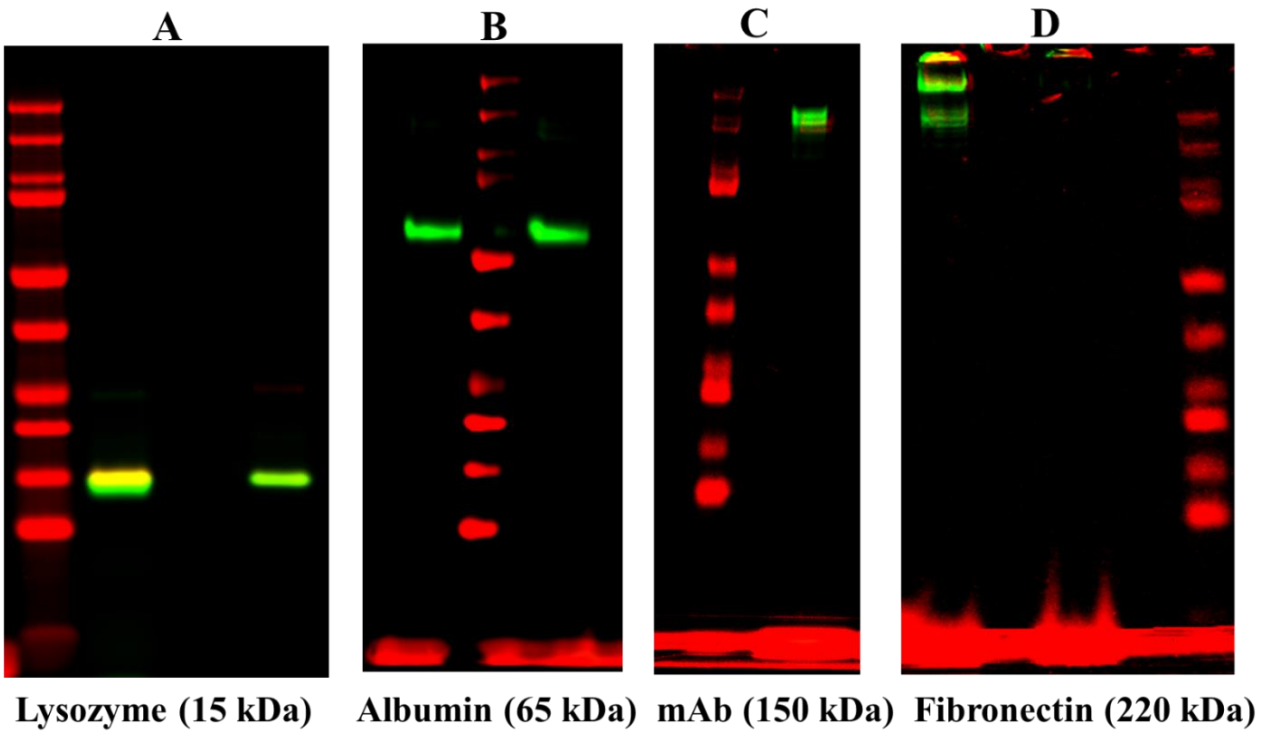

Figure 3.1 The SDS PAGE gels IRdye800CW-labeled (A) 15 kDa Lysozyme, (B) 65 kDa Albumin, (C) 150kDa IgG mAb, and (D) 220 kDa Fibronectin that are imaged using Odyssey CLx imaging system to determine protein purity and the absence of unconjugated IRdy800cw.

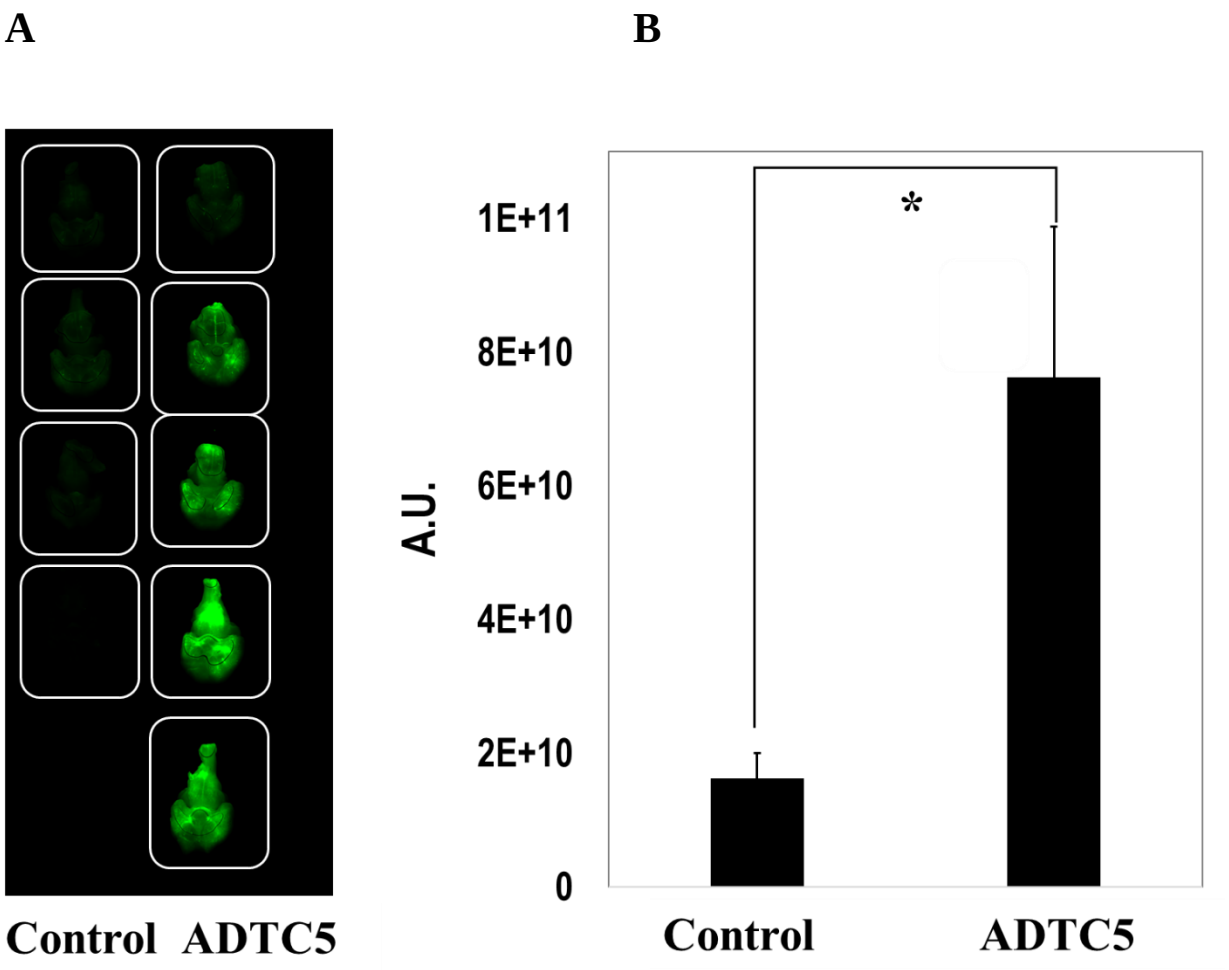

Figure 3.2 The effect of ADTC5 (13 µmol/kg) on improving the brain delivery of IRdye800CW-IgG mAb (21.6 nmol/kg) in SJL/elite mice. **(A)** The image shows whole brain fluorescent of mice that received IRDye800cw-IgG mAb alone (left; n = 4) and IRDye800cw-IgG mAb + ADTC5 (right; n = 5). **(B)** Mean fluorescence intensity of IRDye800cw-IgG mAb for quantitative comparison of NIRF signals between mice that received IRDye800cw-IgG mAb+ADTC5 *vs.* IRDye800cw-IgG mAb alone; asterisk (*) indicates a significant difference from the control group with ADTC5 group with $p < 0.05$. Error bars show the mean ± SE from control and ADTC5-treated group.

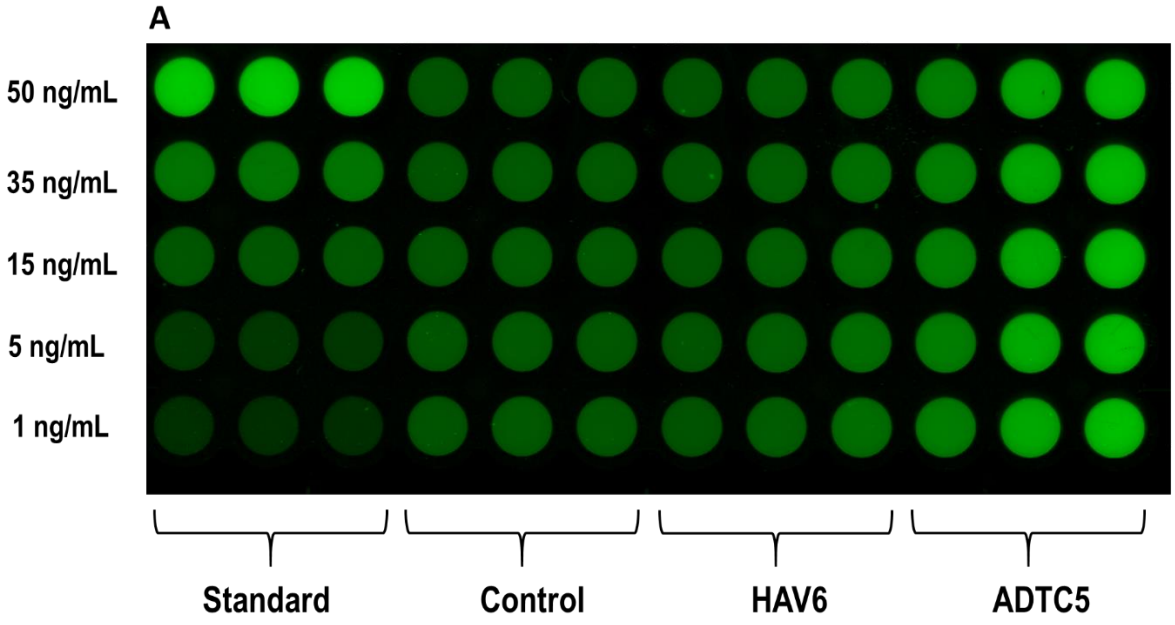
A
50 ng/mL
35 ng/mL
15 ng/mL
5 ng/mL
1 ng/mL
Standard
Control
HAV6
ADTC5

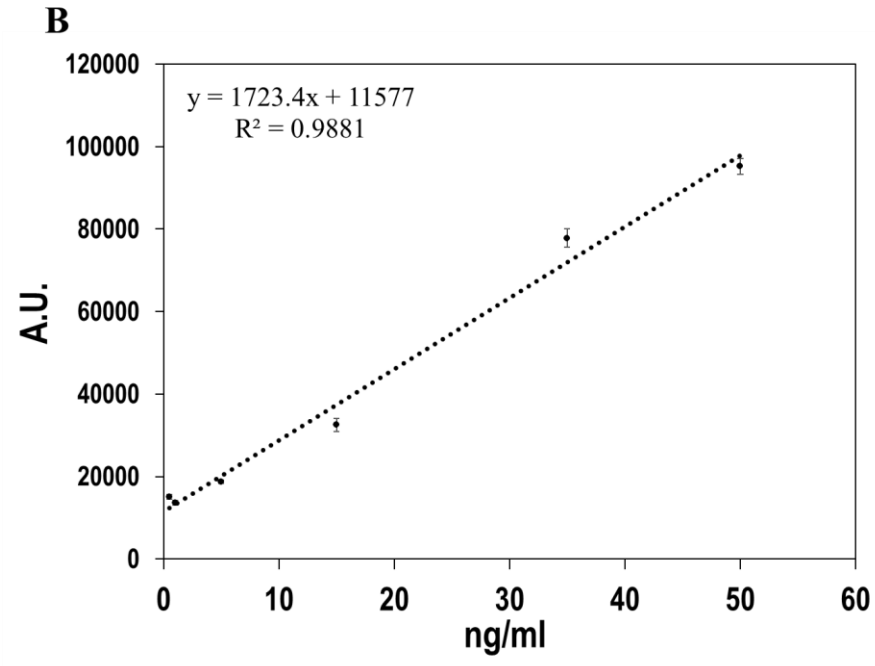
B
y = 1723.4x + 11577
R² = 0.9881
A.U.
ng/ml
120000
100000
80000
60000
40000
20000
0
0
10
20
30
40
50
60

Figure 3.3 Development of the quantification method and standard curve for IRdye800CW-lysozyme using NIRF image of brain homogenates in a 96-well plate scanned using Odyssey CLx imaging system. **(A)** Examples of scanned images of brain homogenates from various concentrations of standard samples as well as samples form HAV6- and ADTC5-treated mice. Each well was scanned to get the NIRF intensity. **(B)** An example of calibration curve for lysozyme ($R = 0.988$) was generated by plotting the concentrations of spiked standard against the fluorescence intensity. The concentrations of lysozyme in the brains of HAV6- and ADTC5-treated mice were determined by interpolating the fluorescence intensity in the standard curve.

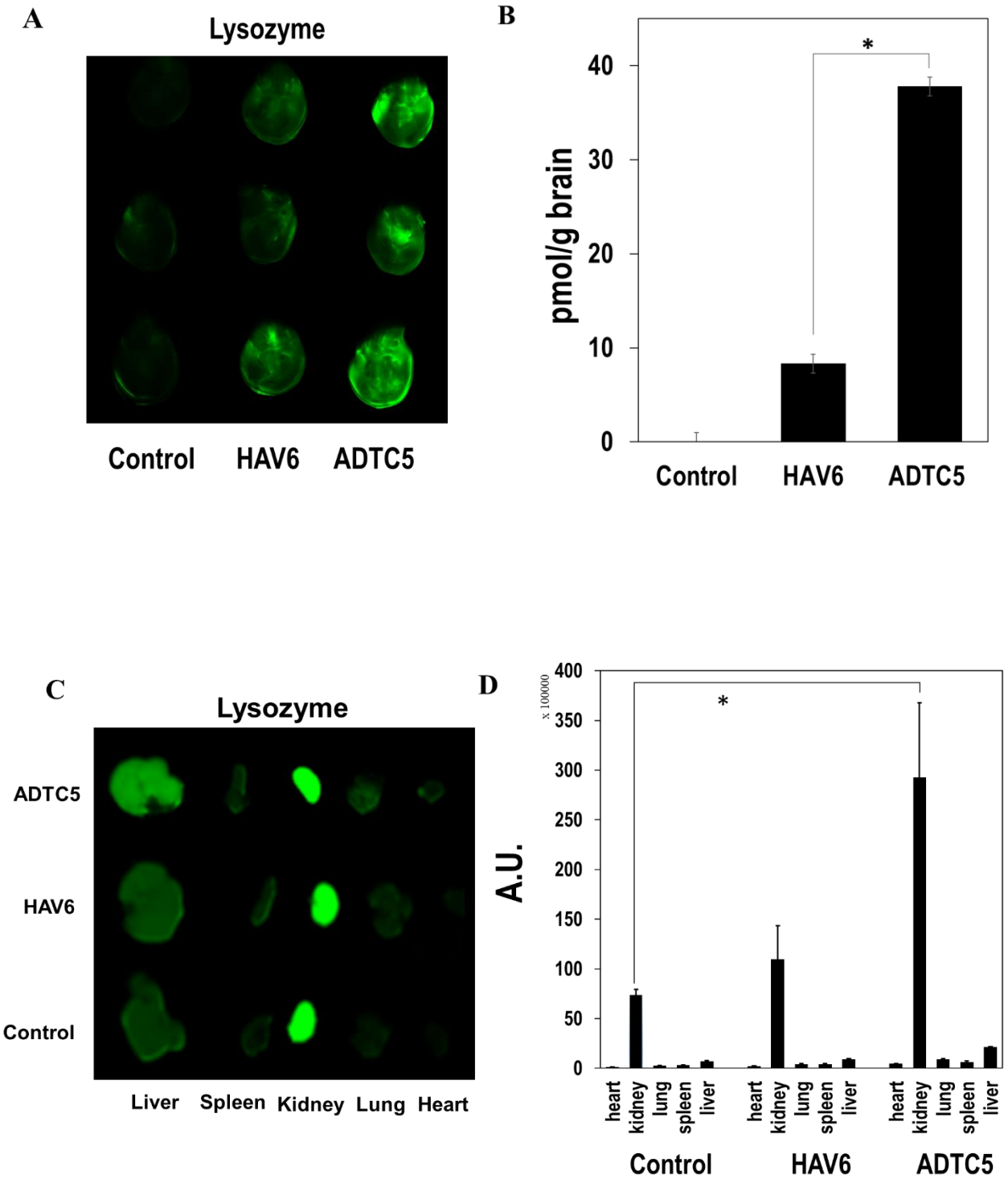
A
Lysozyme
Control
HAV6
ADTC5
B
pmol/g brain
40
30
20
10
0
*
Control
HAV6
ADTC5
C
Lysozyme
ADTC5
HAV6
Control
Liver
Spleen
Kidney
Lung
Heart
D
A.U.
x 100000
400
350
300
250
200
150
100
50
0
*
heart
kidney
lung
spleen
liver
Control
HAV6
ADTC5

Figure 3.4 Qualitative and quantitative comparisons of IRdye800CW-lysozyme (64 nmol/kg) depositions in the brain and other organs when administered alone and along with HAV6 and ADTC5 peptides (13 μmol/kg). **(A)** Qualitative comparison of NIRF brain images from control, HAV-, and ADTC5-treated animals. (B) Quantitative comparisons of lysozyme brain depositions in pmol/g brain for control, HAV6-, and ADTC5-treated mice. **(C)** A representative of lysozyme depositions in heart, kidney, lung, spleen, and liver. **(D)** Comparisons of lysozyme depositions in of various organs using tissue NIRF signal intensities. Asterisk (*) indicates a significant difference from the control group with ADTC5 group with $p < 0.05$. Error bars show the mean ± SE from control and ADTC5-treated group.

A

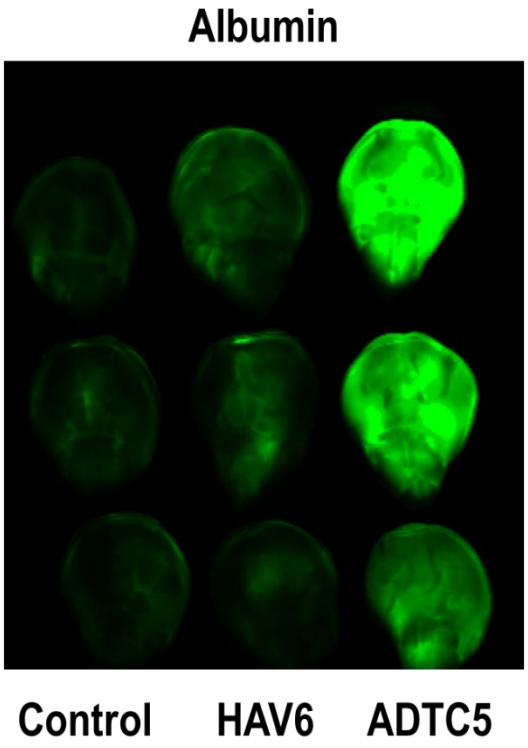
Albumin
Control
HAV6
ADTC5

B

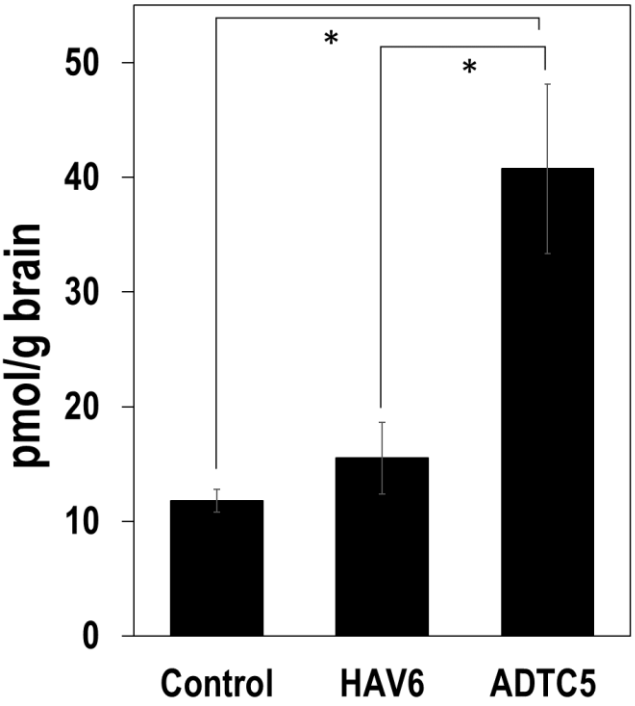
pmol/g brain
0
10
20
30
40
50
*
*
Control
HAV6
ADTC5

C

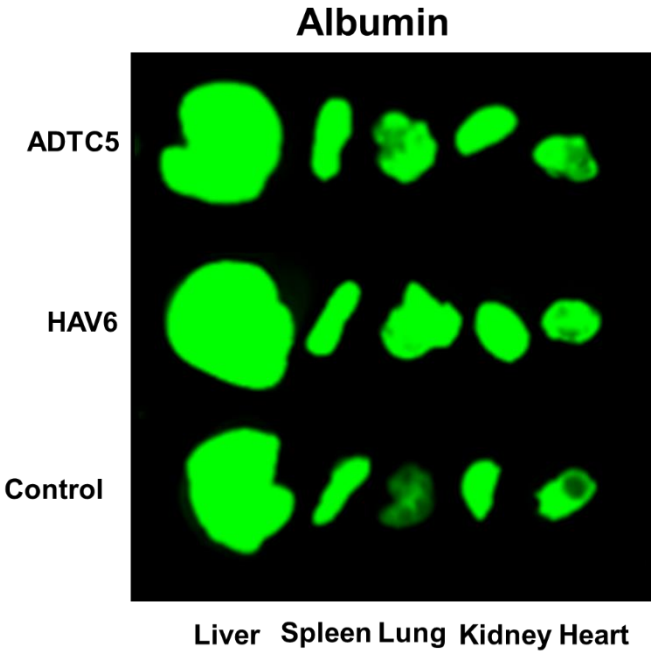
Albumin
ADTC5
HAV6
Control
Liver
Spleen
Lung
Kidney
Heart

D

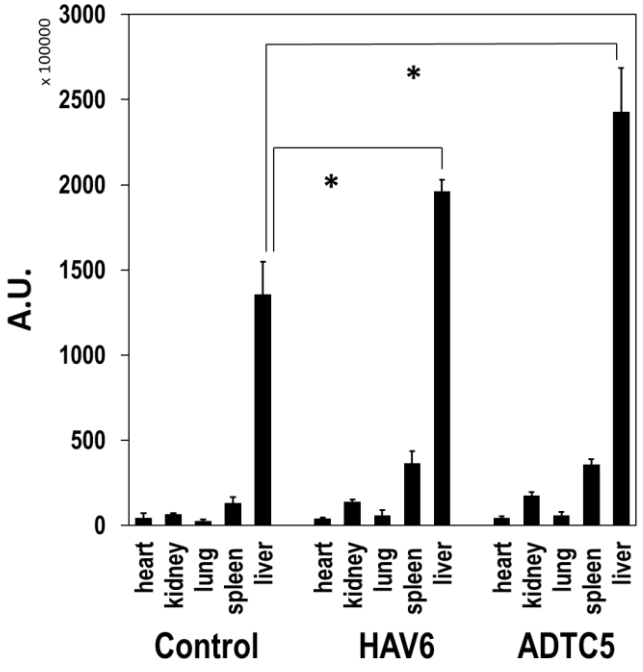
x 100000
A.U.
0
500
1000
1500
2000
2500
3000
*
*
heart
kidney
lung
spleen
liver
Control
HAV6
ADTC5

Figure 3.5 Qualitative and quantitative comparisons of IRdye800CW-albumin (21.6 nmol/kg) depositions in the brain and other organs when administered alone and along with HAV6 and ADTC5 peptides (13 μmol/kg). **(A)** Qualitative comparison of NIRF brain images from control, HAV-, and ADTC5-treated animals. **(B)** Quantitative comparisons of albumin brain depositions in pmol/g brain for control, HAV6-, and ADTC5-treated mice. **(C)** A representative of lysozyme depositions in heart, kidney, lung, spleen, and liver. **(D)** Comparisons of albumin depositions in of various organs using tissue NIRF signal intensities. Asterisk (*) indicates a significant difference from the control group with ADTC5 group with $p < 0.05$. Error bars show the mean ± SE from control and ADTC5-treated group.

A

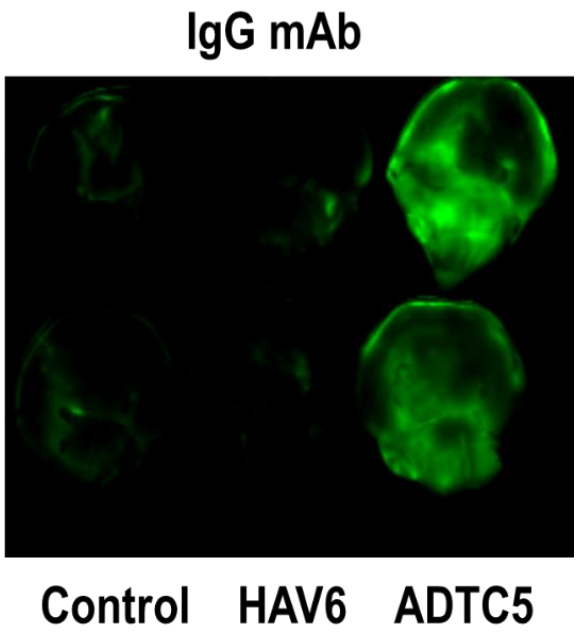
IgG mAb
Control
HAV6
ADTC5

B

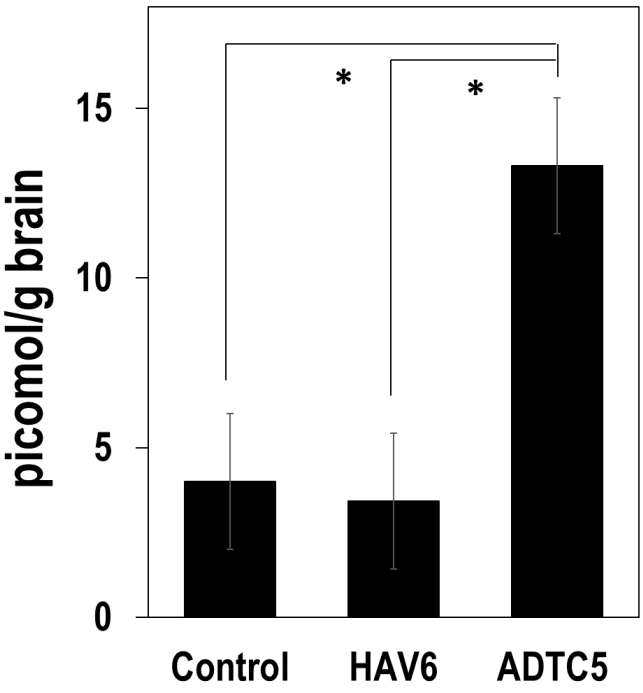
picomol/g brain
0
5
10
15
*
*
Control
HAV6
ADTC5

C

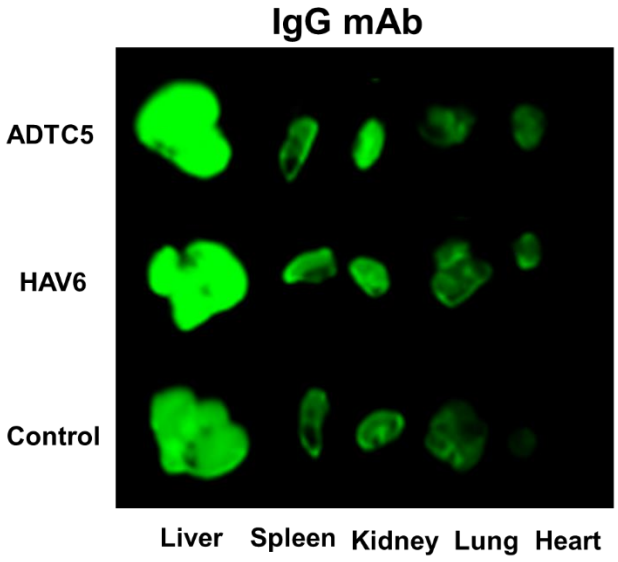
IgG mAb
ADTC5
HAV6
Control
Liver
Spleen
Kidney
Lung
Heart

D

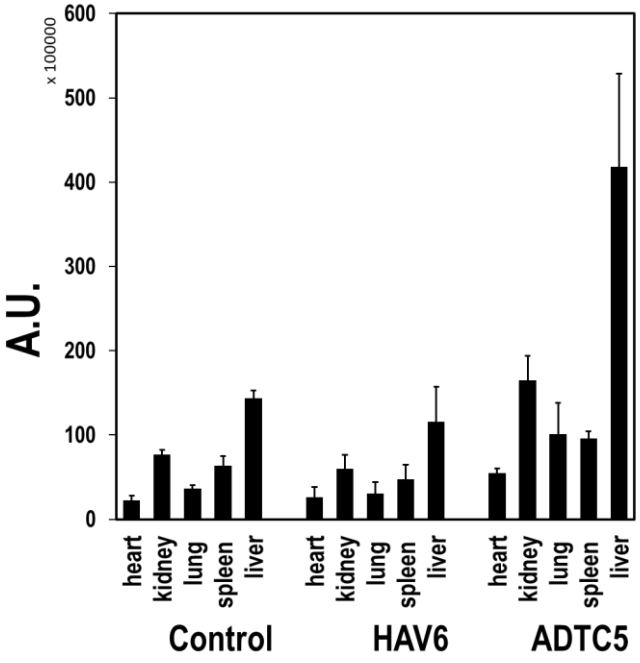
A.U.
x 100000
0
100
200
300
400
500
600
heart
kidney
lung
spleen
liver
Control
HAV6
ADTC5

Figure 3.6 Qualitative and quantitative comparisons of IRdye800CW-IgG mAb (21.6 nmol/kg) depositions in the brain and other organs when administered alone and along with HAV6 and ADTC5 peptides (13 μmol/kg). **(A)** Qualitative comparison of NIRF brain images from control, HAV-, and ADTC5-treated animals. **(B)** Quantitative comparisons of IgG mAb brain depositions in pmol/g brain for control, HAV6-, and ADTC5-treated mice. **(C)** A representative of IgG mAb depositions in heart, kidney, lung, spleen, and liver. **(D)** Comparisons of IgG mAb depositions in of various organs using tissue NIRF signal intensities. Asterisk (*) indicates a significant difference from the control group with ADTC5 group with $p < 0.05$. Error bars show the mean ± SE from control and ADTC5-treated group.

A

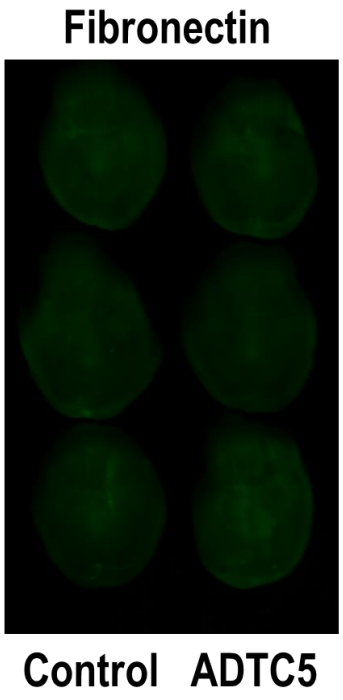
Fibronectin
Control
ADTC5

B

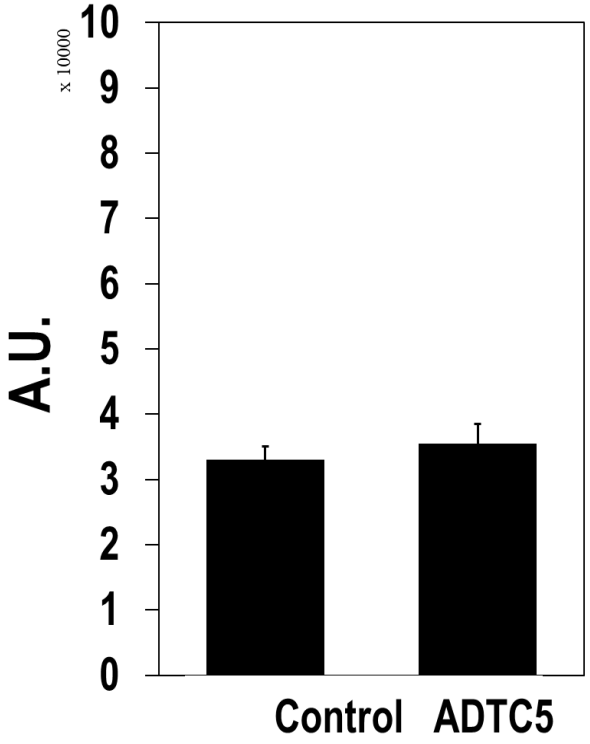
x 10000
10
9
8
7
6
5
4
3
2
1
0
A.U.
Control
ADTC5

C

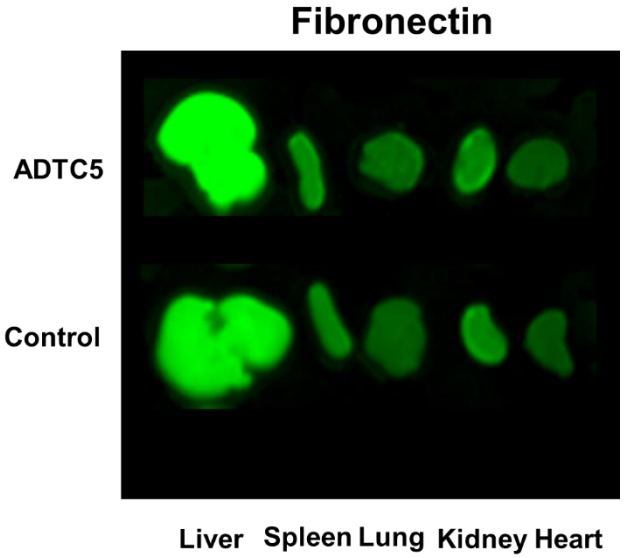
Fibronectin
ADTC5
Control
Liver
Spleen
Lung
Kidney
Heart

D

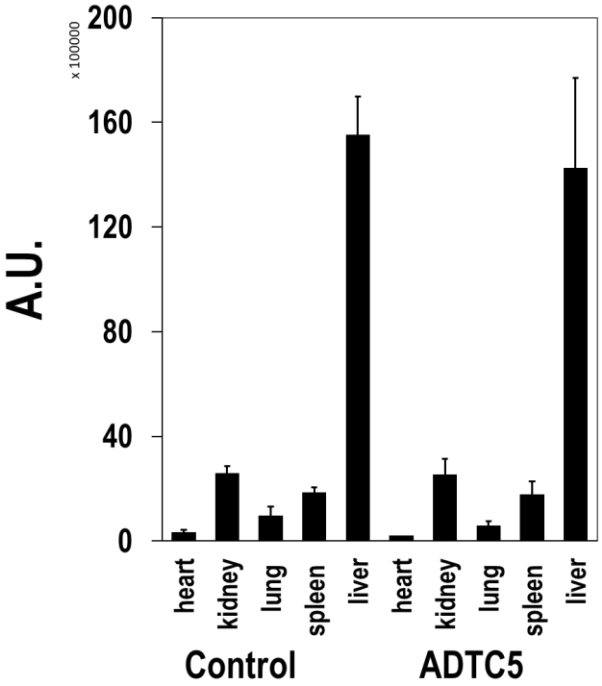
x 100000
200
160
120
80
40
0
A.U.
heart
kidney
lung
spleen
liver
heart
kidney
lung
spleen
liver
Control
ADTC5

Figure 3.7 Qualitative and quantitative comparisons of IRdye800CW-fibronectin (21.6 nmol/kg) depositions in the brain and other organs when administered alone and along with ADTC5 peptide (13 μmol/kg). **(A)** Qualitative comparison of NIRF brain images from control, HAV-, and ADTC5-treated animals. **(B)** NIRF intensities of brain homogenates from ADTC5-treated and control mice. **(C)** A representative of fibronectin depositions in heart, kidney, lung, spleen, and liver. **(D)** Comparisons of fibronectin depositions in of various organs using tissue NIRF signal intensities. Asterisk (*) indicates a significant difference from the control group with ADTC5 group with $p < 0.05$. Error bars show the mean ± SE from control and ADTC5-treated group.

3.7. References

1. Tomlinson, I. M. Next-generation protein drugs. *Nature Biotechnology* **2004,** *22*, 521.
2. Numakawa, T.; Suzuki, S.; Kumamaru, E.; Adachi, N.; Richards, M.; Kunugi, H. BDNF function and intracellular signaling in neurons. *Histol Histopathol* **2010,** *25*, (2), 237-58.
3. Masoudi, R.; Ioannou, M. S.; Coughlin, M. D.; Pagadala, P.; Neet, K. E.; Clewes, O.; Allen, S. J.; Dawbarn, D.; Fahnestock, M. Biological activity of nerve growth factor precursor is dependent upon relative levels of its receptors. *J Biol Chem* **2009,** *284*, (27), 18424-33.
4. Apel, P. J.; Ma, J.; Callahan, M.; Northam, C. N.; Alton, T. B.; Sonntag, W. E.; Li, Z. Effect of locally delivered IGF-1 on nerve regeneration during aging: an experimental study in rats. *Muscle Nerve* **2010,** *41*, (3), 335-41.
5. Laksitorini, M.; Prasasty, V. D.; Kiptoo, P. K.; Siahaan, T. J. Pathways and progress in improving drug delivery through the intestinal mucosa and blood-brain barriers. *Ther Deliv* **2014,** *5*, (10), 1143-63.
6. Kiptoo, P.; Laksitorini, M. D.; Siahaan, T. J., Blood-Brain Peptides: Peptide Delivery. In *Handbook of Biologically Active Peptides*, Kastin, A., Ed. Academic Press: Boston, 2013; pp 1702–1710.
7. Bickel, U.; Yoshikawa, T.; Pardridge, W. M. Delivery of peptides and proteins through the blood-brain barrier. *Adv Drug Deliv Rev* **2001,** *46*, (1-3), 247-79.
8. Carter, P. J.; Lazar, G. A. Next generation antibody drugs: pursuit of the 'high-hanging fruit'. *Nat Rev Drug Discov* **2018,** *17*, (3), 197-223.
9. Ineichen, B. V.; Plattner, P. S.; Good, N.; Martin, R.; Linnebank, M.; Schwab, M. E. Nogo-A Antibodies for Progressive Multiple Sclerosis. *CNS Drugs* **2017,** *31*, (3), 187-198.

10. Ruggieri, S.; Tortorella, C.; Gasperini, C. Anti lingo 1 (opicinumab) a new monoclonal antibody tested in relapsing remitting multiple sclerosis. *Expert Rev Neurother* **2017,** *17*, (11), 1081-1089.

11. Ciric, B.; Howe, C. L.; Paz Soldan, M.; Warrington, A. E.; Bieber, A. J.; Van Keulen, V.; Rodriguez, M.; Pease, L. R. Human monoclonal IgM antibody promotes CNS myelin repair independent of Fc function. *Brain Pathol* **2003,** *13*, (4), 608-16.

12. Fisher, T. L.; Reilly, C. A.; Winter, L. A.; Pandina, T.; Jonason, A.; Scrivens, M.; Balch, L.; Bussler, H.; Torno, S.; Seils, J.; Mueller, L.; Huang, H.; Klimatcheva, E.; Howell, A.; Kirk, R.; Evans, E.; Paris, M.; Leonard, J. E.; Smith, E. S.; Zauderer, M. Generation and preclinical characterization of an antibody specific for SEMA4D. *MAbs* **2016,** *8*, (1), 150-62.

13. Lipinski, C. A. Lead- and drug-like compounds: the rule-of-five revolution. *Drug Discov Today Technol* **2004,** *1*, (4), 337-41.

14. Kobus, T.; Zervantonakis, I. K.; Zhang, Y.; McDannold, N. J. Growth inhibition in a brain metastasis model by antibody delivery using focused ultrasound-mediated blood-brain barrier disruption. *J Control Release* **2016,** *238*, 281-288.

15. Falcone, J. A.; Salameh, T. S.; Yi, X.; Cordy, B. J.; Mortell, W. G.; Kabanov, A. V.; Banks, W. A. Intranasal administration as a route for drug delivery to the brain: evidence for a unique pathway for albumin. *J Pharmacol Exp Ther* **2014,** *351*, (1), 54-60.

16. Neuwelt, E. A.; Barnett, P. A.; Hellstrom, I.; Hellstrom, K. E.; Beaumier, P.; McCormick, C. I.; Weigel, R. M. Delivery of melanoma-associated immunoglobulin monoclonal antibody and Fab fragments to normal brain utilizing osmotic blood-brain barrier disruption. *Cancer Res* **1988,** *48*, (17), 4725-9.

17. Laksitorini, M. D.; Kiptoo, P. K.; On, N. H.; Thliveris, J. A.; Miller, D. W.; Siahaan, T. J. Modulation of intercellular junctions by cyclic-ADT peptides as a method to reversibly increase blood-brain barrier permeability. *J Pharm Sci* **2015,** *104*, (3), 1065-75.

18. Doolittle, N. D.; Muldoon, L. L.; Culp, A. Y.; Neuwelt, E. A. Delivery of chemotherapeutics across the blood-brain barrier: challenges and advances. *Adv Pharmacol* **2014,** *71*, 203-43.

19. Kiptoo, P.; Sinaga, E.; Calcagno, A. M.; Zhao, H.; Kobayashi, N.; Tambunan, U. S.; Siahaan, T. J. Enhancement of drug absorption through the blood-brain barrier and inhibition of intercellular tight junction resealing by E-cadherin peptides. *Mol. Pharm.* **2011,** *8*, (1), 239-49.

20. On, N. H.; Kiptoo, P.; Siahaan, T. J.; Miller, D. W. Modulation of blood-brain barrier permeability in mice using synthetic E-cadherin peptide. *Mol Pharm* **2014,** *11*, (3), 974-81.

21. Tabanor, K.; Lee, P.; Kiptoo, P.; Choi, I. Y.; Sherry, E. B.; Eagle, C. S.; Williams, T. D.; Siahaan, T. J. Brain Delivery of Drug and MRI Contrast Agent: Detection and Quantitative Determination of Brain Deposition of CPT-Glu Using LC-MS/MS and Gd-DTPA Using Magnetic Resonance Imaging. *Mol Pharm* **2016,** *13*, (2), 379-90.

22. Ulapane, K. R.; On, N.; Kiptoo, P.; Williams, T. D.; Miller, D. W.; Siahaan, T. J. Improving Brain Delivery of Biomolecules via BBB Modulation in Mouse and Rat: Detection using MRI, NIRF, and Mass Spectrometry. *Nanotheranostics* **2017,** *1*, (2), 217-231.

23. Alaofi, A.; On, N.; Kiptoo, P.; Williams, T. D.; Miller, D. W.; Siahaan, T. J. Comparison of Linear and Cyclic His-Ala-Val Peptides in Modulating the Blood-Brain Barrier Permeability: Impact on Delivery of Molecules to the Brain. *J Pharm Sci* **2016,** *105*, (2), 797-807.

24. Triguero, D.; Buciak, J.; Pardridge, W. M. Capillary depletion method for quantification of blood-brain barrier transport of circulating peptides and plasma proteins. *Journal of neurochemistry* **1990,** *54*, (6), 1882-8.

25. Dufès, C., Chapter 6 - Brain Delivery of Peptides and Proteins. In *Peptide and Protein Delivery*, Van Der Walle, C., Ed. Academic Press: Boston, 2011; https://doi.org/10.1016/B978-0-12-384935-9.10006-9pp 105-122.

26. Oliveira, S.; Cohen, R.; Walsum, M. S.; van Dongen, G. A.; Elias, S. G.; van Diest, P. J.; Mali, W.; van Bergen En Henegouwen, P. M. A novel method to quantify IRDye800CW fluorescent antibody probes ex vivo in tissue distribution studies. *EJNMMI research* **2012,** *2*, (1), 50.

27. Haas, M.; Kluppel, A. C.; Wartna, E. S.; Moolenaar, F.; Meijer, D. K.; de Jong, P. E.; de Zeeuw, D. Drug-targeting to the kidney: renal delivery and degradation of a naproxen-lysozyme conjugate in vivo. *Kidney Int* **1997,** *52*, (6), 1693-9.

28. Haverdings, R. F. G.; Haas, M.; Greupink, A. R.; deVries, P. A. M.; Moolenaar, F.; de Zeeuw, D.; Meijer, D. K. F. POTENTIALS AND LIMITATIONS OF THE LOW-MOLECULAR-WEIGHT PROTEIN LYSOZYME AS A CARRIER FOR RENAL DRUG TARGETING. *Renal Failure* **2001,** *23*, (3-4), 397-409.

29. Kok, R. J.; Grijpstra, F.; Walthuis, R. B.; Moolenaar, F.; de Zeeuw, D.; Meijer, D. K. Specific delivery of captopril to the kidney with the prodrug captopril-lysozyme. *J Pharmacol Exp Ther* **1999,** *288*, (1), 281-5.

30. Kratz, F. Albumin as a drug carrier: design of prodrugs, drug conjugates and nanoparticles. *J Control Release* **2008,** *132*, (3), 171-83.

31. Kratz, F.; Elsadek, B. Clinical impact of serum proteins on drug delivery. *J Control Release* **2012,** *161*, (2), 429-45.

32. Lin, T.; Zhao, P.; Jiang, Y.; Tang, Y.; Jin, H.; Pan, Z.; He, H.; Yang, V. C.; Huang, Y. Blood–Brain-Barrier-Penetrating Albumin Nanoparticles for Biomimetic Drug Delivery via Albumin-Binding Protein Pathways for Antiglioma Therapy. *ACS Nano* **2016,** *10*, (11), 9999-10012.

33. Alaofi, A.; Farokhi, E.; Prasasty, V. D.; Anbanandam, A.; Kuczera, K.; Siahaan, T. J. Probing the interaction between cHAVc3 peptide and the EC1 domain of E-cadherin using NMR and molecular dynamics simulations. *J Biomol Struct Dyn* **2017,** *35*, (1), 92-104.

34. Wheelock, M. J.; Shintani, Y.; Maeda, M.; Fukumoto, Y.; Johnson, K. R. Cadherin switching. *Journal of cell science* **2008,** *121*, (6), 727.

35. Angst, B. D.; Marcozzi, C.; Magee, A. I. The cadherin superfamily: diversity in form and function. *Journal of cell science* **2001,** *114*, (Pt 4), 629-41.

CHAPTER 4

Improving *In Vivo* Brain Delivery of Monoclonal Antibody Using Novel Cyclic Peptides

4.1. Introduction

Insufficient delivery of drugs across the blood-brain barrier (BBB) has become the major challenge in diagnosing and treating brain-related diseases.[1-3] Many large molecule therapeutics such as neurotrophic factors, enzymes, and antibodies are being developed to treat brain disorders such as neurodegenerative diseases (e.g., multiple sclerosis (MS) and Alzheimer's disease (AD)) and brain tumors (e.g., glioblastoma and medulloblastoma); however, the BBB is one of their major hurdles for entering the brain. Most large molecules such as monoclonal antibodies (mAbs) have low efficiency to enter the brain because any molecule that crosses the BBB requires appropriate physicochemical properties or a specific transporter. The BBB is a very selective barrier whose main function is to regulate the passage of nutrients into brain and provide brain protection against toxic compounds and pathogens. The transcellular pathway, which many hydrophobic drugs utilize to cross the BBB, is also limited to molecules with physicochemical properties that at least satisfy Lipinski's rule of five.[4] Even if a molecule satisfies Lipinski's rule, it can still be prevented from crossing the BBB by efflux pumps.[2]

The paracellular pathway, where a drug molecule can pass through the intercellular junction, is also limited to small ions and hydrophilic molecules with hydrodynamic radius <11 Å.[2] This is due to the presence of tight junctions between two opposing cellular membranes. Therefore, large hydrophilic molecules such as peptides and proteins normally cannot passively diffuse through the paracellular pathway. On the other hand, a selected number of peptides and proteins (e.g., insulin, transferrin) can cross the BBB via the transcellular pathway because they have specific transporter systems (e.g., insulin and transferrin receptors).[3, 5-9] Currently, many neurotrophic factors such as nerve growth factor (NGF)[10] and brain-derived neurotrophic factor (BDNF)[11] have been investigated for treating neurodegenerative diseases such as MS and AD. Unfortunately, as with other proteins, the brain delivery of NGF or BDNF is still very challenging. Therefore, there is an

urgent need to develop methods that are safe and effective for improving delivery of proteins and peptides into the brain.

Several attempts have been made to overcome this challenge using various invasive and non-invasive methods. Intracerebral ventricular (ICV) delivery has currently been used as an invasive injection technique where drug substances are administered directly into the cerebrospinal fluid in cerebral ventricles. Alternatively, many non-invasive methods have been investigated *in vivo* with various levels of successes using receptor-mediated drug delivery systems, liposomes, microbubble-enhanced diagnostic ultrasound (MEUS), and nanoparticles.[12-14] The most successful non-invasive method for delivering drugs to brain tumor patients is the osmotic BBB disruption, which utilizes a mannitol hypertonic solution to shrink the vascular endothelial cells and increase the porosity of the paracellular pathway to improve permeation of antitumor drugs from the blood into the brain.[15-17] Following in the footsteps of the osmotic BBB method, we designed cadherin peptides (e.g., HAV6 and ADTC5) that modulate cadherin-cadherin interactions in the adherens junctions to increase porosity of the BBB paracellular pathways to allow molecules to cross from the bloodstream into the brain.[1, 2] The proposed mechanism is that cadherin peptides inhibit cadherin-mediated cell-cell adhesion in a specific, dynamic, and equilibrium fashion. Both HAV6 and ADTC5 peptides were derived from the extracellular-1 (EC-1) domain of E-cadherin and, collectively, they have been shown to increase the brain delivery of various molecules, including paracellular markers (e.g., ^{14}C-mannitol, 25 kDa IRdye800CW-polyethylene glycols or PEG), anticancer drugs (e.g., ^{3}H-daunomycin, Glu-CPT, adenanthin), efflux pump substrates (e.g., rhodamine 800 (R800), ^{3}H daunomycin), magnetic resonance imaging (MRI)-enhancing agents (e.g., gadopentetic acid or Gd-DTPA), peptides (e.g., IRdye800cw-cLABL and cIBR7), and proteins (e.g., 65 kDa galbumin).[18-23]

Table 4.1. Peptide Names and Peptide Sequences			
Peptide	**Sequence**	**Mass (Da)**	**Exact Mass (Da)**
Cyclic ADTC5	Cyclo(1,7)Ac-CDTPPVC-NH_2	772	795.2778 (+ Na^+)
Linear ADTHAV	Ac-TPPVSHAV-NH_2	847	848.4602
Cyclic ADTHAV	Cyclo(1,8)TPPVSHAV	788	789.9167
Linear HAV6	Ac-SHAVSS-NH_2	627	650.2869 (+ Na^+)
Cyclic HAVN1	Cyclo(1,6)SHAVSS	568	569.2352
Cyclic HAVN2	Cyclo(1,5)SHAVS	481	482.2286

The goal of this study was to design and synthesize novel cyclic peptides derived from HAV6 and ADTC5 peptides to improve their BBB modulatory activity by forming a peptide bond from the N- to C-termini. The hypothesis is that the formation of N- to C-termini cyclic peptides increases backbone rigidity of the peptide to improve binding affinity for the EC1 domain cadherin as well as improving plasma stability of the cyclic peptide compared to its parent linear peptide. Previously, cHAVc3 and ADTC5 cyclic peptides were formed using a disulfide bond between two Cys residues at the N- and C-termini; these cyclic peptides have enhanced BBB modulatory activity and plasma stability compared to their parent linear peptides.[19, 20] However, a disulfide bond in cyclic peptides can be reduced by glutathione in plasma to form a linear peptide that may have lower biological activity. Thus, we designed stable N- to C-termini cyclic peptides (i.e., HAVN1 and HAVN2) derived from HAV6 and cyclic ADTHAV peptide utilizing a combination of sequences from ADT and HAV peptides (**Table 4.1**). A cyclization procedure was developed to make N- to C-termini cyclic peptides using acetonitrile for easy solvent evaporation compared to using dimethylformamide (DMF), which is difficult to evaporate or remove (**Figure 4.1**). The

BBB modulatory activities of new cyclic peptides were compared to current linear HAV6 and cyclic ADTC5 peptides *in vivo* by brain delivery of an IRDye 800CW-labeled IgG mAb in C57BL/6 mice. The effects of the new cyclic peptides on IgG mAb depositions in other organs such as liver, kidney, spleen, lung, and heart were also determined to assess potential off-target tissue effects or side effects of these cadherin peptides.

4.2. Materials and Methods

4.2.1. Chemicals, Reagents, and Animals

Most of the reagents (e.g., trifluoro acetic acid (TFA), hydrogen gas, Pd/C catalyst, triisopropylsilane (TIPS), hexafluorophosphate azabenzotriazole tetramethyl uronium (HATU), diisopropyl ethyl amine (DIEA)) and solvents (e.g., acetonitrile, methanol) were purchased from Sigma Aldrich Chemical Company (St. Louis, MO) and Fisher Scientific Inc. (Hampton, NH). All amino acids for peptide synthesis were purchased from Gyros Protein Technologies Inc. (Tucson, AZ). IRDye800CW Donkey anti-Goat IgG for brain delivery was purchased from LI-COR Inc. (Lincoln, NE). All protocols used for animal studies have been approved by the Institutional Animal Care and Use Committee (IACUC) at The University of Kansas. The animals were maintained in the Animal Care Unit with free access to food and water.

4.2.2. Peptide Synthesis and Purification

A Tribute solid-phase peptide synthesizer (Gyros Protein Technologies, Inc., Tucson, AZ) with Fmoc chemistry was used to synthesize all linear peptide precursors (**Table 4.1**). The HAV6 and linear precursors for cyclic ADTC5 peptide were synthesized using amide resin and were cleaved from the resin with a cocktail mixture of 89% TFA:5% phenol:3% H_2O:3% TIPS. The linear precursors for N- to C-termini cyclic peptides (i.e., HAVN1, HAVN2, and ADTHAV) were synthesized using Fmoc-Val-Wang resin. The carboxylic acid and alcohol groups on the side chains were protected with benzyl groups. The peptides were cleaved using 94% TFA: 3% H_2O:

3% TIPS cocktail solution. The TFA solutions of linear HAV6, ADTC5, ADTHAV were added into cold diethyl ether to precipitate the peptide. In contrast, the cleavage solutions of linear HAVN1 and HAVN2 were directly concentrated by rotary evaporator to yield the crude peptides that were further lyophilized.

To form cyclic ADTC5, a very low concentration of linear peptide precursor without any protecting groups was dissolved in bicarbonate buffer solution at pH 9.0, and then, the solution was bubbled with air to oxidize the two thiol groups in the Cys residues to form a disulfide bond. The end-result produced cyclic ADTC5 peptide in a monomeric form with low side products as dimers, trimers, and oligomers. The desired monomer was purified by semi-preparative HPLC using C18 column Waters XBridge C18 (19 mm × 250 mm, 5 μm particle size; Waters Corporation, Milford, MA). The mobile phase consisted of solvents (A) H_2O: ACN: TFA (94.9:5:0.1) and (B) acetonitrile with a gradient of 40% B (0 min), 40–100% B (17 min), 100% B (2 min), 100–40% B (2 min), and 40% B (6 min). Before combining the collected fractions, each fraction was evaluated using analytical HPLC using a C18 column (Luna C18, 4.6 mm × 250 mm, 5 μm particle size, 100 Å; Phenomenex, Inc., Torrance, CA) to check for purity, and the pure fractions were pooled, concentrated, and lyophilized.

The N- to C-termini cyclizations to produce cyclic ADTHAV, HAVN1, and HAVN2 were carried out in solution phase (**Figure 4.1**). In this case, the acid and alcohol functional groups on the peptide were protected with benzyl ester and ether groups that were removed after cyclization. The optimized molar ratio of peptide: HATU: DIEA for the cyclization reaction was 1:2:4, and the cyclization reaction was done in dilute solution (~ 6.0 mM of peptide) in acetonitrile (ACN). In this case, three separate solutions were prepared: (1) 6.3 mmol peptide in 50 mL of acetonitrile, (2) 12.6 mmol HATU in 50 mL acetonitrile, and (3) 25.2 mmol DIEA in 1 L of acetonitrile. Then

the solutions of peptide and HATU were both added slowly from two different peristaltic pumps into the DIEA solution over 4 h, and the mixture was stirred overnight. The completion time for cyclization reaction was monitored using mass spectrometry every 4 h to observe the disappearance of the linear precursor and the appearance of the cyclic peptide with the loss of 18 amu from removal of one molecule of H_2O. After confirming the complete formation of the cyclic peptide, the acetonitrile was removed by rotary evaporator. A C18 semi-preparative HPLC column was used to isolate the cyclic peptide and the pure peptide was lyophilized. The cyclic peptide was dissolved in methanol and subjected to hydrogenation reaction under balloon pressure in the presence of Pd/C catalyst overnight to remove benzyl ester and ether protecting groups. The final product was purified by semi-preparative HPLC, and the identity of the cyclic peptide was confirmed using mass spectrometry (**Table 4.1**).

4.2.3. EC1 Protein Expression and Purification

For studies of peptide binding to the EC1 domain of E-cadherin, the EC1 domain protein was expressed and purified using our previously published protocol.[24, 25] The protein has 138 amino acids with 110 residues from the EC1 domain and an additional 28 residues at the C-terminus from the interface between the EC1 and EC2 domains. The N-terminus contains an added Streptag I sequence (WSHPQFEK) connected to the IEGR sequence as an interface to the N-terminus of the EC1 domain, and the IEGR sequence can be cleaved by Factor Xa enzyme. The protein was purified using an affinity Strep Tactin II column (5.0 × 0.6 cm; GE Healthcare Life Sciences, Pittsburgh, PA). The protein cDNA (BlueHeron, Bothell, WA) was subcloned into pASK-IBA6 plasmid (Genosys, Woodland, TX) and 2 μL of cDNA vector was mixed into 50 μL of BL21 cells followed by incubation for 30 min in ice. Then, the cells were warmed for 30 s in water bath at 42°C to allow cDNA to enter the cells; that was followed by a cooling period in an ice bath for 3 min. The cell suspension was then added with 200 μL of SOC medium and the resulting mixture

was shaken at 250 rpm and 37 °C for 1 h. The mixture was aliquoted (50 and 100 μL) into different agar plates followed by incubation for 12–16 h at 37 °C. Several colonies were selected from either a 50- or 100-μL-plate and incubated into 10 mL of LB medium (10 g NaCl, 10 g peptone, 5 g yeast, and up to 1 L of dd H_2O) followed by addition of ampicillin solution (10 μL of 100 mg/mL). The mixture was incubated overnight at 37 °C followed by its addition into 1 L of LB medium, which was incubated until the cell density was 0.6–0.8 at OD 600 nm. Cell growth was stimulated by adding 50 μL anhydrotetracycline (2 mg/mL, Promega Inc., Madison, WI) to start expressing the EC1 domain followed by incubation for 4 h at 30°C. The resulting cells were harvested by centrifugation at 10000–12000 rpm, and cell pellets were immediately stored at –80°C.

Prior to the SPR experiment, the EC1-containing cells were taken from the –80°C freezer and subjected to a lysing procedure using the French press in 25 mL binding buffer (100 mM Tris, 150 mM NaCl, 1 M EDTA, 1 mM DTT, 0.02% NaN3, pH 8). The lysed cells were centrifuged at 14000 rpm and 4 °C for 1 h to remove cell debris. The supernatant was isolated and filtered through a 0.2 μm sterile filter. Then, the filtrate was centrifuged using Amicon Ultra tubes (EMD Millipore, Billerica, MA) with 3,000 Da molecular weight cutoff to concentrate the EC1 protein. The concentrated EC1 was purified using a StrepTactin II column. The column was equilibrated and washed with binding buffer before and after protein solution exposure to the column at 5 mL/min flow rate. Pure protein was eluted from the column using an elution buffer containing 2.5 mM desthiobiotin at a flow rate of 2 mL/min. Tris-Bis SDS-PAGE (4–12%) was used to check the purity of the protein fractions from the affinity column. The protein concentration was determined using a UV spectrophotometer at 280 nm with molar absorptivity of 19480 M^{-1} cm^{-1}.

4.2.4. Surface Plasmon Resonance

The binding affinity of cyclic ADTC5 and cyclic ADTHAV peptides to the EC1 protein was determined using surface plasmon resonance (SPR) (OpenSPR instrument, Nicoya Lifesciences,

Waterloo, Canada) equipped with a 100 μL loading loop at 25 °C in a constant flow rate of 25 μL/min. The EC1 protein was injected into a streptavidin sensor chip with a running buffer (100 mM Tris HCl, 150 mM NaCl, 1% BSA, and 0.05% Tween20 at pH 7.4) to immobilize the protein. Next, different concentrations of peptide were injected to evaluate their binding process followed by washing with running buffer. The concentration range used for ADTC5 was from 6.25 μM to 50 μM while the concentration range for cyclic ADTHAV was between 550 nM and 2 μM. After peptide injection, 100 μM of HCl was injected to completely dissociate the complex and regenerate the sensor. Data analysis was done using Trace Drawer software (Ridgeview Instruments AB) as recommended by the manufacturer. Kinetic parameters were calculated using global analysis by fitting the data to a One-to-One binding model.

4.2.5 *In Vivo* Delivery of IRdye800CW IgG mAb

The activity of each peptide in enhancing BBB penetration was evaluated by delivering IRdye800CW Donkey anti-Goat IgG mAb in C57BL/6 mice; the amounts of mAb in the brain were determined using an NIRF imaging method. IgG mAb (21.6 nmol/kg) along with 13 μmol/kg peptide was administered via tail vein, and mAb was administered alone as a control. After the delivered molecules were circulating for 15 min, the mice were sacrificed; then, a mixture of PBS with 0.5% Tween20 was administered for cardiac perfusion to remove the blood and delivered molecules in the brain microvessels. The brain and other organs such as lung, heart, spleen, liver, and kidney were harvested and rinsed with PBS. The isolated organs were scanned with Odyssey® CLx for mAb quantification.

The brain deposition of IgG mAb was also quantified by NIRF imaging in brain homogenates. The isolated brains were mechanically homogenized in 2.0 mL PBS. To make the standard solutions, IRDye800CW IgG mAb stock solution (70 μg/mL) was prepared and it was diluted with various amounts of PBS. To generate a calibration curve, the homogenized mixture (200 μL; n =

8) was aliquoted out to a 96-well plate. 10 μL of solutions with various concentrations of IgG mAb were added to the blank brain homogenates to make standard spiked homogenates with a range of 10–200 ng/mL IgG mAb. Then the wells were scanned using the Odyssey® CLx scanner, and the signal intensities *vs*. concentrations of mAb per gram brain were used to generate a calibration curve.

4.2.6. Statistical Analysis

ANOVA with Student–Newman–Keuls was used to compare the data for determining statistical significance for IgG mAb depositions in the brains. The *p*-value of less than 0.05 was used as a criterion for a significant difference in data comparison.

4.3. Results

4.3.1. Peptide Synthesis and Purification

The solid-phase peptide synthesizer was used to generate all peptides used in this study and the synthesis was done using Fmoc amino acids. A high yield of crude peptide was normally found for peptide synthesis. The cyclization reaction to make cyclic ADTC5 peptide was uneventful and it generated mostly a monomeric cyclic peptide. The syntheses of N- to C-termini cyclic peptides were done by a combination of solid-phase and solution-phase synthetic methods (**Figure 4.1**). As an example, the linear ADTHAV as a precursor to a cyclic peptide was synthesized using solid phase peptide synthesis and the side chains of the Asp, Ser, and Thr residues were protected with benzyl ester and ether protecting groups. These protecting groups were maintained during the cleavage reaction to remove the peptide from the resin. After a semi-preparative HPLC purification, the isolated product was considered acceptable when it has >96% purity as determined by analytical HPLC with a C18 column. The cyclization was done in acetonitrile in high dilution to favor intramolecular peptide bond formation and to prevent formation of dimers, trimers, and oligomers. The major product was a monomeric cyclic peptide. The exact mass of

each N- to C-termini cyclic peptide is shown in **Table 4.1,** where the molecular mass of the cyclic peptide was 18 amu (– H_2O) less than the precursor linear peptide.

4.3.2. Surface Plasmon Resonance

Binding properties between cyclic ADTC5 or ADTHAV peptide to the immobilized EC1 domain protein on streptavidin chips were analyzed using SPR (**Figures 4.2 and 4.3**). The results showed that the dissociation constants (KD) for ADTC5 and cyclic ADTHAV were 26.8 μM and 0.114 μM, respectively (**Table 4.2**), suggesting that cyclic ADTHAV has tighter binding to the EC1 domain than does ADTC5.

Table 4.2. Dissociation Constant (KD) for ADTC5 and ADTHAV Cyclic Peptide

Peptide	K_{on} ($M^{-1}.S^{-1}$)	K_{off} (S^{-1})	KD (μM)
ADTC5	5.33×10^{3}	1.64×10^{-1}	26.8
Cyclic ADTHAV	5.47×10^{4}	6.23×10^{-3}	0.114

4.3.3. In Vivo Delivery of IRdye 800CW IgG mAb

The new cyclic peptides were compared to ADTC5 and HAV6 peptides by evaluating their activities in delivering IgG mAb into the brains of C57BL/6 mice. As a negative control, IgG mAb was delivered in PBS without peptide. Previously, ADTC5 has been shown to improve brain delivery of IgG mAb, which can serve as a positive control. Cyclic HAV peptides (i.e., HAVN1, HAVN2) and linear HAV6 were evaluated to test whether the formation of cyclic peptides could improve their BBB modulatory activity. Cyclic ADTHAV peptide was formed via a combination of ADTC5 and HAV6 sequences to test the potential additive activity of the two sequences.

Because ADTC5 and HAV6 bind to two different binding sites on the EC1 domain, it is proposed that cyclic ADTHAV has two different binding sites on the EC1 domain.

A calibration curve was generated to determine the amount of IgG mAb in the brain by spiking blank brain homogenates with a concentration range from 10 to 200 ng/mL and a good linearity with $R^2 \geq 0.99$ was achieved. As previously found, HAV6 did not enhance brain delivery of IgG mAb compared to control, i.e., IgG mAb alone (**Figure 4.4**, $p > 0.05$). while IgG mAb brain delivery was significantly enhanced by cyclic HAVN1 and HAVN2 peptides compared to HAV6 and control (**Figure 4.4**). These results indicate that cyclic peptide formation increases BBB modulatory activity of HAV peptide. The average amounts of IgG mAb in the brains of HAV6-treated and control animals were 4.0 ± 0.4 and 3.4 ± 0.5 pmol/g brain, respectively. In contrast, the average amounts of mAb in the brains of cyclic HAVN1- and HAVN2-treated mice were 8.6 ± 0.5 and 8.8 ± 0.6 pmol/g brain, respectively (**Table 4.3**). The BBB modulatory activities of ADTC5, linear ADTHAV, and cyclic ADTHAV (**Figure 4.5; Table 4.3**) were also compared to control. The brain delivery of IgG mAb by linear ADTHAV, cyclic ADTHAV, and ADTC5 was significantly better than the PBS control. The average brain depositions of IgG mAb were 11.8 ± 0.5, 15.7 ± 0.8, and 13.3 ± 0.7 pmol/g brain for linear ADTHAV, cyclic ADTHAV, and ADTC5, respectively.

The effects of peptides in the deposition of IgG mAb in other organs such as liver, kidney, heart, spleen and lungs were compared to control. There was no significant difference in IgG mAb deposition in other organs for HAV6-, HAVN1- and HAVN2-treated animals compared to control animals (**Figure 4.6**). These results suggest that these BBB-modulating peptides do not have a significant impact on other organs (**Figure 4.6**). In contrast, ADTC5 and linear ADTHAV peptides have significant effects on the distribution of IgG mAb in the heart and kidney when compared to

control (**Figure 4.7**). Moreover, there were significant increases in depositions of IgG mAb in liver, kidney, spleen, and lungs for cyclic ADTHAV peptide when compared to control (**Figure 4.7**).

Table 4.3. Brain Delivery of IgG mAb with BBB Modulating Peptides

Peptide	pmol/g brain
Control	**4.0 ± 0.4**
HAV6	**3.4 ± 0.5**
HAVN1	**8.6 ± 0.5**
HAVN2	**8.8 ± 0.6**
ADTC5	**13.3 ± 0.7**
Liner ADTHAV	**11.8 ± 0.5**
Cyclic ADTHAV	**15.7 ± 0.8**

4.4. Discussion

Treating brain diseases has become a challenge as it is difficult to deliver drugs through the BBB into the brain. As many approaches to solve this problem have failed clinically, it is important to investigate new methods to improve brain delivery of molecules for diagnosing and treating brain diseases. This study was focused on designing, synthesizing, and evaluating new cyclic peptides for modulating the BBB to increase paracellular protein delivery into the brain. Our previous studies showed that ADTC5 and HAV6 peptides modulate the paracellular pathways of the BBB and increase the permeation of small marker or drug molecules, peptides and proteins

into the brain.[19-23] The aim of this study was to design and synthesize more potent and selective cyclic peptides derived from ADTC5 and HAV6 sequences and evaluate their BBB modulatory effects in delivering IgG mAb to the brain. First, cyclic HAVN1 and HAVN2 peptides derived from linear HAV6 sequence were synthesized by N- to C-termini cyclization. The hypothesis is that cyclic peptides are more selective and conformationally more stable than the parent linear peptides. Second, a combination of ADT and HAV6 sequences was implemented in linear and cyclic ADTHAV peptides. The hypothesis is that the combined sequence and cyclization can enhance the BBB modulatory activity of the parent peptides. Thus, linear and cyclic ADTHAV peptides were compared to ADTC5 in delivering IgG mAb into the brains of C57BL/6 mice.

Previously, the formation of cyclic peptides has been shown to improve biological activity and plasma stability of peptides. Many cyclization methods have been utilized to improve conformational stability and binding properties of peptides to their respective target receptor(s). Various covalent bonds have been utilized to form cyclic peptides by linking two ends of the peptide with an amide, lactone, ether, thioether, or disulfide bond using. The cyclization can be formed via backbone-to-backbone (or N-to-C termini), backbone-to-side chain, or side chain-to-side chain. One of the most popular cyclization methods is by forming the N-to-C (or backbone-to-backbone) cyclization from the amino to carboxyl terminus using an amide bond. In nature, many biologically active cyclic peptides are N-to-C cyclized peptides. Compared to their linear counterparts, cyclic peptides are less flexible or more conformationally rigid, which often enhances the biological activity of the peptide.[26] The rigidity of a cyclic peptide results in a higher affinity toward the target receptor compared to the linear counterpart, which is presumably due to the decrease in the entropy term of the Gibbs free energy. Moreover, the N-to-C cyclic peptides do not have open-ended carboxyl or amino termini that can be subjected to enzymatic degradations

by exo- and endopeptidases; therefore, the cyclic peptide is enzymatically more stable than the parent linear peptide in the plasma.[27] For these reasons, cyclic peptides have been developed successfully as therapeutics in the clinic and there are more than 60 approved peptide-derived drugs available in the United States and other major markets. Among those, a vast majority are derived from natural products such as antimicrobials or human peptide hormones, including widely applied cyclic peptides such as oxytocin, octreotide, vasopressin, vancomycin, daptomycin, and polymyxinB.[28]

It was interesting to find that cyclic HAVN1 and HAVN2 peptides were able to deliver IgG mAb while their parent linear HAV6 peptide could not enhance delivery of IgG mAb. HAVN1 is a cyclic hexapeptide that has the same sequence as HAV6 while HAVN5 is a cyclic pentapeptide with deletion of the C-terminal Ser residue. It is also interesting to find that this Ser deletion in HAVN2 still provided BBB modulatory activity similar to that of HAVN1 in the current experimental conditions. This finding is consistent with our previous study in which the formation of a cyclic HAV peptide called cHAVc3 (cyclo(1,6)Ac-CSHAVC-NH_2) had improved modulatory activity compared to that of linear HAV peptide.[19] It has been shown that HAV6 also did not enhance the delivery of 65 kDa albumin using the current conditions; however, HAV6 could enhance the delivery of 65 kDa galbumin into the brain when the dose of galbumin was increased 27 times compared to the current experimental conditions. This suggests that there is an improvement in the BBB modulatory activity of cyclic HAVN1 and HAVN2 compared to that of linear HAV6, which cannot enhance the delivery of mAb. These results also indicate that cyclic pentapeptide HAVN2 can be used as a lead compound for future mutation studies to improve the BBB modulatory activity and selectivity.

These cadherin peptides interrupt the cadherin-cadherin interactions by binding to the extracellular domains of cadherins allowing delivered molecules to pass through the intracellular junctions of the BBB. The X-ray structure of C-cadherin showed that cadherin molecules can form *cis*- and *trans*-interactions with each other in a homotypic fashion.[29] The *cis*-cadherin interactions were formed by binding of the EC1 domain from one cadherin molecule to the EC2 domain of another cadherin, both of which protrude from the same cell membranes. The *trans*-cadherin interactions were formed by binding between the EC1 domain of a cadherin molecule from one cell membranes to the EC1 domain of another cadherin molecule from the opposing cell membranes. In this case, a Trp residue at the N-terminus of the first EC1 binds to a hydrophobic pocket in the second EC1 from the opposing cell membranes while another Trp the second EC1 binds to a hydrophobic pocket at the first EC1. This process is called "domain swapping". Our previous NMR studies indicated that HAV peptides bind to the EC1 domain of E-cadherin at the interface of *cis*-cadherin interactions; thus, it is proposed that HAV peptides block *cis*-cadherin interactions to open the paracellular pathways.[30] In contrast, ADT peptides bind to the hydrophobic pocket involved in the domain-swapping process to block *trans*-interactions of two opposing EC1 domains. These results presumably suggest why ADT peptides have better modulatory activities than do HAV peptides.

We propose that combining the sequences of ADT and HAV peptides could create a more potent peptide compared to individual ADT or HAV peptides with the rationale that the new peptide can bind to two different binding sites. To test this idea, linear and cyclic ADTHAV peptides were synthesized, and the binding properties of cyclic ADTHAV and ADTC5 to the EC1 domain were determined using SPR, which can evaluate binding kinetics (e.g., binding association and dissociation rates) and binding affinity. In this study, different concentrations of the studied

peptide were passed through a chip surface modified with immobilized EC1 protein. Prior to the binding experiment, it was necessary to check for any non-specific binding (NSB) by injecting the peptide to the bare surface of the chip without any protein. In this study, the binding conditions have been optimized to minimize or eliminate the non-specific binding of the peptide by finding the optimal pH of the running buffer, adding surfactant and blocking agent, and adjusting the salt (NaCl) concentration. In this study, NSB was minimized by adding 1% BSA and 0.05% Tween20 to the running buffer. After optimizing the running conditions, the EC1 protein was immobilized on the streptavidin chip via the Streptag I sequence on the N-terminus of the EC1 domain followed by injection of various peptide concentrations. The binding results that were observed on the sensorgram consisted of three phases: association, dissociation, and regeneration. The obtained KD for ADTC5 was 26.8 μM (**Figure 4.2**), which is in range similar to that of the KD (35 μM) determined by NMR upon titration of the ^{15}N-labeled EC1-domain of E-cadherin using heteronuclear single quantum coherence spectroscopy (HSQC) experiments. It is interesting to find that cyclic ADTHAV has a lower KD (0.114 μM) than that of ADTC5 (35 μM), suggesting that ADTHAV cyclic has better binding affinity than ADTC5 to the EC1-domain of E-cadherin.

Next, the *in vivo* BBB modulatory activities of linear and cyclic ADTHAV peptides as well as ADTC5 to deliver IgG mAb were compared to that of control in C57BL/6 mice. All three peptides were effective in delivering IgG mAb into the brain compared to control (**Figure 4.5;** $p < 0.05$). Cyclic ADTHAV showed a trend of higher activity in delivering IgG mAb compared to linear ADTHAV ($p = 0.07$), while there was no significant difference between cyclic ADTHAV and ADTC5 ($p = 0.20$). There is a significant difference in BBB modulatory activity between cyclic ADTHAV and cyclic HAVN2; however, it was not clear whether the different in the activity was due to different mechanisms of binding to the EC1 domain. In other words, cyclic ADTHAV

potentially has two different binding sites on the EC1 domain to inhibit *cis*- and *trans*-cadherin interactions due to a sequence combination while cyclic HAVN2 has only one binding site on the EC1 domain to inhibit *cis*-cadherin interactions. The potential binding mechanisms of both peptides can be evaluated in the future by NMR experiments.[19] It also proposed that a short circulation time (15 min) may not be adequate to differentiate BBB modulatory activities of ADTC5 and ADTHAV peptides. In the future, we will evaluate the effects of dose and longer circulation times to further differentiate the *in vivo* biological activities of all cyclic peptides that were used in the current study. At the same time, the stability of cyclic ADTHAV and ADTC5 in the systemic circulation can also be compared because it is predicted that the plasma stability of ADTC5 will be lower than that of cyclic ADTHAV; this is due to the instability of the disulfide bridge in ADTC5 peptide that could be reduced by glutathione in the blood.

Because cadherin-mediated cell-cell adhesion is also found in different organs (i.e., liver, kidney, heart, spleen, and lung), the effects of cyclic peptides on IgG mAb depositions in other organs were determined to evaluate the potential side effects. All peptide-treated groups and the control group showed a significantly higher accumulation of IgG mAb in the liver compared to spleen, heart, kidney, and lung because most of the metabolic pathways occur in the liver. When comparing the control group to all groups treated with HAV peptides (i.e., HAV6, HAVN1, and HAVN2), there was no significant difference in depositions of IgG mAb within each specific organ. These results suggest that these peptides did not have any effect on the peripheral organs. Thus, HAV peptides may have higher specificity in modulating the BBB than the peripheral organs. In contrast, cyclic ADTC5 and linear ADTHAV showed a significant increase in IgG mAb depositions in heart and kidney compared to control while the cyclic ADTHAV group had a significant increase in IgG mAb depositions in lungs, spleen, kidney, and liver. The strong effect

of cyclic ADTHAV in peripheral organs was presumably due to its strong binding affinity to the EC1 domain of E-cadherins; thus, further studies are needed to evaluate the role of different doses in IgG depositions in peripheral organs.

The duration of time of the BBB opening is an important factor to consider for using cadherin peptides to deliver molecules to the brain. This is because it is dangerous to keep the BBB open for a long period of time, allowing unwanted molecules to enter the brain. However, it is necessary to keep the opening for an adequate amount of time to allow the delivered molecule to enter the brain with the necessary dose. For example, HAV6 has an opening window of less than 1 h to allow a small molecule such as R800IRdye and gadopentetic acid (Gd-DTPA) to enter the brain, while ADTC5 has a duration of opening between 2 to 4 h for brain delivery of Gd-DTPA.[20, 21] Using a high dose of 65 kDa galbumin, HAV6 peptide can increase the BBB penetration of galbumin when they are delivered together; however, a 10-min delay between the delivery of HAV6 and galbumin does not allow galbumin to cross the BBB. Thus, the BBB window of opening by HAV6 for a large protein such as galbumin is short (< 10 min). In contrast, the opening created by ADTC5 for galbumin is between 10 and 40 min. The results suggest that each peptide produces various populations of pore sizes that can collapse in a time-dependent manner, and each peptide has a cut-off size of molecules that can be delivered through the BBB.

4.5. Conclusion

In this study, we have designed and synthesized novel cyclic peptides that can effectively modulate the BBB to enhance the delivery of mAb into the brains of C57BL/6 mice. The new peptides were designed based on HAV6 and ADTC5 peptides, which modulate cadherin-cadherin interactions in the BBB to improve the delivery of small, medium, and large molecules, including proteins. We have shown that cyclic HAVN1 and HAVN2 peptides have better BBB modulatory effects than their linear counterpart, HAV6 peptide. Cyclic ADTHAV with a combination of ADT

and HAV sequences has better binding affinity to the EC1 domain of E-cadherin than does ADTC5 peptide. Cyclic ADTHAV can significantly enhance brain delivery of IgG mAb compared to control, and it influences the deposition of IgG mAb in peripheral organs while no HAV peptides influence the deposition of IgG mAb in these organs. In the future, all cyclic peptides will be evaluated in longer circulation times to evaluate their effects in delivering mAb and other proteins with various sizes.

4.6. Figures and Legends

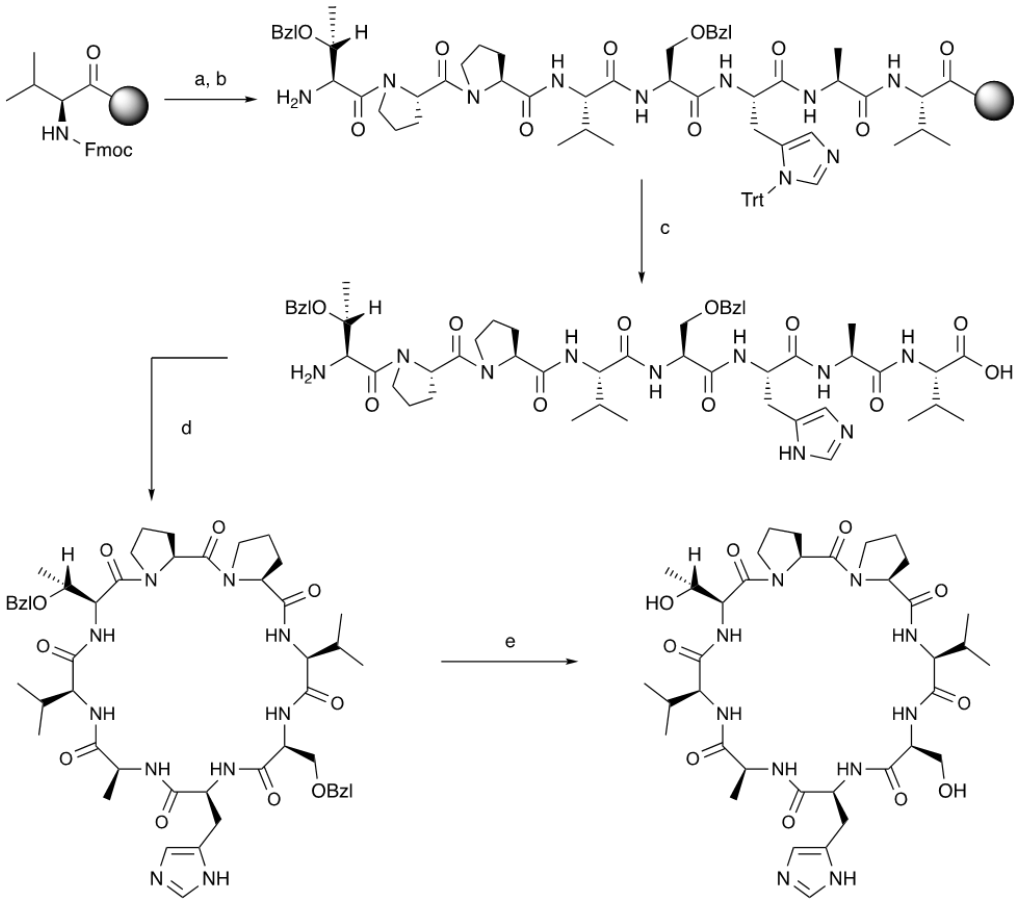

Figure 4.1 A synthetic scheme to make cyclic ADTHAV peptide: **(a)** Fmoc-deprotection: piperidine/DMF (1:4). **(b)** Coupling reaction in DMF using HCTU, NMM, and Fmoc-amino acids: Fmoc-Ala-OH, Fmoc-Ser(Bzl)-OH, Fmoc-Val-OH, Fmoc-Pro-OH, Fmoc-His(Trt)-OH, Fmoc-Thr(Bzl)-OH, and Fmoc-Pro-OH. **(c)** (i) Fmoc-deprotection reaction and (ii) peptide cleavage from the resin: TFA/H_2O/TIPS (94:3:3) at room temperature and 2-h reaction time. **(d)** Solution-phase cyclization reaction using HATU/DIEA/peptide (2:4:1) in acetonitrile at room temperature and 24-h reaction time followed by Prep-HPLC. **(e)** Final hydrogenation reaction for side-chain deprotection peptide/H_2/Pd/C at room temperature and 24-h reaction time.

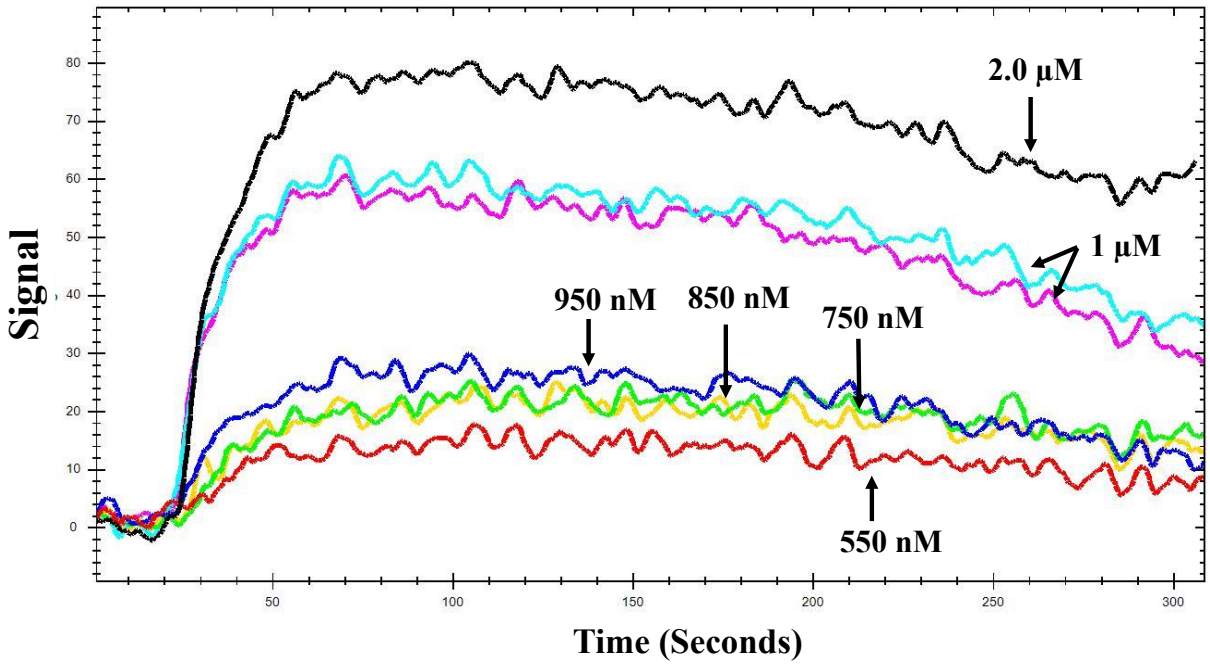

Figure 4.2 SPR sensorgrams of binding between cyclic ADTHAV peptide and the EC1 protein immobilized onto streptavidin chips using the OpenSPR Nicoya instrument. Sensorgrams were recorded using increasing amounts of ADTHAV (550 nM – 2 μM) in running buffer during the association phase.

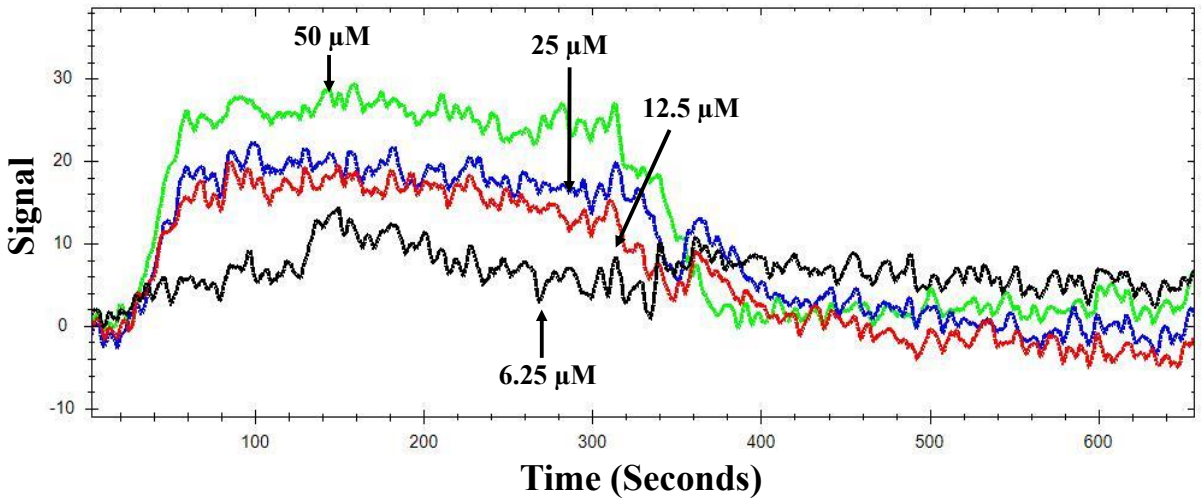

Figure 4.3 SPR sensorgrams of binding between cyclic ADTC5 peptide and the EC1 protein immobilized onto streptavidin chips using the OpenSPR Nicoya instrument. Sensorgrams were recorded using increasing amounts of ADTC5 (6.25 μM – 50 μM) in running buffer during the association phase.

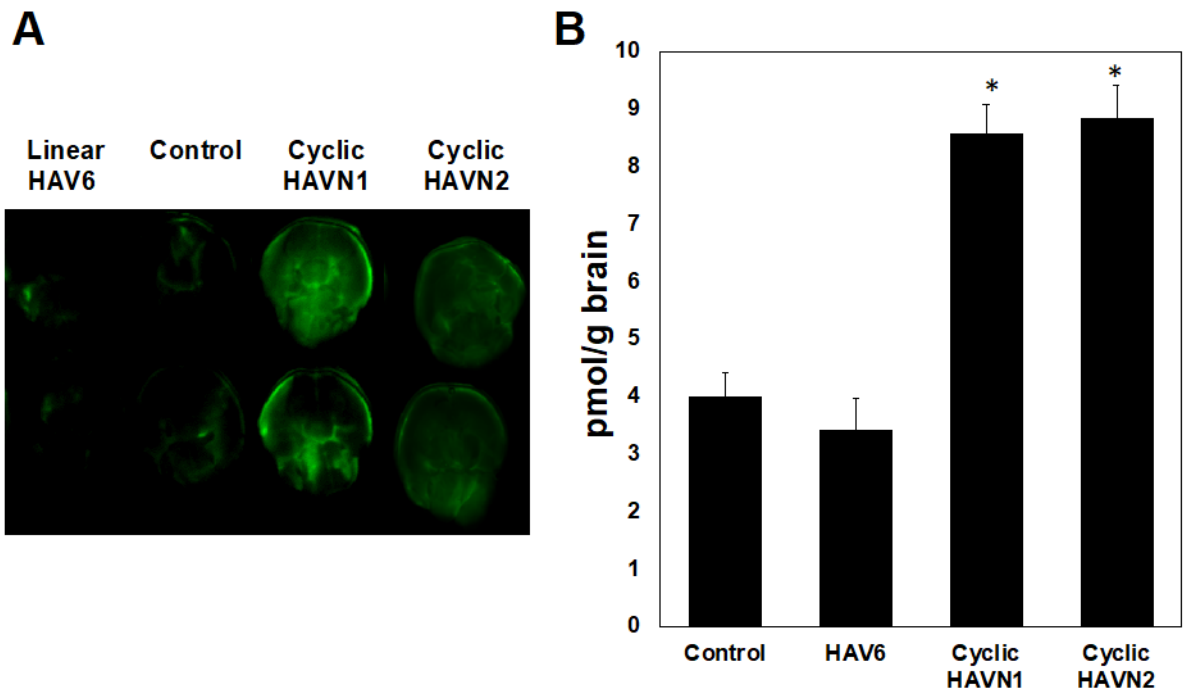

Figure 4.4 (**A**) The levels of brain depositions of IRdye800CW-IgG mAb were qualitatively shown by NIRF imaging after administration of IgG mAb (21.6 nmol/kg) alone as a control or along linear HAV6, cyclic HAVN1, or cyclic HAVN2 (13 μmol/kg) in C57BL/6 mice. (**B**) IRdye800CW-IgG mAb brain depositions were determined quantitatively using NIRF imaging in pmol/g brain after delivery of IgG mAb when delivered alone (21.6 nmol/kg) or delivered with HAV6, HAVN1, or HAVN2 (13 μmol/kg) in C57BL/6 mice. The asterisk symbol (*) was used to designate a significant difference in HAVN1- or HAVN2-treated groups compared to control with $p < 0.05$. Error bars show the mean ± SE with the number of animals, n = 3, for each group.

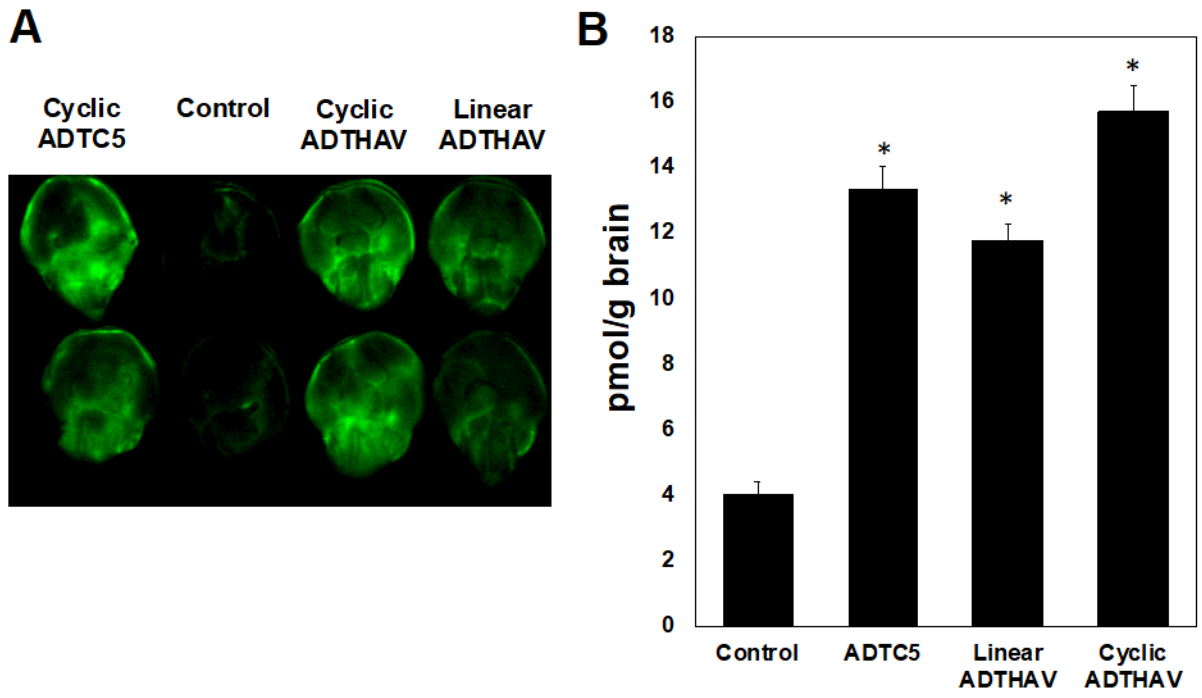

Figure 4.5 (**A**) The qualitative brain depositions of IRdye800CW-IgG mAb shown as NIRF images after its i.v. administration alone (21.6 nmol/kg) as a control and together with cyclic ADTC5, linear ADTHAV, or cyclic ADTHAV (13 μmol/kg) in C57BL/6 mice. (**B**) Quantitative determination of IRdye800CW-IgG mAb brain depositions in pmol/g brain after its administration (21.6 nmol/kg) without peptide as a control group or in the presence of ADTC5, linear ADTHAV, or cyclic ADTHAV (13 μmol/kg) in C57BL/6 mice. The asterisk (*) indicates a significant difference in cyclic ADTC5-, linear ADTHAV-, or cyclic ADTHAV-treated groups compared to control with $p < 0.05$. Error bars show the mean ± SE with the number of animals, n = 3, for each group.

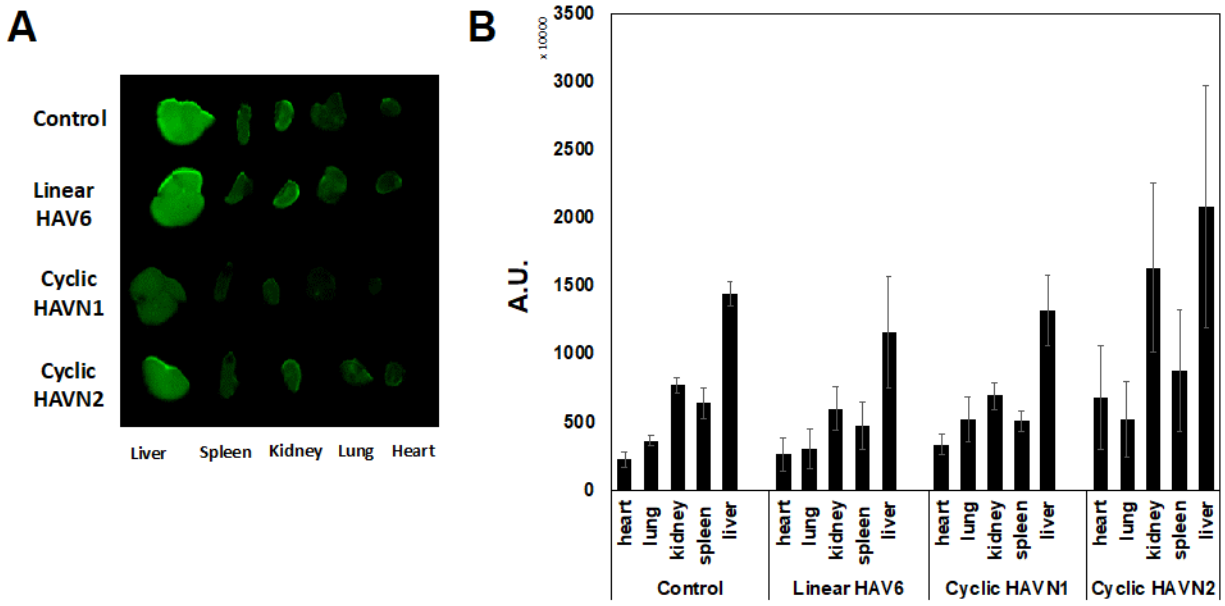

Figure 4.6 The effects of linear HAV6, cyclic HAVN1, and cyclic HAVN2 peptides on the peripheral organ depositions of the IRdye800CW-IgG mAb in heart, lung, kidney, spleen, and liver determined using NIRF signal intensity **(A)** qualitatively and **(B)** quantitatively in absorption unit (A.U.). The IgG mAb depositions were measured by the total NIRF image intensity in each organ. There is no significant difference in the IgG mAb signal intensities for each organ when

comparing the control group and peptide-treated group with $p > 0.05$. Error bars show the mean ± SE with the number of animals, n = 3, for each group.

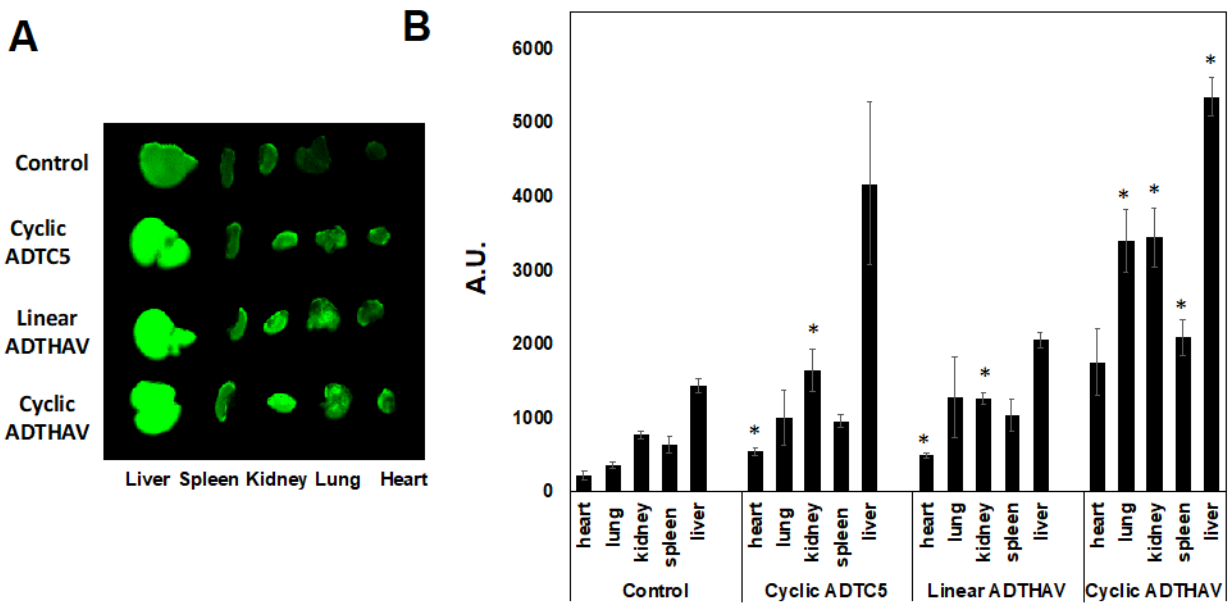

Figure 4.7 The effects of cyclic ADTC5, linear ADTHAV, and cyclic ADTHAV peptides on the peripheral organ deposition of the IRdye800CW-IgG mAb in heart, lung, kidney, spleen, and liver determined using NIRF signal intensity **(A)** qualitatively and **(B)** quantitatively in absorption unit (A.U.). The IgG mAb depositions were measured by the total NIRF image intensity in each organ. There are significance differences in the IgG mAb signal intensities for kidney and heart of ADTC5- or linear ADTHAV-treated mice compared to control ($p > 0.05$). There are significant differences in the IgG mAb signal in all five organs from the cyclic ADTHAV-group compared to the control group. Error bars show the mean ± SE with the number of animals, n = 3, for each group.

4.7. References

1. Kiptoo, P.; Laksitorini, M. D.; Siahaan, T. J., Blood-Brain Peptides: Peptide Delivery. In *Handbook of Biologically Active Peptides*, Kastin, A., Ed. Academic Press: Boston, 2013; pp 1702–1710.
2. Laksitorini, M.; Prasasty, V. D.; Kiptoo, P. K.; Siahaan, T. J. Pathways and progress in improving drug delivery through the intestinal mucosa and blood-brain barriers. *Ther Deliv* **2014,** *5*, (10), 1143-63.
3. Pardridge, W. M. The blood-brain barrier: bottleneck in brain drug development. *NeuroRx* **2005,** *2*, (1), 3-14.
4. Lipinski, C. A. Lead- and drug-like compounds: the rule-of-five revolution. *Drug Discov Today Technol* **2004,** *1*, (4), 337-41.
5. Pardridge, W. M. Blood-brain barrier drug delivery of IgG fusion proteins with a transferrin receptor monoclonal antibody. *Expert Opin Drug Deliv* **2015,** *12*, (2), 207-22.
6. Pardridge, W. M. Delivery of Biologics Across the Blood-Brain Barrier with Molecular Trojan Horse Technology. *BioDrugs : clinical immunotherapeutics, biopharmaceuticals and gene therapy* **2017,** *31*, (6), 503-519.
7. Pardridge, W. M.; Boado, R. J. Pharmacokinetics and safety in rhesus monkeys of a monoclonal antibody-GDNF fusion protein for targeted blood-brain barrier delivery. *Pharm Res* **2009,** *26*, (10), 2227-36.
8. Abbott, N. J.; Romero, I. A. Transporting therapeutics across the blood-brain barrier. *Mol Med Today* **1996,** *2*, (3), 106-13.
9. Chacko, A. M.; Li, C.; Pryma, D. A.; Brem, S.; Coukos, G.; Muzykantov, V. Targeted delivery of antibody-based therapeutic and imaging agents to CNS tumors: crossing the blood-brain barrier divide. *Expert Opin Drug Deliv* **2013,** *10*, (7), 907-26.

10. Masoudi, R.; Ioannou, M. S.; Coughlin, M. D.; Pagadala, P.; Neet, K. E.; Clewes, O.; Allen, S. J.; Dawbarn, D.; Fahnestock, M. Biological activity of nerve growth factor precursor is dependent upon relative levels of its receptors. *J Biol Chem* **2009,** *284*, (27), 18424-33.
11. Numakawa, T.; Suzuki, S.; Kumamaru, E.; Adachi, N.; Richards, M.; Kunugi, H. BDNF function and intracellular signaling in neurons. *Histol Histopathol* **2010,** *25*, (2), 237-58.
12. Brasnjevic, I.; Steinbusch, H. W. M.; Schmitz, C.; Martinez-Martinez, P. Delivery of peptide and protein drugs over the blood–brain barrier. *Progress in Neurobiology* **2009,** *87*, (4), 212-251.
13. Rotman, M.; Welling, M. M.; Bunschoten, A.; de Backer, M. E.; Rip, J.; Nabuurs, R. J.; Gaillard, P. J.; van Buchem, M. A.; van der Maarel, S. M.; van der Weerd, L. Enhanced glutathione PEGylated liposomal brain delivery of an anti-amyloid single domain antibody fragment in a mouse model for Alzheimer's disease. *J Control Release* **2015,** *203*, 40-50.
14. Kobus, T.; Zervantonakis, I. K.; Zhang, Y.; McDannold, N. J. Growth inhibition in a brain metastasis model by antibody delivery using focused ultrasound-mediated blood-brain barrier disruption. *J Control Release* **2016,** *238*, 281-288.
15. Farrell, C. L.; Shivers, R. R. Capillary junctions of the rat are not affected by osmotic opening of the blood-brain barrier. *Acta neuropathologica* **1984,** *63*, (3), 179-89.
16. Neuwelt, E. A.; Barnett, P. A.; Hellstrom, I.; Hellstrom, K. E.; Beaumier, P.; McCormick, C. I.; Weigel, R. M. Delivery of melanoma-associated immunoglobulin monoclonal antibody and Fab fragments to normal brain utilizing osmotic blood-brain barrier disruption. *Cancer Res* **1988,** *48*, (17), 4725-9.

17. Neuwelt, E. A.; Barnett, P. A.; McCormick, C. I.; Frenkel, E. P.; Minna, J. D. Osmotic blood-brain barrier modification: monoclonal antibody, albumin, and methotrexate delivery to cerebrospinal fluid and brain. *Neurosurgery* **1985,** *17*, (3), 419-23.

18. Kiptoo, P.; Sinaga, E.; Calcagno, A. M.; Zhao, H.; Kobayashi, N.; Tambunan, U. S.; Siahaan, T. J. Enhancement of drug absorption through the blood-brain barrier and inhibition of intercellular tight junction resealing by E-cadherin peptides. *Mol Pharm* **2011,** *8*, (1), 239-49.

19. Alaofi, A.; On, N.; Kiptoo, P.; Williams, T. D.; Miller, D. W.; Siahaan, T. J. Comparison of Linear and Cyclic His-Ala-Val Peptides in Modulating the Blood-Brain Barrier Permeability: Impact on Delivery of Molecules to the Brain. *J Pharm Sci* **2016,** *105*, (2), 797-807.

20. Laksitorini, M. D.; Kiptoo, P. K.; On, N. H.; Thliveris, J. A.; Miller, D. W.; Siahaan, T. J. Modulation of intercellular junctions by cyclic-ADT peptides as a method to reversibly increase blood-brain barrier permeability. *J Pharm Sci* **2015,** *104*, (3), 1065-75.

21. On, N. H.; Kiptoo, P.; Siahaan, T. J.; Miller, D. W. Modulation of blood-brain barrier permeability in mice using synthetic E-cadherin peptide. *Mol Pharm* **2014,** *11*, (3), 974-81.

22. Ulapane, K. R.; On, N.; Kiptoo, P.; Williams, T. D.; Miller, D. W.; Siahaan, T. J. Improving Brain Delivery of Biomolecules via BBB Modulation in Mouse and Rat: Detection using MRI, NIRF, and Mass Spectrometry. *Nanotheranostics* **2017,** *1*, (2), 217-231.

23. Tabanor, K.; Lee, P.; Kiptoo, P.; Choi, I. Y.; Sherry, E. B.; Eagle, C. S.; Williams, T. D.; Siahaan, T. J. Brain Delivery of Drug and MRI Contrast Agent: Detection and Quantitative Determination of Brain Deposition of CPT-Glu Using LC-MS/MS and Gd-DTPA Using Magnetic Resonance Imaging. *Mol Pharm* **2016,** *13*, (2), 379-90.

24. Makagiansar, I. T.; Ikesue, A.; Duc Nguyen, P.; Urbauer, J. L.; Bieber Urbauer, R. J.; Siahaan, T. J. Localized production of human E-cadherin-derived first repeat in Escherichia coli. *Protein Expression and Purification* **2002,** *26*, (3), 449-454.

25. Prasasty, V. D.; Krause, M. E.; Tambunan, U. S.; Anbanandam, A.; Laurence, J. S.; Siahaan, T. J. (1)H, (13)C and (15)N backbone assignment of the EC-1 domain of human E-cadherin. *Biomol NMR Assign* **2015,** *9*, (1), 31-5.

26. Edman, P. Chemistry of amino acids and peptides. *Annual review of biochemistry* **1959,** *28*, 69-96.

27. Joo, S. H. Cyclic peptides as therapeutic agents and biochemical tools. *Biomol Ther (Seoul)* **2012,** *20*, (1), 19-26.

28. Zorzi, A.; Deyle, K.; Heinis, C. Cyclic peptide therapeutics: past, present and future. *Current opinion in chemical biology* **2017,** *38*, 24-29.

29. Boggon, T. J.; Murray, J.; Chappuis-Flament, S.; Wong, E.; Gumbiner, B. M.; Shapiro, L. C-Cadherin Ectodomain Structure and Implications for Cell Adhesion Mechanisms. *Science* **2002,** *296*, (5571), 1308.

30. Alaofi, A.; Farokhi, E.; Prasasty, V. D.; Anbanandam, A.; Kuczera, K.; Siahaan, T. J. Probing the interaction between cHAVc3 peptide and the EC1 domain of E-cadherin using NMR and molecular dynamics simulations. *J Biomol Struct Dyn* **2017,** *35*, (1), 92-104.

CHAPTER 5

Summary, Conclusions and Future Directions

5.1 Summary and Conclusions

The overall objective of this project was to enhance the brain delivery of peptides and proteins in mouse and rat models. The objectives of this project were to (a) develop methods to detect the delivery of peptides and proteins into the brains; (b) modulate the blood-brain barrier (BBB) for brain delivery of peptides and proteins using cadherin peptides; and (c) design and evaluate new cyclic cadherin peptides to improve BBB modulatory activity to deliver proteins into the brain. The BBB acts as a physical and enzymatical barrier to delivery of foreign molecules, including drugs, to the brain; therefore, this makes the development of diagnostics and drugs for brain diseases challenging.

In the second chapter, we found that BBB-modulating peptides (i.e., HAV6, cHAVc3, and ADTC5) enhance the delivery of various molecules such as a 65 kDa galbumin and peptides (i.e., cIBR7, IRdye800cw-cLABL) in both mice and rats. These BBB-modulating peptides significantly enhanced the brain delivery of 65 kDa galbumin compared to control in Balb/c mice as quantified by magnetic resonance imaging (MRI). A 10-min pretreatment with ADTC5 peptide significantly increased brain delivery of galbumin; however, no enhancement was observed after a 10-min pretreatment with HAV6. There was no enhancement of galbumin deposition following 40-min pretreatment with ADTC5 or HAV6, suggesting a short duration of the BBB opening for large molecules. Next, near IR fluorescence (NIRF) was used to detect the enhanced delivery of IRdye800cw-cLABL peptide in the presence of ADTC5 peptide, which resulted in a 3.5-fold improved brain delivery compared to control in Balb/c mice. Finally, as a proof of study, a non-labeling method, LC-MS/MS, was used to evaluate the BBB modulator activity of ADTC5 to deliver cIBR7 peptide *in vivo* using Sprague-Dawley rats. LC-MS/MS was developed and validated for accuracy, precision, stability and linear calibration curves. Extraction procedures

were optimized for efficient extraction of peptides from the brain homogenates. Deposition of cIBR7 peptide in the presence of ADTC5 and absence (controls) were quantified and showed that ADTC5 peptide as a BBB modulator enhanced the delivery of cIBR7 peptide into rat brain about 4-fold compared to control. Overall, we showed that ADTC5 was capable of modulating the BBB to enhance peptide and protein delivery to the brain using both labelled and non-labeled quantifying methods.

Currently, biologics or protein drugs have drawn attention to inventing new medicines, mainly for brain diseases because limited effective treatments exist for many brain conditions, including brain tumors, autoimmune diseases, neurodegenerative diseases, infectious diseases, and genetic disorders. Although many biological drugs have been developed and are already on the market, there are no successful biological drugs targeting neurological conditions and brain diseases such as, Alzheimer's, Parkinson's and multiple sclerosis. This is mainly due to the inability to deliver those drugs to the brain due to their large molecular size. In our previous study, we successfully delivered galbumin (65 kDa) to the brain by modulating the BBB. The next goal of this work is to evaluate and quantitatively determine the delivery of large proteins into the brain using cadherin peptides, ADTC5, and HAV6.

In Chapter 3, we have compared two BBB modulator peptides (i.e., ADTC5 and HAV6) in improving the delivery of different sized proteins from 15 kDa to 220 kDa in C57BL/6 mice. Lysozyme (15 kDa), albumin (65 kDa), IgG mAb (150 kDa), and fibronectin (220 kDa) were labeled with IRdye800CW to be quantified after the *in vivo* delivery using NIRF imaging. A novel NIRF quantifying method was developed and validated for accuracy, precision, stability and linear calibration curves according to the FDA guidelines. With our *in vivo* studies, it showed that ADTC5 peptide significantly enhanced brain delivery of lysozyme, albumin and IgG mAb but not

fibronectin compared to controls. In contrast, HAV6 peptide significantly enhanced the brain delivery of lysozyme but not albumin and IgG mAb. Thus, there is a cut-off size of proteins that can be delivered by each peptide. Overall, we showed that ADTC5 is a better BBB modulator than HAV6 in delivering various sizes of proteins into the brain.

Since HAV and ADT peptides showed different binding sites in EC1 of the cadherin protein in our previous NMR studies, it was interesting to design novel peptides with a combination sequence targeting for a better modulatory effect. Moreover, it is well known that cyclic peptides have shown a higher stability and better biological activity than their linear counterparts. The main goal in Chapter 3 was to design novel cyclic peptides and evaluate their activity *in vitro* and *in vivo* for the BBB modulation. While HAV6 is a linear peptide and ADTC5 is a disulfide bridged cyclic peptide, both peptides have shown promising BBB-modulating activity to improve brain delivery of various molecules. We have designed and synthesized cyclic and linear ADTHAV peptides derived from both sequences of ADTC5 and HAV6 peptides. We also designed and synthesized cyclic HAVN1 and HAVN2 peptides that are C-to-N cyclized peptides derived from linear HAV6 peptide. It is hypothesized that by combining the two sequences and forming N-to-C terminal cyclization, the resulting peptides will be more stable and have a higher BBB modulatory effect. All the novel peptides were compared with ADTC5, HAV6, and control (with no peptide to modulate the BBB) for delivery of an IRdye800CW IgG mAb to C57BL mice. It is interesting to show that both HAVN1 and HAVN2 peptides showed higher accumulations of IgG mAb in mice brains compared to HAV6 and control. In Chapter 3 we have shown that there is no significant difference between HAV6 and control brains for deposition of IRdye800cw-IgG mAb; however, after cyclizing the HAV6 peptide using N-to-C terminal cyclization there was a significant difference in brain delivery of mAb by either HAVN1 or HAVN2 compared to control.

Moreover, cyclic and linear ADTHAV peptides showed higher deposition of IRdye800cw-IgG mAb, but there was no significance difference compared to ADTC5. It is assumed that the current condition of 15-minute circulation time was not adequate to detect significant differences among the cyclic peptides. Therefore, longer circulation times will be investigated to differentiate the activities of the cyclic peptides. In addition, more experiments will be carried out to evaluate the stability and efficacy of cyclic ADTHAV in the future.

5.2 Future Directions

5.2.1 Brain Delivery of Neuroregenerative Molecules

Neurodegenerative diseases such as multiple sclerosis (MS) and Alzheimer's disease (AD) affect people of all ages and result in progressive degeneration and death of neurons. In MS patients, the myelin sheaths of the neuronal axons are attacked and damaged by their own immune cells.[1,2] Repairing and protecting myelin is one of the approaches in treating MS. Unfortunately, while all of the available drugs are capable of preventing further injury to nerves and axons by suppressing the immune response, none of the available drugs can repair the neuronal damage that has already occurred. In AD, neuronal degeneration relates to accumulation of extracellular amyloid plaques and intracellular neurofibrillary tangles in the brain.[3,4] Even though several antibody treatments targeting amyloid beta have shown some promising results for treating AD, most of them have failed clinically due to ineffectiveness in delivering them to the brain.[5,6]

One way to reverse the neuronal damage in neurodegenerative diseases is to deliver neuroregenerative molecules such as brain-derived neurotrophic factor (BDNF),[7-9] nerve growth factor (NGF),[10] or insulin-like growth factor 1 (IGF-1)[11] to the CNS. In our previous studies we have successfully shown that we can enhance the delivery of various sizes of proteins up to monoclonal antibodies (150 kDa) to healthy mice using ADTC5 as the BBB modulator. In future

studies, BDNF can be delivered to MS and AD mouse models using ADTC5 or any of the novel peptides as the BBB modulator. With our promising results for enhanced antibody delivery in previous studies, an effective BDNF delivery is expected and it will induce the remyelination and neuroregeneration. The results can be evaluated according to (a) disease scores, (b) behavior, (c) physical appearance, (d) pathology of neuroregeneration/repair, and (e) mechanism of neuroregeneration in the brain by detecting upregulation of signal proteins induced by BDNF delivery.

5.2.2 Brain Delivery of Antibody Drugs to Treat Brain Tumors

Because the BBB is a barrier to many developed drugs, our BBB-modulating peptides have increased brain delivery by modulating the cadherins in the intracellular junction. In Chapters 2, 3, and 4 we have shown that our BBB-modulating peptides can improve the delivery of various molecules, including peptides, proteins, and monoclonal antibodies.

Among many biological drugs such as monoclonal antibodies (mAbs), Fab fragments, and mAb-drug conjugates such as avastin (bevacizumab), herceptin, kadcyla, and mylotarg have been used successfully to treat tumors outside of the brain. But none of them can be used to treat brain tumors (e.g., glioblastoma, medulloblastoma) due to their inability to cross the BBB and enter the brain. Therefore, our BBB modulating peptides, ADTC5, and novel ADTHAV peptides could be used to improve the brain delivery of anti-tumor drugs to improve its paracellular permeability to the brain. A mixture of the BBB-modulating peptide and an unlabeled or labeled antibody drug can be administered intravenously (i.v.) in normal or brain-tumor mouse models.

5.2.3 Novel Peptides for Brain Delivery of Proteins

In Chapter 3, we have shown that ADTC5 can improve the brain delivery of various proteins up the size of a monoclonal antibody (150 kDa) with a cut-off size of 220 kDa using current

conditions—peptide (13 µmol/kg), protein (21.6 nmol/kg), and 15-min circulation time. In Chapter 4, we have designed and synthesized novel cyclic peptides with the hypothesis that, by combining the two sequences of ADTC5 and HAV6 peptides (ADTHAV peptides) and cyclizing through N to C terminal cyclization, better modulatory peptides with higher stability would result. Even though we see higher modulatory effects for the cyclic peptides HAVN1 and HAVN2 compared to their linear counterpart HAV6, there was no significant difference between the ADTHAV peptides and ADTC5 peptide. It is assumed that the current cyclization time (15 min) was not sufficient to show a significant effect on stability. It can be hypothesized that the deposition of protein in the brain is correlated to the time of circulation. Therefore, increasing the circulation time should eventually show a significant difference in protein deposition with different peptides. Thus, the effects of circulation time on brain deposition can be optimized to find the optimal circulation time. Also, *in vitro* plasma stability experiments can be done with the peptides to evaluate their half-lives and other kinetic parameters.

5.3 References

1. Lassmann, H. Axonal and neuronal pathology in multiple sclerosis: what have we learnt from animal models. *Exp Neurol* **2010,** *225*, (1), 2-8.
2. Compston, A.; Coles, A. Multiple sclerosis. *Lancet* **2008,** *372*, (9648), 1502-17.
3. Milward, E. A.; Papadopoulos, R.; Fuller, S. J.; Moir, R. D.; Small, D.; Beyreuther, K.; Masters, C. L. The amyloid protein precursor of Alzheimer's disease is a mediator of the effects of nerve growth factor on neurite outgrowth. *Neuron* **1992,** *9*, (1), 129-37.
4. Kim, J.; Choi, I. Y.; Michaelis, M. L.; Lee, P. Quantitative *in vivo* measurement of early axonal transport deficits in a triple transgenic mouse model of Alzheimer's disease using manganese-enhanced MRI. *NeuroImage* **2011,** *56*, (3), 1286-92. ID: 3098472

5. Mullard, A. Anti-amyloid failures stack up as Alzheimer antibody flops. Nat Rev Drug Discov 2019.

6. Mehta, D.; Jackson, R.; Paul, G.; Shi, J.; Sabbagh, M. Why do trials for Alzheimer's disease drugs keep failing? A discontinued drug perspective for 2010-2015. *Expert Opin Investig Drugs* **2017**, 26, (6), 735-739.

7. Zagrebelsky, M.; Korte, M. Form follows function: BDNF and its involvement in sculpting the function and structure of synapses. *Neuropharmacology* **2014,** *76 Pt C*, 628-38. ID

8. Greenberg, M. E.; Xu, B.; Lu, B.; Hempstead, B. L. New insights in the biology of BDNF synthesis and release: implications in CNS function. *J Neurosci* **2009,** *29*, (41), 12764-7. ID: PMC3091387

9. Numakawa, T.; Suzuki, S.; Kumamaru, E.; Adachi, N.; Richards, M.; Kunugi, H. BDNF function and intracellular signaling in neurons. *Histol Histopathol* **2010,** *25*, (2), 237-58.

10. Masoudi, R.; Ioannou, M. S.; Coughlin, M. D.; Pagadala, P.; Neet, K. E.; Clewes, O.; Allen, S. J.; Dawbarn, D.; Fahnestock, M. Biological activity of nerve growth factor precursor is dependent upon relative levels of its receptors. *J Biol Chem* **2009,** *284*, (27), 18424-33. ID: 2709390

11. Apel, P. J.; Ma, J.; Callahan, M.; Northam, C. N.; Alton, T. B.; Sonntag, W. E.; Li, Z. Effect of locally delivered IGF-1 on nerve regeneration during aging: an experimental study in rats. *Muscle Nerve* **2010,** *41*, (3), 335-41. ID: PMC3045758